REGULATION OF GLIOSIS IN THE MOUSE RETINA

A Dissertation

Submitted to the Faculty

of

Purdue University

by

Subramanian Dharmarajan

In Partial Fulfillment of the

Requirements for the Degree

of

Doctor of Philosophy

August 2017

Purdue University

Indianapolis, Indiana

THE PURDUE UNIVERSITY GRADUATE SCHOOL
STATEMENT OF COMMITTEE APPROVAL

Dr. Teri Belecky-Adams

Department of Biology

Dr. Jason S. Meyer

Department of Biology

Dr. Stephen Randall

Department of Biology

Dr. AJ Baucum

Department of Biology

Dr. Yuk Fai Leung

Department of Biological Sciences

Approved by:

Dr. Theodore R. Cummins

Head of the Graduate Program

To my wife Akshaya
and my daughter Ananya.

ACKNOWLEDGMENTS

I would like to thank my advisor, Dr. Teri Belecky-Adams, for all of her support, encouragement and mentorship. You have helped me become the researcher I am today. In addition to my advisor, I would also like to thank my committee members Dr. AJ Baucum, Dr. Yuk Fei Leung, Dr. Jason Meyer and Dr. Stephen Randall. I appreciate your insightful comments and assistance throughout my project which have helped develop my skills.

To my fellow graduate students and staff of the department of Biology, I would like to thank you for lending a helping hand whenever I needed it. I would like to also thank the faculty of the department of Biology for all their help with my projects and career advise.

I am grateful to my friends Nilesh, Chetan, Rishi, Shrikant and Amrit. The game nights, dinners, road trips and general help and friendship helped me feel at home and was a welcome distraction from my lab work.

Finally, this work would not be complete without the unwavering support of my wife Akshaya. She has been a great companion, loved and encouraged me throughout this challenging period, to make them the best years of my life. I would also like to thank my parents for their unconditional love and support in allowing me to follow my ambitions.

TABLE OF CONTENTS

Page

Page

Page

LIST OF TABLES

LIST OF FIGURES

Figure Page

ABBREVIATIONS

Angiomotins	AMOT
Aquaporin	AQ
Blood retinal barrier	BRB
Bone morphogenetic proteins	BMP
Chemokine ligand	CCL
Chondoritin sulphate proteoglycans	CSPG
Ciliary neurotrophic factor	CNTF
Connective tissue growth factor	CTGF
Day	d
Endothelial growth factor receptor	EGFR
Fibroblast growth factor	FGF
Glial cell line derived neurotrophic factor	GDNF
Glial fibrillary acidic protein	GFAP
Glutamate aspartate transporter	GLAST
Glutamine synthetase	GS
Granulocyte macrophage colony stimulating factor	GM-CSF
Hour	h
Insulin like growth factor	IGF
Interferon	IFN
Interleukin	IL
Inwardly rectifying potassium channels	Kir
Janus kinase	JAK
Leukemia inhibitory factor	LIF
Lipocalin	LCN

Matrix metalloproteinases	MMP
Minute	min
Neurocan	NCAN
Nitric oxide	NO
Nuclear factor kappa light chain enhancer of activated B cells	NF-κB
Paired homeobox	PAX
Phosphacan	PCAN
Platelet derived growth factor	PDGF
Ribonucleic acid	RNA
Seconds	sec
Sex determining region Y box 2	SOX2
Secreted phosphoprotein	SPP1
Signal recognition particle	SRP
Signal transducer and activator of transcription	STAT
Succinate dehydrogenase	SDHA
TGF-β activated kinase	TAK
Thioredoxin interacting protein	TXNIP
Thrombospondin	THBS
Tissue inhibitor of metalloproteinases	TIMP
Toll like receptor	TLR
Transcriptional co-activator with PDZ binding motif	TAZ
Transcriptional enhancer associated domain	TEAD
Transforming growth factor-beta	TGF-β
Tumor necrosis factor-alpha	TNF-α
Vascular endothelial growth factor	VEGF
Vehicle	Veh
Vimentin	VIM
X linked inhibitor of apoptosis	XIAP
Yes activated protein	YAP

ABSTRACT

Dharmarajan, Subramanian Ph.D., Purdue University, August 2017. Regulation Of Gliosis In The Mouse Retina. Major Professor: Teri Belecky-Adams.

The glial cells of the retina aid in function and maintenance of the retina. The macroglia, Müller cells and the retinal astrocytes, become reactive following injury or disease in the retina, a response that is characterized by hypertrophy, de-differentiation, loss of functionality, proliferation, and remodeling of tissue and extracellular matrix (ECM). The microglia which are the resident macrophages, also respond to injury/disease becoming activated, undergoing characteristic molecular and morphological changes, which include regulation of secreted factors, changes in inflammatory response and increased phagocytosis. Reactivity in Müller glia is thought to be the result of secreted signals, such as epidermal growth factor, ciliary neurotrophic factor, and fibroblast growth factor, which are released at the injury site to interact with quiescent glial cells. Furthermore, microglia and macroglia have been shown by some studies to interact following activation. While BMPs are known to be upregulated following injury in the CNS, little information is available concerning their role in reactive gliosis in the retina. We hypothesize that BMP7 indirectly triggers Müller gliosis by activating microglia. Using RT-qPCR, immunofluorescence and western blot, we assessed changes in gliosis markers in the mouse retinal glia following treatment with BMP. Our results showed that BMP7 was able to trigger Müller cell gliosis in the retina *in vitro* and *in vivo*. Furthermore, ablation of microglia lead to a subdued gliosis response in the mouse retina following BMP7 exposure. Thus, BMP7 triggers activation of retinal microglia in addition to the Müller glia. IFN-γ and IL6 could play a role in microglia mediated activation of Müller glia, following exposure to BMP7. We also assessed the role of the Hippo/YAP pathway in the regulation of

gliosis in the retina. We demonstrated that YAP was localized to the nucleus of the Müller cells of the retina and was upregulated in IFN-γ induced gliosis in the mouse retina.

1. INTRODUCTION

1.1 Mammalian retina

The retina is a highly organized neural tissue located at the back of the eye which converts light to an electrical impulse giving us vision [1]. The mature mammalian retina is organized into three nuclear layers, separated by two plexiform layers made up synapses of the neurons from adjacent layers. The nuclear layers are: the outer nuclear layer, made up of the rod and cone photoreceptor cells; the inner nuclear layer, made up of bipolar, horizontal and amacrine interneurons and the ganglion cell layer made up of the retinal ganglion cells. Synapses of the photoreceptor cells and the bipolar cells are found in the outer plexiform layers, while the inner plexiform layer consists of the synapses between the bipolar cells and the retinal ganglion cells. The axons of the ganglion cells form the nerve fiber layer and exit the retina through the optic nerve, carrying the signal to the brain. The Müller glia, which are the primary glial or non-neural support cells, are found in the inner nuclear layer with the processes extending the length of the retina. The retina also consists of the retinal astrocytes, found in the nerve fiber layer and ganglion cell layer. The microglia, which are the resident macrophages, are distributed throughout the retina (Figure 1.1) [2].

The photoreceptor cells include the rod and the cone cells. The rod cells are greater in number in comparison to the cone cells and are involved in providing vision in situations of dim light and are particularly good for detecting motion. In contrast the cones are active in bright light and help in object and color recognition, and shape analysis. There are at least three different types of cone cells identified in human and non-human primate retinas, classified as short, medium and long wavelength cones, which aid in color discrimination. Rods outnumber the cones 97:1 in primates and

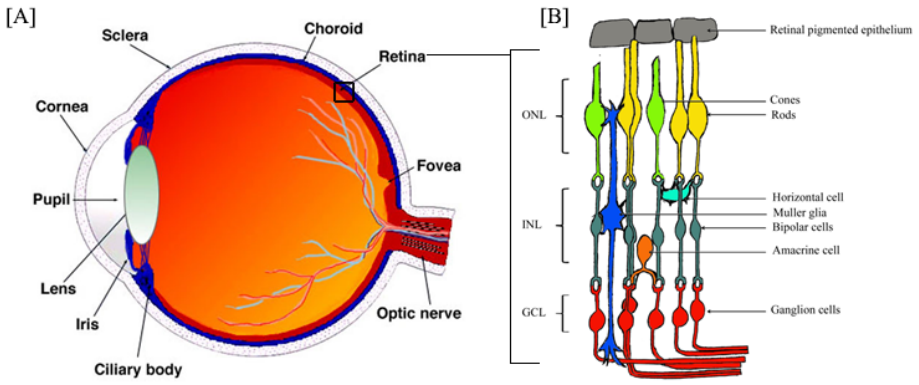

Fig. 1.1. Vertebrate eye and the retina. (A) Structure of the mature mammalian eye, (B) Organization and cells of the mature mammalian retina [3].

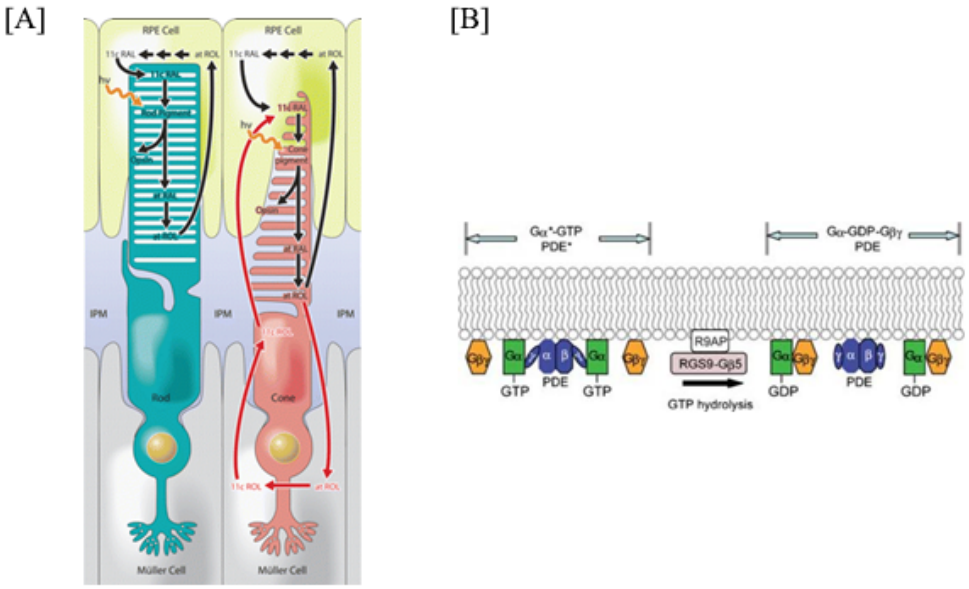

Fig. 1.2. Photoreceptor cell and light activation. (A) Diagramatic representation of the structure of rod and cone photoreceptor cells, (B) Light induced activation of G-protein coupled receptors in photoreceptors which ultimately leads to generation of an impulse [4].

animal models such as mice. The photoreceptor cells convert light to an electrical impulse, a process known as phototransduction. Structurally, the photoreceptor cells consist of an outer segment, containing a stack of membrane discs and an inner segment linked by a connecting cilium. The outer segments contain all the molecular phototransduction machinery including, the visual pigment, a G-protein coupled receptor (GPCR) made up of opsin and cis-retinal. When a photon is absorbed by the visual pigment, the energy from the photon converts the cis-retinal to trans-retinal. This induces the pigment to the active metarhodopsin-II form, leading to activation of the transduction cascade. cGMP gated ion channels are closed as a result of cascade in the outer segment, leading to hyperpolarization of the cell (Figure 1.2). The light induced signals are transferred to the horizontal cells and bipolar cells through synapses formed with the synaptic terminal of the photoreceptor cells in the outer plexiform layer. The bipolar interneurons, along with the amacrine cells synapse with the ganglion cells in the inner plexiform layer to transmit the signal to the ganglion cells. The horizontal and amacrine cells of the outer and inner plexiform layers, respectively, help in reducing the noise/background of the input signal [4, 5].

The axons of the retinal ganglion cells exiting the retina through the optic nerve terminate in four regions of the diencephalon: the thalamus, pretectum, hypothalamus and superior colliculus. Most of the axons terminate in the lateral geniculate nuclei (LGN) in the thalamus. Axons from here project on to the visual cortex. These form the retinogeniculostriate pathway which is the primary visual pathway. This pathway processes most of the input visual stimuli. A small percentage of ganglion cell axons also project to the pretectum, which regulates the pupillary light reflex, the hypothalamus which involved in the circadian rhythms of the body and to the superior colliculus which coordinates head and eye movements (Figure 1.3) [6].

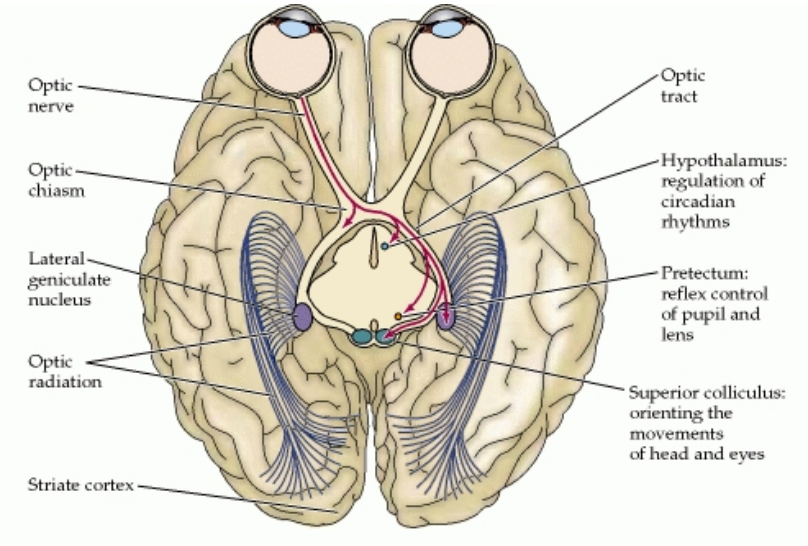

Fig. 1.3. Projections of the retinal ganglion cells. Diagramatic representation of the projections of axons from the ganglion cells which exit from the retina through the optic nerve, crossover at the optic chiasm and project onto different regions of the brain [7] .

1.2 Development of the retina

The vertebrate eye develops from the eye field, in the anterior neural plate. This region is characterized by expression of eye field transcription factors such as Six3, Six6, Rax, Pax6, Lhx2 and Tbx3. Following formation of the neural tube, sonic hedgehog (SHH) induces the eye field to split, forming the optic grooves. These optic grooves evaginate to form the optic vesicles, which come into close proximity with the overlying head ectoderm. Reciprocal signaling between the optic vesicle and the overlying ectoderm induces the formation of the lens placode from the ectoderm, which ultimately become the lens [8]. The proximal part of the vesicle forms the optic stalk, through which the optic nerve exits the eye sending signals to the brain. The layer close to the lens placode differentiates to form the neural retina, while the distal part of the vesicle gives rise to the retinal pigmented epithelium [9]. The retinal progenitors undergo symmetric and asymmetric divisions to give rise of the different cell types of the retina. The retinal cell types are derived in a sequential

manner with the retinal ganglion cells being the first born cells. The horizontal cell, cone photoreceptors and the amacrine cells differentiate in the next wave, while the bipolar cells, the rod photoreceptors and the Müller glia differentiate last from the retinal progenitors (Figure 1.4) [10].

1.3 Retinal glia

The glial cells are the non-neural support cells found in the neural tissue. Broadly, they can be classified into macroglia and microglia. The retinal macroglia consist of two cell populations: the Müller glia, which are the primary glial cell type of the retina, and the retinal astrocytes. The Müller cell bodies are found in the inner nuclear layer, with the processes extending throughout the length of the retina, from the inner limiting membrane near the vitreal edge to the outer limiting membrane just beneath the inner and outer segments of the rods and cones. The retinal astrocytes are found in the nerve fiber layer [11].

The Müller glia arise from multipotent retinal progenitor cells. The retinal progenitor cells give rise to ganglion cells first followed by horizontal cell, cone photoreceptor cells and amacrine cells. The Müller glial cells are one of the last group of cells that differentiate from these progenitor cells along with the rod photoreceptors and the bipolar cells [8]. The retinal astrocytes originate in the optic nerve from glia restricted precursors. The astrocytes migrate into the retina through the optic disc and move into the nerve fiber layer [12, 13]. The Müller glia exhibit a radial glia like morphology with their cell bodies in the inner nuclear layer and their processes spanning the entire retina contacting neighboring neurons. In contrast, the retinal astrocytes exhibit a stellate morphology, and are found in the nerve fiber layer and ganglion cell layer [8]. Both the macroglial cell types perform similar functions in supporting and protecting the retina as listed in the sections below. The microglial cells are

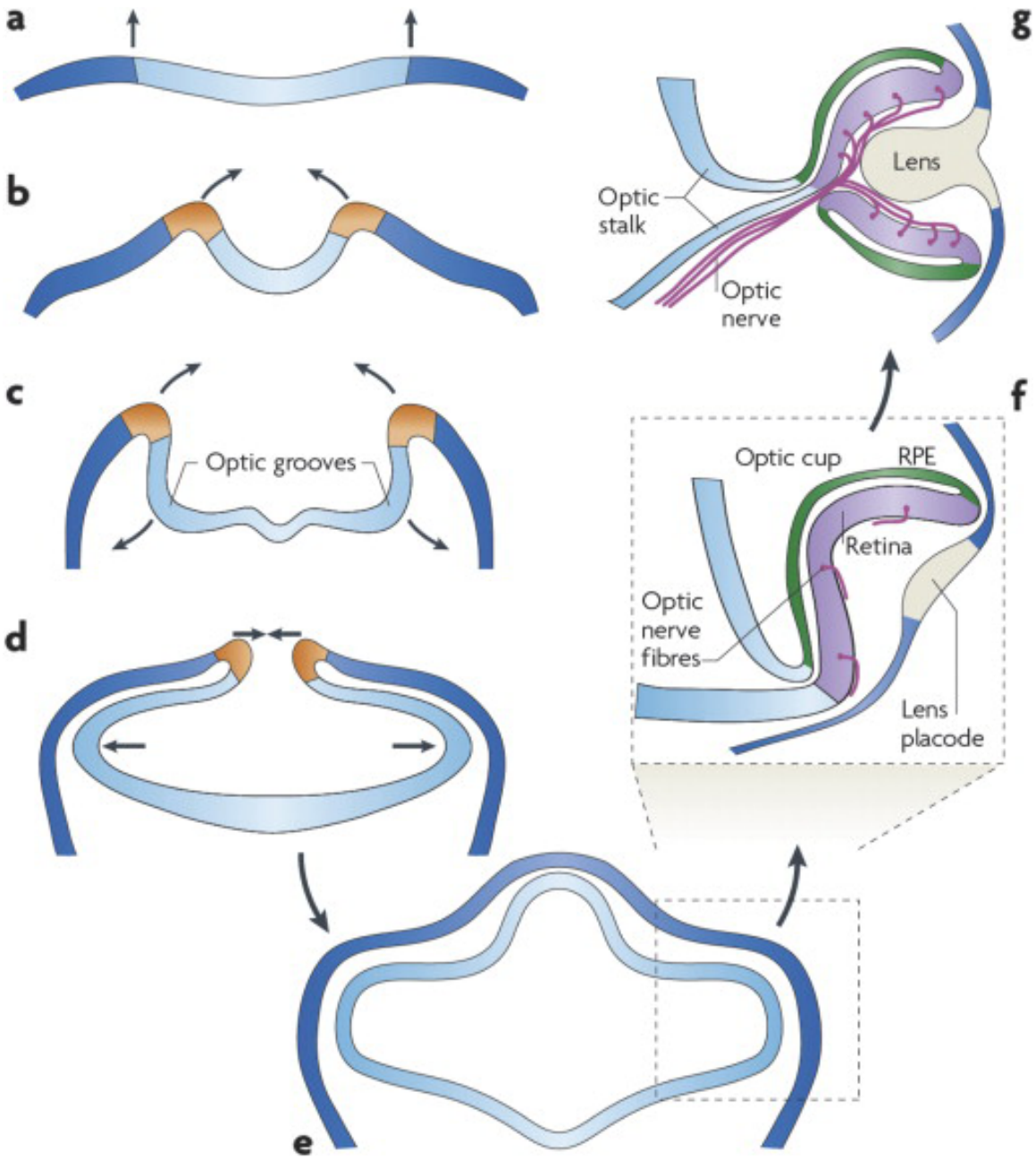

Fig. 1.4. Development of the vertebrate eye. (A) Neural plate, (B) Formation of the neural tube, (C) Splitting of the eye field to generate optic grooves, (D) Evagination of the optic grooves towards head ectoderm, (E) Closure of the neural tube bringing the optic grooves in close proximity to the head ectoderm, (F) Formation of the optic cup and the lens placode, and (G) Region of the optic cup proximal to the lens placode differentiates into the retina, while the distal portion gives rise to the retinal pigmented epithelium [10].

derived from embryonic yolk sac blood islands and migrate into the optic cup early in development [14]. In addition some vertebrate retinas contain oligodendrocytes that myelinate the retinal ganglion cell axons in the nerve fiber layer; however the murine retina does not contain oligodendrocytes [15]. The avian retina also contains a novel glial cell type termed the non-astrocytic inner retinal glia (NIRG) [16].

1.4 Retinal glial functions

The retinal glia play an important role in maintaining retinal homeostasis and supporting normal function of the neurons. They are required for neuronal survival as well as serve as a conduit for exchange of molecules [17]. Broadly, they play a role in regulating the neurotransmitter uptake, releasing factors for neuronal survival, protecting the neurons from oxidative stress, formation and maintenance of the blood retinal barrier, as well as regulating water and ion homeostasis (Figure 1.5).

1.4.1 Regulating glucose metabolism

The brain utilizes 25% of the glucose present in the human body, most of which is utilized due to neuronal activity [18]. The neurons are reliant on external sources, particularly the glial cells, for the supply of nutrients for the oxidative metabolism. Furthermore, the glial cells also store excess glucose in the form of glycogen to meet neuronal demands during increased neuronal metabolic rates. Enzymes involved in glycogen metabolism such as glycogen synthase kinase 3β and glycogen phosphorylase have been shown to be localized to the retinal glia. Studies have shown that the Müller glia convert excess glucose to glycogen in an insulin dependent manner (PerezLeon et al. 2013; Pfeiffer-Guglielmi et al. 2005). Glucose uptake in the glial cells is mediated by the glucose transporter 1 (GLUT 1) receptor. Most of the glucose consumed is converted to lactate and released into the extracellular space via the

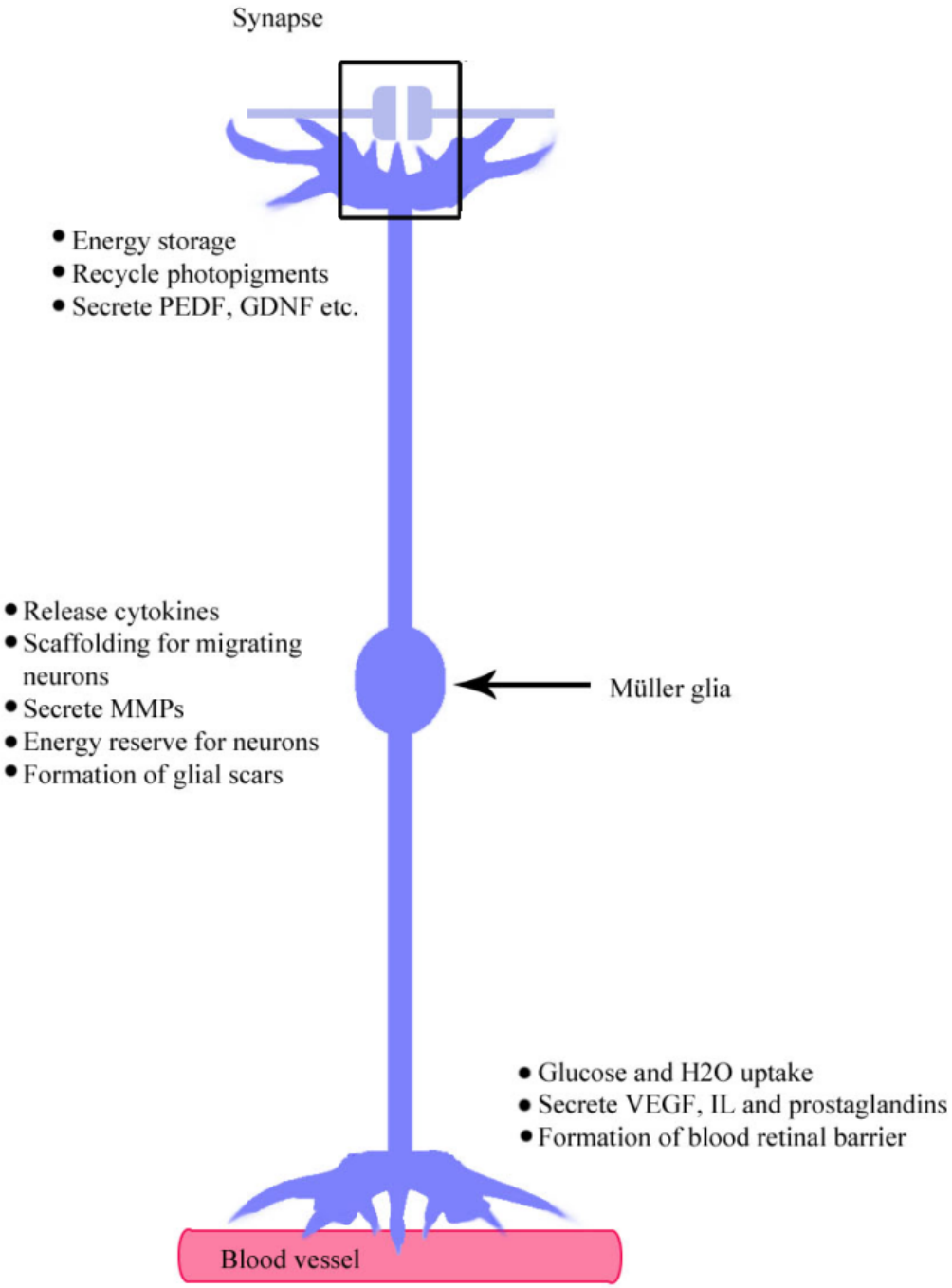

Fig. 1.5. Functions of the Müller glia. The Müller glia play a role in support and maintenance of normal neuronal function as well as establishing the blood retinal barrier, secreting growth factors, energy storage, neurotransmitter recycling and water and ion homeostasis [3].

monocarboxylase transporter 2 (MCT2), which is then taken up by the surrounding neurons [19].

1.4.2 Regulation of glutamate metabolism

Glutamate is the most prominent neurotransmitter released by the photoreceptors, bipolar and ganglion cells of the retina. The Müller glia and astrocytes are involved in removal of the excess glutamate from the extracellular sites via the excitatory amino acid transporters (EAAT1 – 5) [20]. The major glutamate transporter of the Müller cells however, is the glutamate aspartate transporter (GLAST/EAAT1). After its uptake, glutamate is rapidly metabolized by the enzyme glutamine synthetase to glutamine or utilized for the production of glutathione, an antioxidant. Glutathione is localized to the retinal glia, and only released under conditions associated with oxidative stress. Glutamine synthetase is localized throughout the cytosol of the Müller glia and astrocytes in the retina. The glutamine produced by Müller glia is released and taken up by neurons for synthesis of glutamate and gamma aminobutyric acid (GABA) [21]. Bipolar cells and ganglion cells are highly dependent on glutamine from the Müller glia as revealed by studies inhibiting glutamine synthetase [22]. The transport and uptake of glutamine from the glia to the neurons is mediated by neutral amino acid carrier systems A and L (ATA and LAT); and the sodium dependent amino acid exchanger (ASCT2) [21].

1.4.3 Synaptic function

The processes of the macroglia have been found to be in close association with the synaptic region of retinal neurons. They have been shown to promote synapse formation *in vitro* [23]. Furthermore, it is thought energy substrates, neurotransmitter precursors, ions and neurotrophic factors such as glial cell line derived neurotrophic fac-

tor (GDNF), released by the glial cells help in maintaining normal synaptic function (Pfrieger and Barres 1996). Furthermore, macroglia have been thought to be directly involved in regulating synaptic signaling via release of gliotransmitters (GABA, ATP, glutamate). The processes of the glial cells involved in the modulation of synapse are hypothesized to form a tripartite synapse with the pre and post synaptic terminals [24].

1.4.4 Development and maintenance of blood retinal barrier

The blood retinal barrier is a physical barrier that separates the circulating blood and the extra cellular fluid in the retina. This barrier makes the retina an immune privileged site and also regulates the chemical environment within the tissue. In the retina, the blood retinal barrier (BRB) consists of the outer barrier, formed by the retinal pigmented epithelium, and the inner barrier, formed by the endfeet of the retinal glia and cells of the retinal vasculature [25]. The inner barrier is formed by the tight junctions between adjacent endothelial cells, stabilized by pericytes and the covered by the macroglia endfeet. These tight junctions regulate the movement of fluids and other substances between the blood and the retina. The Müller glia secrete factors such as pigment epithelium derived factor (PEDF) and GDNF which enhance the barrier function of the retina [26].

1.4.5 Maintenance of ion homeostasis in the retina

Müller glia help maintain homeostasis by regulating extracellular pH, Na+, K+ ions, and water. The Müller glia express inwardly rectifying potassium (Kir) channels through which they regulate the extracellular potassium concentrations. The Kir 4.1 channel, localized to the vitreal endfeet and perivascular membrane, and the Kir 2.1, distributed throughout the Müller glia, are the two main types of the Kir channels

involved in potassium regulation [27]. They take up the excess ions released at the synapses by neurons and transport it to the blood or the vitreous through these channels [28]. The Müller glia also express the glial water channel, aquaporin-4 (AQP4), expressed primarily in the perivascular membrane and endfeet [29]. The Müller glia also help regulate the CO_2 and pH by the action of carbonic anhydrase and acid/base transporters present at the endfeet. The glia specific enzyme, carbonic anhydrase, transfers the CO_2, a by-product of metabolic activity in the neurons, to HCO_3- and also generates a proton. The HCO_3- is redistributed via the H^+/HCO_3- exchanger into the perivascular membrane or the blood vessels [17, 30].

1.5 Microglia

The microglia are the resident macrophages of the retina, migrating within the retina to clear cellular debris and surveying the microenvironment. The microglia are found in the nerve fiber, ganglion and inner plexiform layers, while deeper microglia lie within the outer plexiform layer (Figure 1.6). The microglial cells appear to be originating from the embryonic yolk sac blood islands and migrate into the very early developing brain, suggesting that these may be present in the optic pits prior to closure of the neural tube and development of the optic cups [14].These resting or ramified microglia have highly motile processes which scavenge their local surroundings for cellular debris and various other metabolic products and phagocytose these substances [31]. They have also been found to be important regulators of neuronal differentiation as well as synapse modification [32]. The microglial cells play an important role in immune and inflammatory response in the retina. They express receptors such as toll like receptors, scavenger receptors, cytokine and chemokine receptors, as well as MHC receptors. Expression of receptors such as the toll like receptors mediates their response to lipopolysaccharide, bacteria and viruses. They also express fractalkine receptors CX3CR and CCR which are required for normal physiological

functions. Activation of these receptors due to invading pathogens or neuronal injury mediates the release of chemokines, cytokines and other inflammatory factors [33].

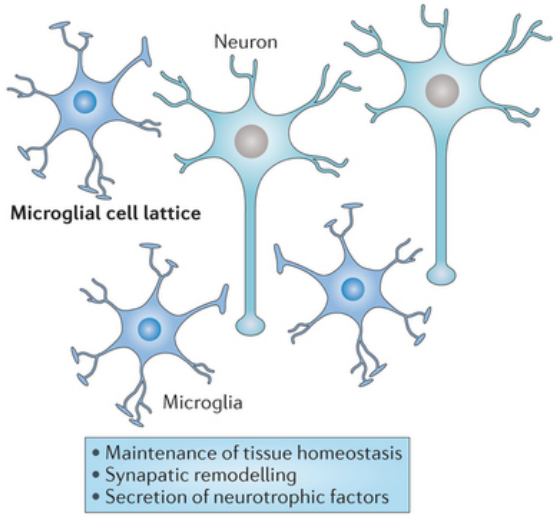

Fig. 1.6. Functions of microglia. Resting microglia constantly survey their surroundings and are involved in debris removal via phagocytosis, secretion of neurotrophic factors and secretion of neurotrophic factors as well as mediating synaptic remodeling [24].

During development the microglia have been shown to play a role in neuronal survival by secreting factors such as insulin like growth factor-1 (IGF-1), phagocytosis of immature/degenerating ganglion cells via the activation of triggering receptor expressed on myeloid cells-2 (TREM2) or fractalkine signaling, and in synaptic pruning [34–37]. Evidence suggests that the microglia, in addition to the macroglia, play a role in angiogenesis. Microglial cells have been shown to recognize the capillary forming tip cells, and subsequently aid in branching and new vessel formation. While mice lacking microglia did show decreased vascular branching in the retina and CNS during development, the vasculature recovered as development progressed indicating the microglia facilitated, but are not essential to branching [38]. Alternately, injection of microglia in damaged retinas has been shown to promote vascular repair [39]. Microglia are a highly dynamic cell. In their resting state, confocal microscopy has

revealed their processes to be in constant motion, surveying the surroundings. This constant surveillance of the surrounding environment is aimed at maintaining homeostasis through absorption of cellular debris, uptake of excess neurotransmitter, and regulating synaptic activity [40].

1.6 Reactive gliosis

Reactive gliosis is a stereotypical response characteristic of astrocytes and Müller glial cells following injury or during disease that is accompanied by loss of function, growth factor expression, hypertrophy, extracellular matrix remodeling, de-differentiation, and proliferation (Figure 1.7). Reactive glia are observed in many states of central nervous system (CNS) injury such as ischemia, trauma, hypoxia and neurodegenerative diseases such as Alzheimers disease [41]. In the eye, retinal gliosis is observed in all forms of retinal injury or disease such as glaucoma, diabetic retinopathy, photic damage, ischemia and retinal trauma [42].

The hallmark of reactive gliosis is hypertrophy due to increase in the intermediate filament glial fibrillary acidic protein (GFAP). Protective and regenerative responses of astrocytes and Müller glia involve, among others, the production of neurotrophic factors, the release of antioxidant agents, the uptake of excess glutamate, the restoration of the bloodbrain barrier, the promotion of neovascularization and remyelination, and the support of axonal regeneration and synaptic remodeling. These responses from the glial cells can be described by a wide range of molecular changes in the glial cells. These include regulation of intermediate filaments such as vimentin and GFAP; extracellular matrix molecules such as chondroitin sulfate proteoglycans (CSPGs) and matrix metalloproteinases (MMPs); enzymes regulating oxidative stress such as nitric oxide synthase; growth factor production; calcium binding proteins such as S100β; glial components involved in neurotransmitter regulation such as glutamine

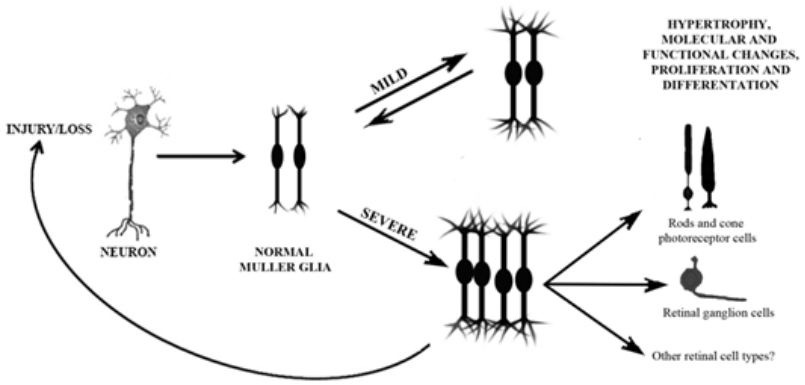

Fig. 1.7. Reactive gliosis in the Müller glia. Damage/loss of neurons due to an injury or disease induces Müller glia to undergo molecular and functional changes, a response classified as reactive gliosis or activation. In mild injuries, the changes in the Müller glia are transient and the cells revert back to the normal/resting stage upon removal of the stimulus. In severe injuries, the cells also undergo proliferation, de-differentiation and mediate changes to the extra cellular matrix leading to formation of a glial scar. They also secrete factors which can exacerbate the damage/loss to retinal neurons [3].

synthetase and EAAT; inflammatory regulators such as cytokines; molecules involved in fluid and ion homeostasis such as aquaporins and Kir channels; and transcriptional regulators such as nuclear factor kappa-light-chain-enhancer of activated B cells (NF-κB) and SMADs. These changes are stimulus dependent and response observed may be any combination of the above changes [43, 44].

Gliosis is an injury dependent response and in cases of widespread damage, glial cells can also remodel the extracellular matrix leading to the formation of a glial scar. The glial scar is a physical barrier which permanently sequesters the injured tissue from neighboring healthy tissue, as well as secretion of factors which can prevent axon regeneration [41, 45]. They also secrete inflammatory factors such as tumor necrosis factor alpha (TNF-α), interleukin-1 beta (IL-1β) and IL-6, which can lead to chronic inflammation via microglia activation, and can further exacerbate the gliosis response [46,47]. Further, increased Müller cell proliferation in severe or chronic reti-

nal damage leads to loss of its functional properties, for example due to reduction of Kir channels, which could be detrimental to the neuronal function and survival [48]. A very small percentage of reactive Müller glial cells have also been shown to re-enter the cell cycle, become proliferative and express progenitor markers under certain conditions [49].

The initial gliosis response of macroglia is essential to protect the neurons from further damage. Release of neurotrophic factors such as leukemia inhibitory factor (LIF) and ciliary neurotrophic factor (CNTF), antioxidants such as glutathione, uptake of excess glutamate and release of nitric oxide serve to increase neuronal survival and prevent oxidative and excitotxic damage to the neurons. Secretion of inflammatory cytokines and chemokines serve to attract microglia to the site of injury to aid in phagocytosis of cellular debris, thereby, indirectly protecting the retinal tissue. However, at the later stages or if the injury is more severe, gliosis becomes detrimental to retinal tissue. As previously stated, severe gliosis can lead to formation of a glial scar and increased production of inflammatory factors. Prolonged expression of factors such as vascular endothelial growth factor (VEGF), inflammatory markers and NO, which initially serve to be protective, now lead to detrimental effects on the neurons. Excessive VEGF can lead to vascular leakage and neovascularization. While low concentrations of nitric oxide (NO) protect the neurons against glutamate excitotxicity, increased NO production can lead to oxidative damage of neurons [45, 50]. In this state, some Müller cells also undergo proliferation and de-differentiation. This leads to loss of supportive functions such as reduced glutamate, ion and water uptake, increasing the susceptibility of neurons to damage [51].

1.7 Microglia activation

Microglia in response to pathogen invasion, tissue damage, disease or injury undergo a change in the morphology as well a change in expression of various markers. This response is termed microglial activation. Microglial activation is observed in many retinal diseases including retinitis pigmentosa, glaucoma, age related macular degeneration and in diabetic retinopathy, to name a few. The activated microglia change from a ramified morphology to a more amoeboid shape, exhibit enhanced proliferation and migration (Figure 1.8). Primarily, active microglia exhibit increased levels of cytokine such as TNF-α, interferon gamma (IFN-γ), interleukins, chemokines such as chemokine ligand 2 (CCL2 or monocyte chemoattractant protein 1 MCP1), CCL5 (RANTES) and growth factors such as macrophage colony stimulating growth factor (M-CSF/CSF), granulocyte macrophage colony stimulating factor (GM-CSF) and transforming growth factor-beta1 (TGF-β1) [52–54].

Expression of these factors serves to aid in migration of the microglia to the tissue damage site as well as induce the inflammatory response. Depending on the expression of markers, the activated microglia are further classified into the classically activated M1 phenotype or the alternatively activated M2 phenotype. The M1 phenotype is characterized as the response of microglia resulting in: upregulation of primarily pro-inflammatory cytokines such as TNF-α, IL-1β, and IL-6, increased production of reactive oxygen species and upregulation MHC proteins to serve as antigen presentation cells [55]. The M2 phenotype, however, is primarily ascribed to the tissue repair and anti-inflammatory function of the microglia. Upregulation of anti-inflammatory cytokines such as IL-10, IL-18, extracellular matrix proteins such as YM1, ornithine to promote wound repair and receptors such as TREM2 which aides in debris clearance [56].

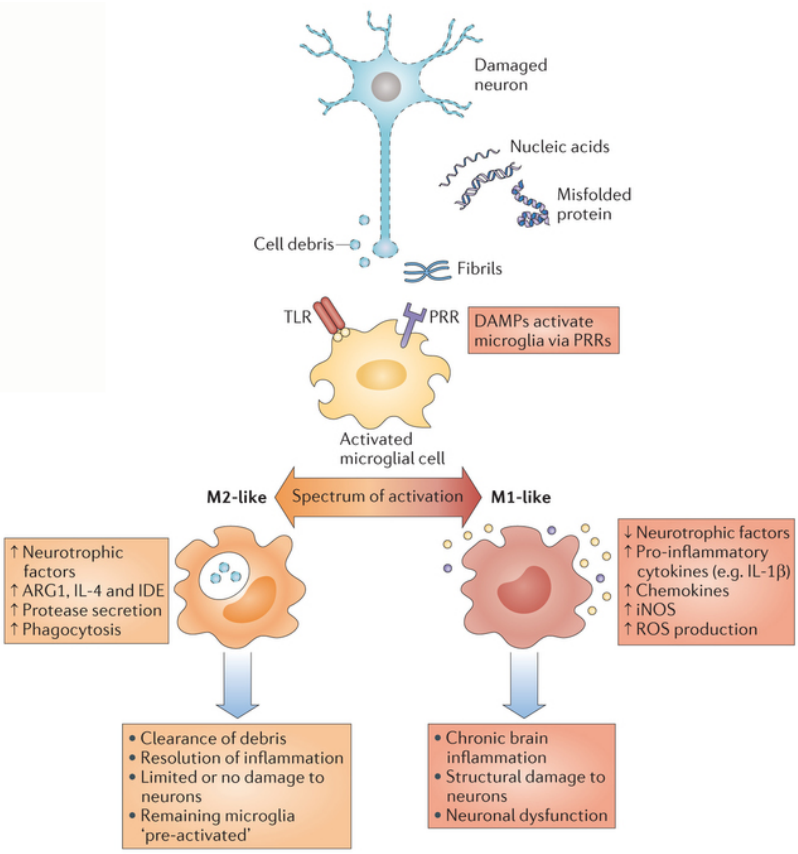

Fig. 1.8. Changes in microglia following activation. Diagramatic representation of changes to the microglia following activation. Microglia can be activated into a pro-inflammatory M1 state or an anti-inflammatory M2 state [24].

1.8 Müller glia and microglia interaction in the retina

Reactive gliosis and microglia activation are responses seen in the retina in various disease and injury models. Furthermore, studies characterizing the glial responses have revealed close association between the two cell types. For example, in the normal retina, microglia morphology and motility of the processes regulated by ATP released from the Müller glia, which in turn is regulated by extracellular glutamate levels [57, 58]. These signals thus, constitute a mode of communication between the Müller glia and the resting microglia in the normal retina. Similarly in the injured retina, signals from activated microglia can potentially affect the state of the Müller

glia, and vice versa. Wang et al., 2011 showed Müller cells respond to microglia activated through exposure to lipopolysaccharide (LPS), increased expression of neuron survival factors such as GDNF and LIF [59]. These cells also increased expression of inflammatory markers such as IL-1β and IL-6, which in turn was able to able to activate resting microglia. Similarly, in a study modeling neurodegeneration *in vitro*, astrocytes were showed to be essential for microglial activation [60].

Factors such as TNF-α, inducible nitric oxide synthase (iNOS), IL-1β have been identified as potential factors which could be playing a role in the interaction between the two glial populations [61]. While microglia derived factors have been shown to trigger gliosis in the macroglia, the pro-inflammatory factors derived from astrocytes/Müller glia could contribute to the chronically active microglia, which can cause further damage to the neural tissue [62]. Furthermore, changes to the extracellular matrix by reactive macroglia can also trigger activation of microglia leading to a prolonged inflammatory response, which is detrimental [63]. However, astrocytes have been shown to negatively regulate microglia activation through TGF-β signaling by downregulating expression of pro-inflammatory cytokines and antigen presentation markers [64].

1.9 Factors in gliosis

Many factors have been identified which could trigger reactive gliosis including reactive oxygen species, hypoxia, growth factors such as CNTF and LIF; and factors associated with inflammatory response such as TNF-α and IFN-γ (Figure 1.9) [3]. The breakdown of the blood retinal barrier (BRB), observed in most of the retinal diseases, has been determined to be the major cause for loss of vision and reactive gliosis. Oxidative stress, hypoxic and hyperglycemic conditions in diabetic retinopathy, glaucoma, AMD, retinitis pigmentosa (RP) etc. lead to breakdown of the BRB, which in turn cause an upregulation of inflammatory cytokines and chemokines, as

well as factors such as CNTF, LIF and vascular endothelial growth factor (VEGF). These signals regulate gliosis either on their own or in combination with other factors.

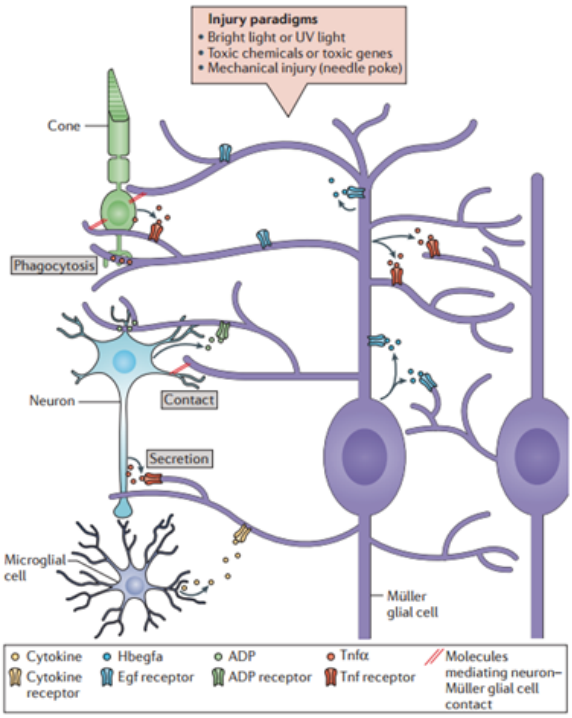

Fig. 1.9. Known factors regulating gliosis. Gliosis has been described in all retinal injuries and disease conditions. Factors which trigger gliosis include: mechanical injury, an increase in inflammatory markers, reactive oxygen species as well as factors such as CNTF [65].

TNF-α has been shown to upregulate GFAP expression in astrocytes through mitogen associated protein kinase (MAPK) signaling [66, 67]. It has also been shown to upregulate expression of other inflammatory cytokines such as IL-1β, IFN-γ and TNF-α, from the glial cells [59]. Similarly, IFN-γ and IL-1β have been shown to regulate expression of inflammatory cytokines as well as GFAP levels in the macroglia. CNTF regulates a wide range of gliosis markers in astrocytes and Müller glia primarily via the janus kinase-signal transducer and activator of transcription (JAK-STAT) pathway. These include growth factors and cytokines such as TGF-β and TNF-α, GFAP and other genes such as S100β, lipocalin-2 and ion channels, previously shown

to be regulated in gliosis [68]. Fischer et al., 2004 demonstrated the effect of different factors on retinal gliosis in the chick retina. While CNTF induced an upregulation of GFAP in the Müller glia, FGF2 induced vimentin upregulation [69]. In the zebrafish retina, IL-6 has been shown to induce proliferation of Müller glia via the JAK-STAT pathway [70]. Platelet derived growth factor (PDGF) has also been shown to influence retinal macroglia. Yamada et al., 2000 demonstrated that PDGFA induced astrocyte migration, GFAP upregulation as well release of factors such as insulin like growth factor (IGF) and VEGF in the macroglia [71]. TGF-β, another factor regulated during gliosis has been shown to influence the extracellular matrix composition, inducing expression of chondroitin sulphate proteoglycans (CSPGs) via the SMAD independent AKT-mTOR pathway [72].

1.10 Bone morphogenetic proteins (BMP) in the retina

The BMPs consist of a large number of signaling molecules belonging to the TGF-β superfamily. The BMP ligands signal primarily by forming homo- or hetero-dimers, which then bind to the receptor associated proteins. The BMP receptors are serine threonine kinase receptors, classified into 2 groups: the type I and type II receptors. The BMP type I receptors act downstream of the type II receptors and determine the specificity of the signal. Three type I (Alk -2, -3 and -6) and type II (BMPRII, ActR II A and ActR II B) receptors have been identified which bind BMP ligands. While the BMP ligands have specificity to certain receptors, for example Alk1 for BMP9 and Alk2 for BMP7, they bind with lower affinity to other receptors and mediate their downstream pathways [73]. Binding of the ligand leads to phosphorylation and activation of the receptors, which then phosphorylate the receptor-bound signaling mediators (Figure 1.10). The BMPs signal canonically via the SMAD pathway and non-canonically via the TAB-TAK pathway or FRAP-STAT pathway. Binding of ligand to the receptor leads to activation of the bound mediators: SMADs (SMAD

-1, -5 and -8), x-linked inhibitor of apoptosis (XIAP) protein and the immunophilin FKBP12. Upon BMP activation, the SMADs are phosphorylated and dimerize with SMAD4, and are then translocated to the nucleus to bind to specific sequences in the DNA, bringing about transcriptional regulation of target genes. XIAP leads to the formation of a XIAP-TAB1-TAK1 complex, activating the MAPK pathway, while phosphorylation of the FKBP12 protein activates the FRAP (FKBP12 rapamycin associated protein) molecule which then activates and phosphorylates STAT leading to transcriptional regulation [74, 75].

Spinal cord and retinal injury models have shown an upregulation of BMPs (4 and 7) at the injury site, as well as an increase in phospho SMAD 1/5/8 in glial cells in the retina [77, 78]. BMP4 regulates survival of amacrine neurons and proliferation of Müller glial cells in a retinal injury model [79]. BMP7 has been found to be neuroprotective in spinal cord injury models in rats and activation of the SMAD pathway in murine retinas following injury has been shown to promote the survival of the ganglion neurons [78,80]. Furthermore, the opposing effect of activation of 2 different BMP receptors on gliosis has also been determined by Sahni et al,. 2010 [81]. Thus, the BMPs are implicated to be regulated during gliosis, although the mechanism and effects are not fully understood. Furthermore, the crosstalk between the downstream signaling components of the canonical and non-canonical pathways with each other or other pathways may be involved.

1.11 Hippo pathway and role in gliosis

While gliosis has been universally described in disease and injury states of the central nervous sustem, it is unclear at this time whether the factors that regulate gliosis act through a common mechanism to trigger de-differentiation. Part of this dissertation is directed at the hypothesis that angiomotins and the Hippo pathway may be a com-

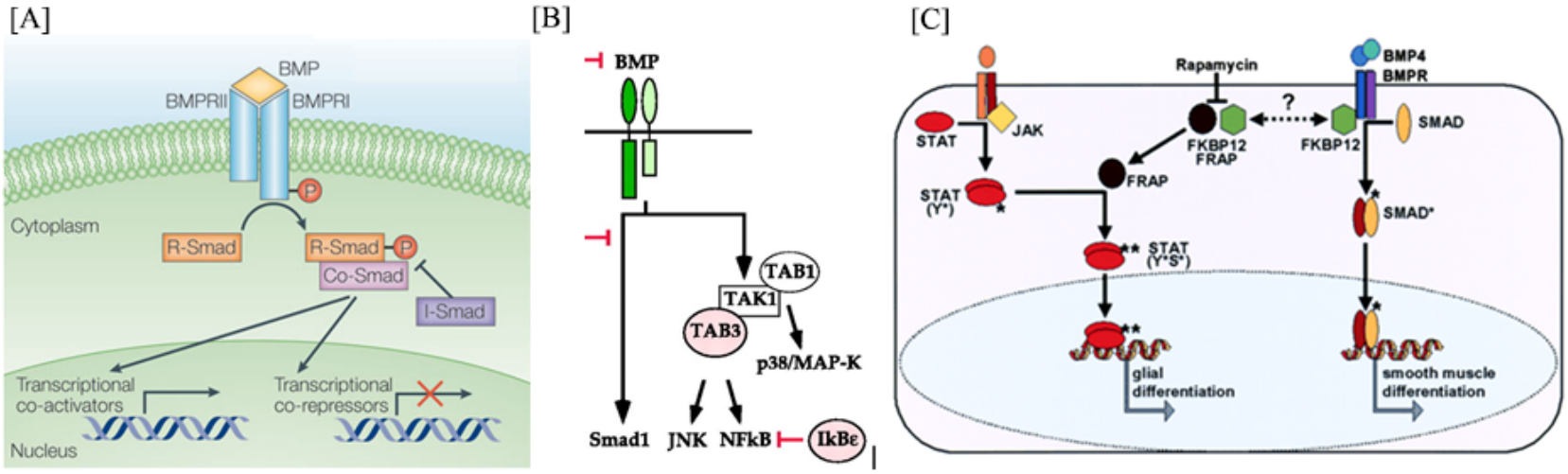

Fig. 1.10. BMP pathway: canonical and non-canonical signaling. (A) Canonical BMP signaling mediated by binding of BMP ligand to its receptor which activates the signaling cascade through the receptor bound SMAD. (B) BMP signaling activates TAB1 which phosphorylates and activates TAK1, which in turn activates p38 and MAPK leading to transcriptional regulation, (C) Binding of BMP ligand to the receptor leads to the activation of receptor bound FKBP12, which dimerizes with FRAP and phosphorylates/activates FRAP leading to transcriptional regulation [74, 76].

mon mechanism by which external signals trigger de-differentation that accompanies gliosis. The Hippo pathway is known to be an important regulator of tissue formation and organogenesis by regulation of proliferation, growth and differentiation. Activation of upstream regulators, primarily found in apical junction, leads to activation of the core kinases of the hippo pathway, MST1/2 and Lats1/2 (Figure 1.11). Regulators of the core kinases of the hippo pathway include apical and basal junction proteins such as neurofibromatosis 2 (NF2), scribble and crumbs, as well as proteins associated with the cytoskeleton such as E-cadherin, α-catenin and angiomotins (AMOT), growth factors such as EGF and G-protein coupled receptors [82,83]. When activated, these regulators activate MST kinases which in turn activate the LATs kinases. The activated core kinases phosphorylate the yes activated protein (YAP) and leads to its cytoplasmic localization. In the unphosphorylated state, YAP is localized to the nucleus, and along with co regulator transcriptional co-activator with PDZ-binding motif (TAZ). Within the nucleus, it binds with the transcription factor transcriptional enhancer associate domain (TEAD) and brings about regulation of target genes in the cell [84]. The YAP/TAZ complex has also been shown to bind to other transcription factors such as SMAD and RUNX to mediate transcriptional regulation. In the nucleus, the primary targets of the YAP/TAZ/TEAD complex include growth promoting and anti-apoptotic genes such as connective tissue growth factor (CTGF), Sox4, c-Myc and baculoviral IAP repeat containing protein (BIRC), proteins involved in regulation of cell cycle such as cell division cycle 6 (CDC6), protein c-ets1 (ETS1) and kinesin family member 23 (KIF23) [85].

As mentioned in the previous section, one of the factors regulating Hippo/YAP pathway are the AMOTs. The AMOTs were initially identified for their role in endothelial cell migration and angiogenesis. The AMOTs consist of a PPXY protein interaction motif and a WW binding motif in the N terminal domain, a coiled-coiled domain and a C-terminal PDZ binding motif [87]. AMOTs have been shown to interact with tight junction proteins Merlin and Rich1 to maintain tight junction integrity [88].

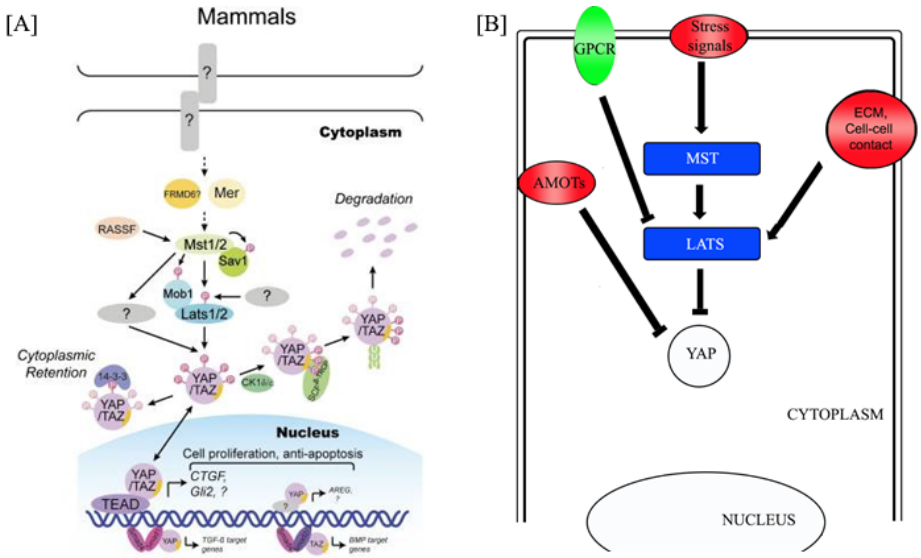

Fig. 1.11. Hippo pathway and its regulation. (A) Hippo pathway cascade is mediated by a core of kinases (MST1 and LATs1) which phosphorylate YAP. When hippo pathway is turned on, YAP is phosphorylated and sequestered to the nucleus and in the absence of signal, the unphosphorylated YAP translocates to the nucleus regulating target genes by binding to the TEAD co-factor. (B) The Hippo pathway is regulated angiomotins, extra-cellular matrix, stress signals and G-protein coupled receptors [86].

The AMOTs also interact with YAP via the PPXY motif to sequester YAP to the cytoplasm and inhibiting it. Furthermore, AMOTs can also inhibit YAP by activating LATs and MST through an unknown mechanism, which can phosphorylate and inhibit YAP [86].

Research has shown that Hippo pathway components are involved in cross talk with other signaling pathways including the Wnt pathway, TGF-β/BMP pathway, EGF signaling and Notch signaling [84, 89]. YAP/TAZ complex can inhibit and promote Wnt signaling. Cytoplasmic YAP/TAZ sequester β-catenin and SHP2 to the cytoplasm due to phosphorylation, thereby, inhibiting Wnt signaling [90, 91]. However, Xin et al,. 2011 showed that nuclear YAP can upregulate IGF signaling which in

turn leads to activation of β-catenin and the Wnt pathway [92]. Alcaron et al,. 2009 showed YAP mediated SMAD regulation of transcription activity in mouse embryo development [93]. Furthermore, BMP4 and TGF-β are known targets of YAP/TAZ complex. Similarly, YAP/TAZ/TEAD complex also regulates notch signaling by up-regulating transcription of Jag1, Notch 2 and Sox9 [94]. Thus, the hippo pathway appears to be a key regulator of cellular homeostasis and has the potential to regulate multiple pathways in the cell.

The aim of this dissertation is to expand the understanding of retinal gliosis by addressing the following hypothesis: BMP7 triggers a response gliosis in the retina by regulating activation of the glial cells. We further propose that regulation of the Hippo pathway during gliosis may be a common pathway that links this response following different stimuli and that it mediates the de-differentiation response of the Müller glia. We propose to address these questions through the following aims: 1) Determining the effect of BMP7 on the retinal macroglia, 2) Determining the effect of BMP7 on the microglia and potential cros-talk with the macroglia, and 3) Determining the regulation of the Hippo/YAP signaling in retinal gliosis.

2. BONE MORPHOGENETIC PROTEIN 7 REGULATES REACTIVE GLIOSIS IN RETINA ASTROCYTES AND MÜLLER GLIA

2.1 Introduction

The mature mammalian retina contains several types of macroglial cells; Müller glia, retinal astrocytes, and, in some cases oligodendrocytes and non-astrocytic retinal glial cells (NIRG) [95–97]. The Müller glia arise from neural retinal progenitor cells late in retinal development. The Müller cells span nearly the entire width of the retina from the outer limiting membrane, where Müller processes form connections with photoreceptors, to the inner limiting membrane where Müller and retinal astrocyte processes form the boundary between the retina and the vitreous [17]. The retinal astrocytes migrate into the retina from the developing optic nerve and their cell bodies populate the nerve fiber layer and send processes into the ganglion cell layer [13]. While the NIRG cell origins are unknown, they have been hypothesized to migrate from the developing optic nerve [96]. Both the Müller glia and retinal astrocytes have been shown to play very important roles in supporting and protecting the retinal neurons. For instance, both are critical to the formation of the blood-retinal barrier, neurotransmitter recycling, removal of toxins, and growth factor supplementation of ganglion cells [11, 46, 98–100].

An important property of the glial cells is their response to any damage/injury to nearby neurons; a response known as reactive gliosis. The Müller glia and, retinal, and optic nerve astrocytes become reactive in various disease states such as glaucoma, retinal ischemia, and diabetes [50, 101]. One particularly interesting aspect of gliosis is the molecular diversity in the reaction of the macroglia to various disease

states and injuries [44, 69, 102]. For instance, insult-dependent increase or decreases in the expression of glial fibrillary acidic protein (GFAP), vimentin, glutamine synthetase (GS), and extracellular matrix molecules (ECM) have been noted in Müller glial cells and/or astrocytes [50, 103–105]. This variance has been hypothesized to be the result of the release of various factors that drive different aspects of reactive gliosis [43, 69, 106]. Further diversity in the response is introduced by virtue of the fact that reactive astrocytes fall on a continuum from mild to severe, in which cells display one or more of the following; hypertrophy, de-differentiation, loss of function, proliferation, inflammation, and remodeling of the tissue and vasculature [3, 107]. Furthermore, some of the cellular responses are dual in nature. An example of this is the hypertrophy of Müller glia and astrocytes that results from an increase in the intermediate filaments GFAP and vimentin. On one hand the hypertrophied cellular processes may form a barrier around the injured region, inhibiting the spread of inflammatory molecules into healthy tissue; on the other hand, these processes can also block the regeneration of axons and synapses [107].

Severe reactive gliosis is also accompanied by tissue remodeling that includes excessive hypertrophy of the glial cell bodies and processes as well as the turnover of the extracellular matrix to a regeneration-inhibitory matrix, together referred to as a glial scar. One of the major components of the ECM are the chondroitin sulfate proteoglycans (CSPGs), a family of molecules that includes neurocan (NCAN), phosphacan (PCAN), versican, aggrecan, brevican, nerve/glial antigen 2 (NG2), and CD44 [108]. Although the mechanisms and triggers have not been completely characterized, a variety of growth factor signaling mechanisms are found to be important in reactive gliosis such as epidermal growth factor (EGF), fibroblast growth factor (FGF), tumor necrosis factor-α (TNF-α), ciliary neurotrophic factor (CNTF), insulin and WNTs [43, 107, 109]. Data from several laboratories have indicated that each pathway may regulate specific characteristics associated with reactive gliosis. For instance, CNTF appears to be associated with the upregulation of GFAP, while

EGF and FGF are associated with proliferation [104, 110]. Studies using different CNS injury models have shown that the BMP pathway is upregulated at the site of injury in the CNS and can trigger reactive gliosis [77, 111, 112]. Furthermore, BMP receptor 1A has been linked to hypertrophy, whereas BMPR1b has been associated with glial scars [81]. While the BMPs have been associated with penetrating wounds in the spinal cord, no information is available regarding the role of BMPs within the retina and in disease states of the CNS.

BMPs interact with two different types of receptors; type I and type II, both of which are serine-threonine kinases. The type II receptors phosphorylate and activate the type I receptors, and the type I receptors then can activate several intracellular pathways. The intracellular pathways are subdivided into different pathways, the canonical pathway and several non-canonical pathways [75]. The canonical pathway consists of the activation of receptor SMADs (R-SMADs) 1, 5, and 8 by the type I BMP receptors. Once activated, the R-SMADs form heterodimers with the co-SMAD, SMAD4, whereupon they localize to the nucleus to interact with other transcription factors and regulate gene expression. BMP receptors type IA and IB have also been shown to activate X-chromosome-linked apoptosis protein (XIAP). XIAP connects the BMPRIA and IB to the kinase Transforming growth factor -β activated kinase 1 (TAK1), which activates downstream pathway members such as p38, Nuclear factor kappa light chain enhancer of activated B cells (NFκB), and c-Jun N-terminal kinases (JNK) [113]. Another non-canonical pathway that has been identified is the FKBP12/rapamycin associated protein - signal transducer and activator of transcription (FRAP-STAT) pathway. Activation of this pathway occurs via phosphorylation of FK506 rapamycin binding protein (FKBP12) by BMPR IA and/or IB, eventually leading to the activation of STAT proteins, leading to changes in transcription [74].

In this study, we hypothesized that BMP7 plays a role in initiating reactive gliosis in glial cells of the retina. As a first step, we characterized the BMP receptors and

intracellular signaling molecules present in the Müller glial cells of normal adult uninjured retina. Using *in vitro* systems, we observed differential regulation of molecules typically associated with reactive gliosis in retinal astrocytes and human Müller glial cells following treatment with BMP7. Both retinal astrocytes and MIO-M1 Müller cells showed modest increased *Gfap* and *Pax2* levels following treatment with BMP7, but only retinal astrocytes appeared to show changes in matrix metalloproteinases (Mmps) and CSPGs. In contrast, addition of BMP4 *in vitro* appeared not to lead to reactive gliosis in either retinal astrocytes or MIO-M1 Müller glial cells. Injection of BMP7 into the mature mouse eye led to more robust increases in molecules associated with reactive gliosis, such as *Gfap, Pax2, Mmps*, and CSPGs *Ncan* and *Pcan*. These results are consistent with the hypothesis that BMP7 acts as a trigger for reactive gliosis in disease states in the eye.

2.2 Materials and methods

2.2.1 Tissue Processing and Fluorescent Immunohistochemistry

Eyes from C57BL/6J (Jackson Laboratories, Bar Harbor, ME) were dissected from the heads of euthanized animals, washed in phosphate buffer saline (PBS; 40mM K2HPO4, 123.2mM NaCl, 8.4mM NaH2PO4; Fisher Scientific, Pittsburgh, PA), and fixed in 4% paraformaldehyde (Fisher Scientific) for immunohistochemistry. The eyes were then incubated in an ascending series of sucrose (Fisher Scientific) (5%, 10%, 15% and 20%) made in 0.1M phosphate buffer, pH 7.4 overnight. The tissues were frozen in a 3:1 20% sucrose-in phosphate buffer and OCT solution (Sakura Finetek Inc., Torrance, CA). Thick sections (10 μm) were cut using a Leica CM3050 S cryostat and placed on Superfrost Plus slide (Fisher Scientific) treated with Vectabond (Vector Labs, Burlingame, CA), and were stored at -80°C until used for immunohistochemistry. Antibodies used for immunohistochemistry are listed in Table 2.1.

For immunohistochemistry, sections were fixed with 4% paraformaldehyde for 30 min. Sections were then washed in 1X PBS, permeabilized in methanol (Fisher Scientific) and subjected to antigen retrieval by placing the sections in 1% SDS (Fisher Scientific) in 0.01 M PBS for 5 min. To aid in autofluorescence reduction, sections were treated with 1% sodium borohydride in PBS (Fisher Scientific) for 2 min at room temperature, then rinsed with PBS. Tissue was blocked by incubating with 10% serum in 1X PBS containing 0.25% Triton X-100 (Bio-Rad, Hercules, CA) at room temperature for 1 h and incubated with the primary antibody, diluted in 0.025% TritonX-100 PBS with 2% blocking serum, overnight at 4°C. The following day, the slides were incubated in Dylight conjugated secondary antibody (Jackson Immunoresearch, West Grove, PA) at 1:800 diluted with 1X PBS, for 1 h at room temperature, then washed twice with 1X PBS for 5 min each rinse, and mounted with ProLong Gold with DAPI (Invitrogen, Grand Island, NY) or counterstained with Hoechst solution (diluted 1:500 in 1X PBS; Sigma-Aldrich, St. Louis, MO) and mounted with AquaPoly/Mount (Polysciences, Warrington, PA).

Table 2.1.
List of antibodies used

Antibody	**Company**	**IHC concentration**	**Western blot concentration**
ALK2	Genetex	1:250	
βTubulin	Sigma		1:1000
BMPR1A	Abgent	1:50	
BMPR1B	SantaCruz	1:100	
FKBP12	ThermoScientific	1:100	
GFAP	Dako (polyclonal)	1:250	
GFAP	Dako (monoclonal)		1:1000
NEUROCAN	R&D	1:100	
PAX2	Aviva		1:500
phosphoSMAD 1/5/8	Cell Signaling	1:50	
phosphoTAK	Abcam	1:500	
S100β	Abcam	1:300	1:1000
SMAD1	Abcam	1:100	
SOX2	SantaCruz	1:250	
TAK1	Abcam	1:250	
TXNIP	SantaCruz	1:250	

For labeling of mouse tissue slides with glutamine synthetase (GS), blocking and overnight incubation with primary antibody was performed as specified by the Vector mouse-on-mouse immunodetection kit (Vector Labs). For immunolabeling with NCAN, SMAD, BMP receptor 1A, 1B and TAK1, biotin streptavidin amplification was performed. Following overnight incubation with the primary antibody, the sections were first incubated with biotinylated antibody (1:1000, Vector Labs) for 1 h and then streptavidin conjugated Dylight (1:33, Vector Labs) for 1 h at room temperature. For colabels of phospho-SMAD1/5/8 and phospho-TAK1 with sex determining region Y box 2 (SOX2), sections were subjected to heat antigen retrieval following methanol incubation. Briefly, the sections were incubated in sodium citrate buffer (10mM sodium citrate; Fisher Scientific, 0.05%Tween 20; Fisher Scientific, pH 6.0) at 65°C for 1 h, allowed to cool for 20 min, rinsed 3X in water, 1X in PBS and blocked with 10% horse serum in 1X PBS containing 0.25% Triton X-100 for 1 h at room temperature. Following overnight incubation with the primary antibodies, the slides were incubated with biotinylated horse anti rabbit (1:300, Vector Labs) for 1 h and then Alexa flour anti goat (1:500, Invitrogen) and HRP (1:500, Biolegend, San Diego, CA) for 1 h. The slides were then washed 2X in TNT buffer (0.1M Tris-HCl, 0.15M NaCl, 0.05%Tween 20) and incubated with fluorescin plus amplification reagent diluted 1:300 in 1X tyramide signal amplification (TSA) amplification diluent (Perkin Elmer, Waltham, MA) for 5 min. The slides were washed 2X in TNT buffer, 2X in PBS, counterstained with Hoechst solution and mounted with Aqua-Poly/Mount (Polysciences). Slides were viewed under Olympus Fluoview FV 1000 confocal microscope.

2.2.2 Isolation of RNA and protein

Isolated retinas were processed and used for RT-qPCR and western analysis. Briefly, animals were euthanized by CO_2 exposure. Eyes were then dissected using sterile

forceps and the retina isolated. The retinas were homogenized and processed for RNA using RNeasy Mini Kit as per manufacturers protocol (Qiagen, Valencia, CA). Briefly, isolated retinal tissue or cells were homogenized in buffer RLT. 70% ethanol was added and the solution centrifuged in a RNeasy spin column. The flow through was discarded, 700μl of buffer RW1 was added and centrifuged. Following this step, 500μl of buffer RPE was added to the spin column and centrifuged. This step was repeated once, following which the RNA was eluted with 40μl of RNase free water. RNA was quantified using NanoDrop 2000c (ThermoScientific, Rockford, IL).

For protein isolation, retinas isolated were homogenized and incubated with radioimmunoprecipitation assay (RIPA) lysis buffer (0.1%SDS, 50mM Tris-HCl pH 7.5, 1% Triton-X100) supplemented with 0.01mM phenyl methyl sulfonyl fluoride (PMSF; Roche Diagnostics, Indianapolis, IN) and 1:25 protease inhibitor cocktail (RPI Corp, Mount Prospect, IL) for 2 h at 4°C. The tube was then centrifuged at 13680 g for 20 min at 4°C and the supernatant aspirated into a new tube.

2.2.3 Cell Isolation, Cytospin, and Immunocytochemistry

Retinal cells were isolated as previously described [114]. Briefly, mouse retinas were prepared in sterile 0.9% saline. Approximately 200 mg of retinal tissue was incubated with saline containing 0.4 mg/ml papain (Roche) for 30 min at 37°C. The tissues were triturated with a siliconized pipette and dissociated single cells were centrifuged at 500 X g for 10 min. The cells were fixed in 4% paraformaldehyde for 10 min, centrifuged, and washed with saline. The cells were placed onto a Superfrost Plus slide (Fisher Scientific) treated with Vectabond (Vector Labs) using a Cytospin4 (Thermoscientific) and stored at -80°C until used for immunocytochemistry. For immunocytochemistry, the cells were permeabilized in methanol, incubated with 1% SDS in 0.01M PBS, and washed in 1X PBS. The slides were then incubated with 1% sodium borohydride,

blocked using the mouse on mouse kit (Vector Labs), and co-labeled with GS and the BMP receptor antibodies (BMPR1A, BMPRIB and activin receptor like kinase 2; ALK2). Following overnight incubation with the primary, the slides were incubated with the appropriate secondary antibodies with biotin streptavidin amplification used for the receptor antibodies. The slides were then washed, counterstained with Hoechst solution, and mounted with Aqua-Poly/Mount (Polysciences).

2.2.4 Cell culture

The mouse retinal astrocytes were isolated as previously stated [115, 116]. Cells were cultured in DMEM (Catalogue # D1152, Sigma-Aldrich, St. Louis, MO) containing EC growth supplement (Sigma-Aldrich), 1% Pencillin/Streptomycin (Sigma-Aldrich), 1 mM Sodium pyruvate (Life Technologies, Grand Island, NY), 20 mM HEPES (Sigma-Aldrich), 2 mM Glutamine (Life Technologies), 1x non-essential amino acids (Sigma-Aldrich), Heparin (Sigma-Aldrich), 10% fetal bovine serum (Atlanta Biochemicals, Lawrenceville, GA) and 44U/ml of murine recombinant interferon γ (R & D systems, Minneapolis, MN). The cells were grown on Cellbind dishes (Fisher Scientific) in an incubator with 5% CO_2 at 33°C and passaged every 3-4 days using trypsin-EDTA (Sigma-Aldrich). The human MIO-M1 Müller glial cell line was obtained from Dr. GA Limb at the Institute of Ophthalmology, University College London (Limb, Salt, et al. 2002). MIO-M1 cells were grown in DMEM containing 10% fetal bovine serum and 200 mM Glutamine (Life Technologies). The cells were grown in sterilized tissue culture dishes (BD Falcon, Corning, NJ) in an incubator 5% CO_2 at 37°C and passaged every 6-7 days using trypsin-EDTA and the medium changed every 3-4 days.

Treatment of retinal astrocytes and MIO-M1 cultures *in vitro* with sodium peroxynitrite (Cayman Chemicals, Ann Arbor, MI) was performed as previously stated [117]. Briefly, confluent astrocyte cell cultures were washed 3 times with phosphate buffer

saline (PBS) supplemented with 0.8 mM MgCl2, 1 mM CaCl2, and 5 mM glucose. They were then incubated in 1 ml of 1X PBS (50 mM Na2HPO4, 90 mM NaCl, 5 mM KCl, 0.8 mM MgCl2, 1 mM CaCl2, and 5 mM glucose, pH 7.4), followed by three additions of sodium peroxynitrite at a concentration of 0.15 mM. The first bolus of sodium peroxynitrite was added to one edge of the dish and the buffer was swirled to allow mixing of the peroxynitrite throughout the dish. This step was repeated twice while changing the edge at which the addition was made and then incubated for 5 min. The buffer was then removed, replaced with the respective growth medium and placed in the appropriate incubators. The cells were then processed after 32 h for protein or RNA. Some cultures were treated with recombinant BMP7 and BMP4 (R & D systems) reconstituted in 0.4% HCl-PBS. Dishes were treated with either vehicle or 100 ng/ml of BMP7 or BMP4 for 24 or 36 h. Cells were then processed for either RNA or protein for analysis via RT-qPCR or Western blotting, respectively.

2.2.5 BMP7 injections *in vivo*

The mice were injected intravitreally with BMP7 (1 μl of 20 ng/μl). Intravitreal injections were performed with a pump microinjection apparatus (Harvard Apparatus, Holliston, MA) and pulled glass micropipettes. Each micropipette was calibrated to deliver 1 μL of vehicle or vehicle containing BMP7. The mice were anesthetized under a dissecting microscope; the sharpened tip of the micropipette was passed through the sclera, just behind the limbus, into the vitreous cavity. Once the micropipette was in place, the vehicle or BMP7 was injected using a PL-1000 picospritzer (Harvard Apparatus). D3 or D7 post-injection, the animals were sacrificed and retinas were dissected for RNA and protein preparations. Each experiment was performed in triplicate.

2.2.6 Western blot analysis

Antibodies used for western blot analyses are listed in Table 2.1. The total protein was quantified using Pierce BCA Protein Assay Kit (ThermoScientific) as per manufacturers protocol. Briefly, 5μl of sample was mixed with 495μl of working reagent (prepared by mixing Pierce BCA Reagent A and B in 50:1 ratio) and 500μl of water. This solution was incubated at 65°C for 30 min, followed by colorimetric analysis using a NanoDrop 2000c spectrophotometer (Thermscientific). Fifty micrograms of the total protein mixed with the loading dye (containing 5% β–mercaptoethanol) in a 3:1 ratio was then loaded and run on a 4-20% SDS polyacrylamide gel (Expedeon, San Diego, CA) at 125 volts for 1 h. Proteins were transferred to a Polyvinylidene fluoride (PVDF) membrane (Bio-Rad) via a wet transfer and subjected to immunoblotting. Prior to incubation with the antibody, the membrane was blocked using a 5% milk solution in Tris Buffered Saline-Tween (TBST; composition 20mM Tris base, 137mM NaCl, 1M HCl, 0.1% Tween-20, at pH 7.6) for 1 h. The blots were then incubated with the primary antibody diluted in TBST at 4°C overnight. The blots were washed twice with TBST and then incubated with a peroxidase conjugated secondary antibody (ThermoScientific) diluted to 1:5000 in TBST for 1 h in the dark at room temperature. The blots were incubated with either Pierce ECL Western Blotting Substrate (ThermoScientific) or SuperSignal West Femto Chemiluminescent Substrate (ThermoScientific) and the bands visualized on x-ray films (ThermoScientific). β-TUBULIN was used as a loading control and densitometry of the blots was performed using the Image J software (http://rsbweb.nih.gov/ij/).

2.2.7 Real Time-Quantitative PCR (RT-qPCR)

Prior to cDNA synthesis, RNA samples were run on a 1% agarose gel to confirm the overall quality of the total RNA. The cDNA was synthesized from 1 μg of total RNA with iScript cDNA Synthesis Kit (Bio-Rad) according to the manufacturers protocol

and diluted 1:20 before adding to qPCR wells. RT-qPCR was performed using 7300 RT detection system (Applied Biosystems, Carlsbad, CA) using the Power SYBR green PCR master mix (Invitrogen, Grand Island, NY). The primer pairs used have been listed in Table 2.2 (Mouse) and Table 2.3 (Human). Total volume for each reaction was 20 μl using the diluted cDNA, corresponding to 5ng of initial total RNA and 0.4mM of each primer. The cycler conditions used were as follows: initial denaturation at 95°C for 10 min, 45 cycles of denaturation at 95°C for 10 sec, annealing at 60°C for 20 sec and extension at 72°C for 20 sec, followed by a final extension at 72°C for 5 min.

Efficiency of the primer sets was determined by the standard curve method, where efficiency, E= ((10(-1/Ct2 Ct1)) 1) X 100. Primer sets with an efficiency between 90% and 110% were used for our experiments. A no template control and an internal control using primers specific for *β 2 Microglobulin* (*β2M*) were used for each run. The amplified samples were run on a 2% agarose gel to confirm amplification was of the right size. The change in the gene expression levels was done using the $2^{-\delta\delta Ct}$ method, where C_t is the crossing threshold value.

2.2.8 Statistical Analysis

Statistical analysis of RT-qPCR data was by unpaired t-test between the control and treated groups. Statistical analysis of densitometry results was by students t-test. All analyses were performed using SPSS software (IBM) and Excel 2010 (Microsoft).

Table 2.2.
Mouse RT-qPCR primers

Gene	**Primer**	**Sequence**	**Length (bp)**
β2 M	Forward	TCGCGGTCGCTTCAGTCGTC	135
	Reverse	CATTCTCCGGTGGGTGGCGTG	
Ednrb	Forward	TTGACCTCCCCATCAACGTG	140
	Reverse	AGCACAGAGGTTCAAGACGG	
	Reverse	CATTCTCCGGTGGGTGGCGTG	
Gal3	Forward	GGCGGGTGGAGCACTAATC	74
	Reverse	TAAGCGAAAAGCTGTCTGCC	
Gfap	Forward	TAGCCCTGGACATCGAGATCGCC	141
	Reverse	GGTGGCCTTCTGACACGGATTTGG	
Glast	Forward	GATTTGCCCTCCGACCGTAT	185
	Reverse	ATAGACTACAGCGCGCATCC	
Gs	Forward	GCGCTGCAAGACCCGTACCC	145
	Reverse	GGGGTCTCGAAACATGGCAACAGG	
Kir2.1	Forward	GACCCTCCTCGGACCTTACG	151
	Reverse	ACTGGCCGTTCTTCTTGACA	
Lcn2	Forward	AATGTCACCTCCATCCTGGTCA	145
	Reverse	CCACTTGCACATTGTAGCTCT	
Mmp9	Forward	TGTGCCCTGGAACTCACACGAC	135
	Reverse	ACGTCGTCCACCTGGTTCACCT	
Mmp11	Forward	ACTGACTGGCGAGGGGTACCTT	128
	Reverse	GCAGATGGACCCCATGTTTGCTGT	
Mmp14	Forward	TGGGCCCAAGGCAGCAACTT	89
	Reverse	CGTTGTGTGTGGGTACGCAGGT	
Ncan	Forward	CCTGACAAGCGTCCATTCGCCA	90
	Reverse	ACTGTCCGGTCATTCAGGCCGAT	
Pax2	Forward	ACCCTGGCAGGAATGGTGCCT	70
	Reverse	AGGCGGTGTACTGGGGATGGC	

Table 2.2 (Continued)

Gene	**Primer**	**Sequence**	**Length (bp)**
Pcan	Forward	ATCCCTGAGTGGGGAAGGCACA	96
	Reverse	AGCAGGGGATGCTGGGTGATGA	
S100β	Forward	GACTGCGCCAAGCCCACACC	142
	Reverse	TCCAGCTCGGACATCCCGGG	
Spp1	Forward	TCCTTGCTTGGGTTTGCAGT	188
	Reverse	GTCACTTTCACCGGGAGGG	
Tlr4	Forward	TGCCTGACACCAGGAAGCTTGA	102
	Reverse	AGGAATGTCATCAGGGACTTTGCTG	
Timp2	Forward	GCAACAGGCGTTTTGCAATG	71
	Reverse	CGGAATCCACCTCCTTCTCG	
Txnip	Forward	CCTACAGCAGGTGAGAACGA	103
	Reverse	TAAAGGATGTTCCCAGGGGC	
Vim	Forward	AGGAAGCCGAAAGCACCCTGC	78
	Reverse	TCCGTTCAAGGTCAAGACGTGCC	

Table 2.3.
Human RT-qPCR primers

Gene	**Primer**	**Sequence**	**Length (bp)**
β2 M	Forward	AGATGAGTATGCCTGCCGTG	120
	Reverse	TCATCCAATCCAAATGCGGC	
Ednrb	Forward	TGCTTGCTTCATCCCGTTCA	197
	Reverse	TCCCGTCTCTGCTTTAGGTG	
Egfr	Forward	AAACAACACCCTGGTCTGGA	126
	Reverse	GGGATCTTAGGCCCATTCGT	
Gal3	Forward	GCCTTCCACTTTAACCCACG	74
	Reverse	TAAGCGAAAAGCTGTCTGCC	
Gfap	Forward	GCACGCAGTATGAGGCAATG	139
	Reverse	TAGTCGTTGGCTTCGTGCTT	
Glast	Forward	GGCTAGCCTGCCTGCTTAC	165
	Reverse	TGTCTGGGAATCACCCACAG	
Gs	Forward	CTTAACCCACCAACCTGCCTG	221
	Reverse	AGGTGGTCATGGTGGAAGGT	
Kir2.1	Forward	ACTCTCGTCGGACCCTCC	183
	Reverse	GCGACTTGTTGCTCAGGTTG	
Lcn2	Forward	GACCCGCAAAAGATGTATGCC	197
	Reverse	CTCACCACTCGGACGAGGTA	
Mmp9	Forward	CGACGTCTTCCAGTACCGA	81
	Reverse	TTCAACTCACTCCGGGAACTC	
Mmp11	Forward	CTGGGAGAAGACGGACCTCA	242
	Reverse	TCTTGGGGAAGAAGGCATGG	
Mmp14	Forward	GTGGTCTCGGACCATGTCTC	143
	Reverse	AGCCATATTGCTGTAGCCAGG	
Ncan	Forward	GAGGTGCACTCAGATCCCTG	196
	Reverse	GGCAGACAAAGCCATTGACC	
Pax2	Forward	CCAGTTGTGACTGGTCGTGA	206
	Reverse	GGCATTAGTAAGGCGGGGTT	
Pcan	Forward	TCCACAGATTTCAGTTTTGCAG	198
	Reverse	CCCCTCAGCTAGACCAATACG	

Table 2.3 (Continued)

S100β	Forward Reverse	GACCAGGAAGGGGTGAGACA TGATGAGCTCCTTCAGTTCGG	141
Spp1	Forward Reverse	AGCCAAACAACAAATGGGCA AGATGGGTCAGGGTTTAGCC	199
Tlr4	Forward Reverse	GTGAGACCAGAAAGCTGGGA TGCCTAAATGCCTCAGGGGA	151
Timp2	Forward Reverse	GGCGTTTTGCAATGCAGATG TCGTTTCCAGAGTCCACTTCC	72
Txnip	Forward Reverse	TCAAGATGCCGAACCCTGTG AGTGAGGGGCCAATATCCCT	130
Vim	Forward Reverse	GCAGGATTTCTCTGCCTCTTC CTGCACTGAGTGTGTGCAATTT	198

2.3 Results

2.3.1 Müller glia express bone morphogenetic protein type IA, IB and activin receptor like kinase 2 receptors

BMPs bind preferentially to 3 type I receptors; receptor IA, IB, or activin receptor like kinase 2 (ALK2). Double-label immunofluorescence was used to define if any of the type I BMP receptors was expressed by Müller cells and/or retinal astrocytes. Sections through adult murine retina were co-labeled with antibodies specific for GS, which labels Müller glial cells and retinal astrocytes, and BMPR1A, BMPR1B, or ALK2 (Figure 2.1). All three receptors showed similar labeling patterns in the retina with Müller glial cell processes labeled in the outer nuclear layer (ONL), outer plexiform layer (OPL), and ganglion cell layer (GCL; Figure 2.1A–C). Photoreceptor outer segments and ganglion cell bodies were also clearly labeled for all three receptors. To confirm the label of Müller glial cells and their processes by antibodies to type I receptors, enzymatically dissociated cells were co-labeled with antibodies to GS and BMPR1A, BMPR1B, or ALK2 (Figure 2.1J–L). Immunolabeled Müller glia were readily apparent in dissociated samples as they had retained their shape throughout the processing. All three receptors appeared to co-label GS (+) cells, indicating that the cells are responsive to BMPs *in vivo*.

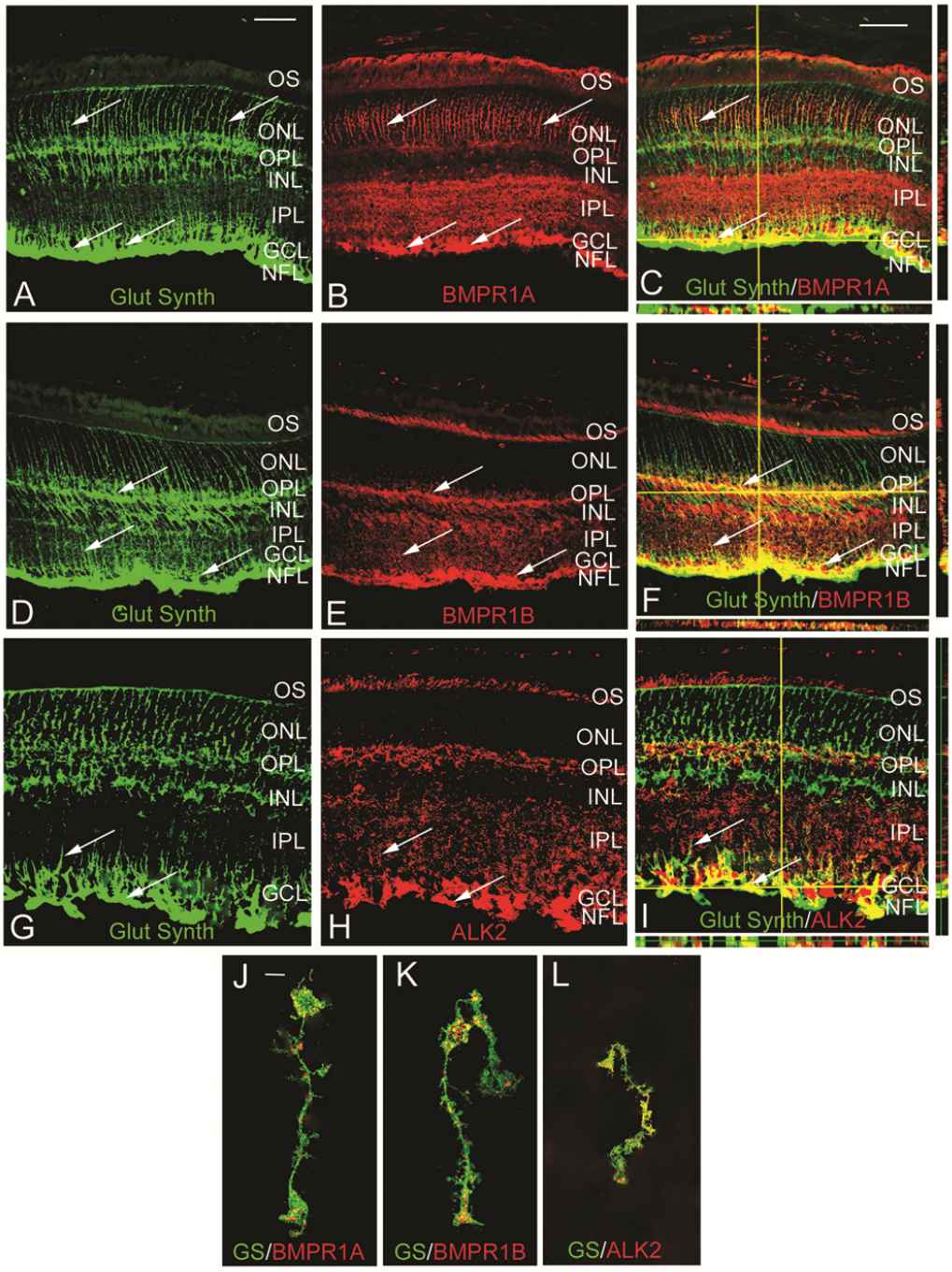

Fig. 2.1. Bone morphogenetic protein (BMP) type I receptors in the mature mouse retina (Continued on next page).

Fig. 2.1. Bone morphogenetic protein (BMP) type I receptors in the mature mouse retina. A: Retinal sections of 4 week-old retina double-labeled using antibodies that recognize Müller glial and retinal astrocyte marker glutamine synthetase (GS) and BMP receptor 1A (BMPR1A). Thin plane confocal microscopy with y,z (strips to right of panels), and x,z planes (strips at bottom of panels) are shown in the last panels in the row. BMPR1A was localized to the Müller glial processes in the outer nuclear layer (ONL) and in Müller glial cell or retinal astrocyte processes in the ganglion cell layer (GCL, arrows A–C). BMPR1A was also detectable in the photoreceptor outer segments, the inner plexiform layer (IPL), cell bodies within the ganglion cell layer, and the nerve fiber layer (NFL). B: Retinal sections of 4 week-old retina double-labeled using antibodies that recognize GS and BMPR1B. BMPR1B appeared to be localized to the outer segments (OS), outer plexiform layer (OPL) and IPL and, Müller glial cell processes as well as Müller glial/retinal astrocyte processes in the GCL and NFL (arrows). C: Retinal sections of 4 week-old retina double-labeled using antibodies that recognize GS and activin receptor like kinase 2 (ALK2). The distribution of ALK2 receptors was similar to that of BMPR1A, with the majority of signal being localized to the end feet within the GCL and NFL. D: Müller glia isolated from P30 retinas were co-labeled for GS and BMPR1A, 1B and ALK2. The isolated cells showed the distribution of receptors to be primarily in the processes and the end feet of the Müller glia, as seen in the P30 tissues. n=3 different eyes for each label. Scale bar A=50 μm applies to A–I. Scale bar J=30 μm applies to J–L.

2.3.2 Bone morphogenetic protein 7 signaling components in the retinal glia

The BMP signaling pathway members present in the Müller glial and retinal astrocytes were also investigated to determine which pathways might be activated in the presence of BMPs. To investigate the canonical BMP pathway, sections were co-labeled with antibodies against SOX2, which labels Müller glial cells, retinal astrocytes and cholinergic amacrine cells in the mature murine retina, and SMAD1. SMAD1 was localized throughout cells of the INL and GCL, and was co-localized with SOX2 (+) cells (Figure 2.2). To determine if the BMP-kinase pathway could be activated in response to BMPs, sections through adult retina were co-labeled with antibodies to GS and TAK1 (Figure 2.2). While TAK1 was prominently expressed in the retina, most notably in a subpopulation of INL and GCL, little to no co-expression could be detected in GS (+) cells (Figure 2.2). Last, potential involvement of the FRAP-STAT pathway in Müller glial BMP signaling was investigated by co-labeling sections with GS and FKBP12 (Figure 2.2). FKBP12 label was noted in the INL, GCL, and inner plexiform layers (IPL). No apparent co-label was detected of FKBP12 and GS (Figure 2.2).

2.3.3 Bone morphogenetic protein 7 can trigger changes in retinal astrocytes and MIO-M1 Müller cells resembling mild reactive gliosis

The role of BMP7 in reactive gliosis was first tested by addition of the factor to an *in vitro* system using isolated retinal astrocytes or a Müller glial cell line, MIO-M1 (Scheef et al. 2005; Sehgal et al. 2009; Limb, Salt, et al. 2002). Previously characterized, retinal astrocytes have been shown to express paired box 2 (PAX2), neurogenin 2 (NG2), and GFAP [115,116,118]. In order to use these cells, their ability to exhibit changes associated with reactive gliosis had to first be determined. The cells were briefly treated with vehicle or sodium peroxynitrite, a strong oxidizing agent that is released by injured neurons and has been shown to trigger reactive gliosis (Pacher,

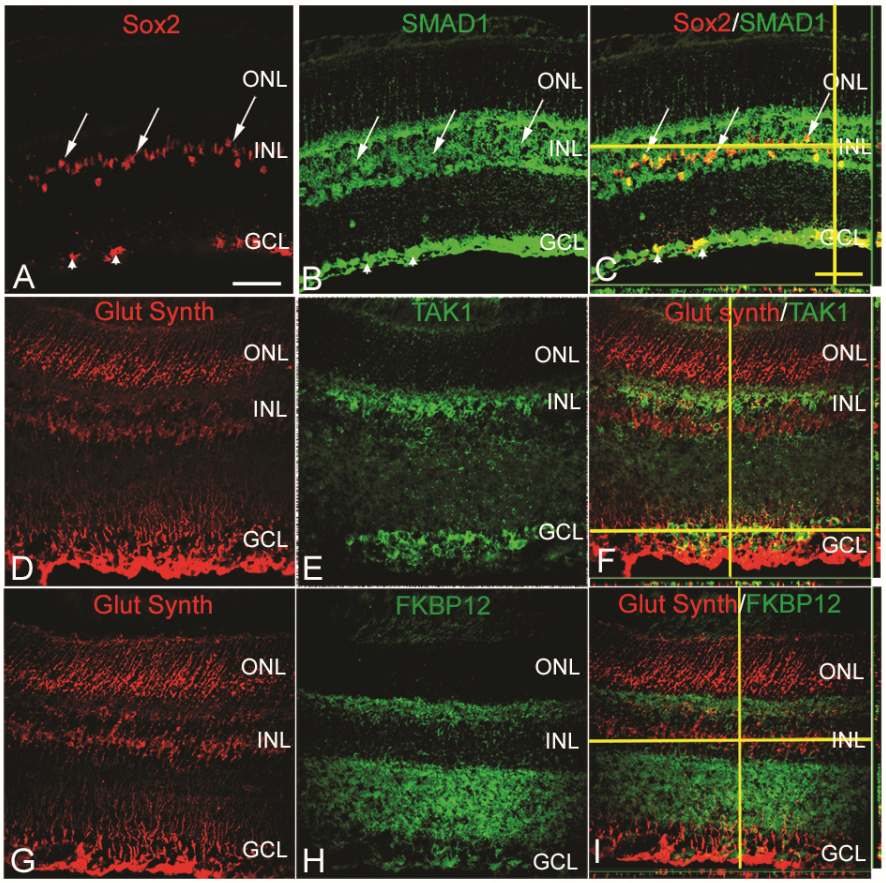

Fig. 2.2. Bone morphogenetic protein (BMP) signaling components in the Müller glia of adult mouse retina. A: Sections of 4 week-old retina were subjected to double-label immunofluorescence with antibodies specific for sex determining region Y box 2 (SOX2), which labels Müller glia, retinal astrocytes, and cholinergic amacrine cells, and intracellular members of the BMP pathway SMAD1 . SMAD1 (+) cells were localized to the inner nuclear layer (INL) and ganglion cell layer (GCL) of P30 retina. A subpopulation of SOX2 (+) Müller glia (arrows) and retinal astrocyte cells (arrowheads) were also positive for SMAD1. B: Sections of 4 week-old retina were subjected to double-label immunofluorescence with antibodies for SOX2, and TGF-β activated kinase 1 (TAK1). Cells positive for the protein TAK1 were found to be localized in the INL and GCL. C: Sections of 4 week-old retina were subjected to double-label immunofluorescence with antibodies for SOX2, and FK506 rapamycin binding protein (FKBP12). FKBP12, also part of the non-canonical BMP pathway, was found to be localized in the INL along with sparse localization in the GCL. Very little to no co-label was seen with glutamine synthetase (GS; +) and TAK1 or FKBP12 (+) cells (B, C). Scale bar A=50 μm applies to all panels.

Beckman, and Liaudet 2007). Following treatment, levels of mRNAs known to be regulated during reactive gliosis were examined 16 (not shown) and 32 h after treatment using RT-qPCR (Figure 2.3).

In the analysis of the RT-qPCR levels throughout this study, two thresholds had to be met in order for the change to be considered a convincing change; 1) the comparative change with controls had to be statistically significant, and 2) an average increase in levels had to reach the level of 1.5 fold or above that of controls or, similarly, a decrease had to reach a level 0.5-fold or below. No statistically significant changes in expression were noted between vehicle and peroxynitrite 16 h following treatment (not shown). In contrast, there were statistically significant increases that reached the 1.5-fold threshold in the level of many mRNAs within the reactive gliosis panel in peroxynitrite treated cells in comparison to vehicle-treated, including *Pax2*, lipocalin2 (*Lcn2*), matrix metalloproteinase 9 (*Mmp9*), phosphacan (*Pcan*), *S100β*, toll-like receptor 4 (*Tlr4*), tissue inhibitor of matrix metalloproteinase 2 (*Timp2*), and glial fibrillary acidic protein (*Gfap*) (Figure 2.3A). There was also a statistically significant decrease in the glutamate aspartate transporter (*Glast*) that also reached the level of 0.5 and below threshold. Levels of protein were investigated by western blotting for 3 proteins; namely GFAP, thioredoxin-interacting protein (TXNIP), and PAX2 (Figure 2.3). While there was a modest increase in GFAP and PAX2 protein in comparison to control vehicle-treated cells, there was no increase in levels of TXNIP 36 h post-treatment (Figure 2.3).

To test whether BMP7 treatment could also trigger signs of reactive gliosis *in vitro*, retinal astrocytes were treated with either vehicle or BMP7 for 24 or 36 h. Following 24 h of vehicle or BMP7 treatment, retinal astrocytes treated with BMP7 showed a statistically significant increase in transcript levels above the 1.5-fold threshold for *Ncan, Pcan, Asci1, Glast, Txnip, Pax2*, and *Gfap* (Figure 2.3). There was also a decrease in levels of *Mmp14* in BMP-treated versus vehicle-treated retinal astrocytes

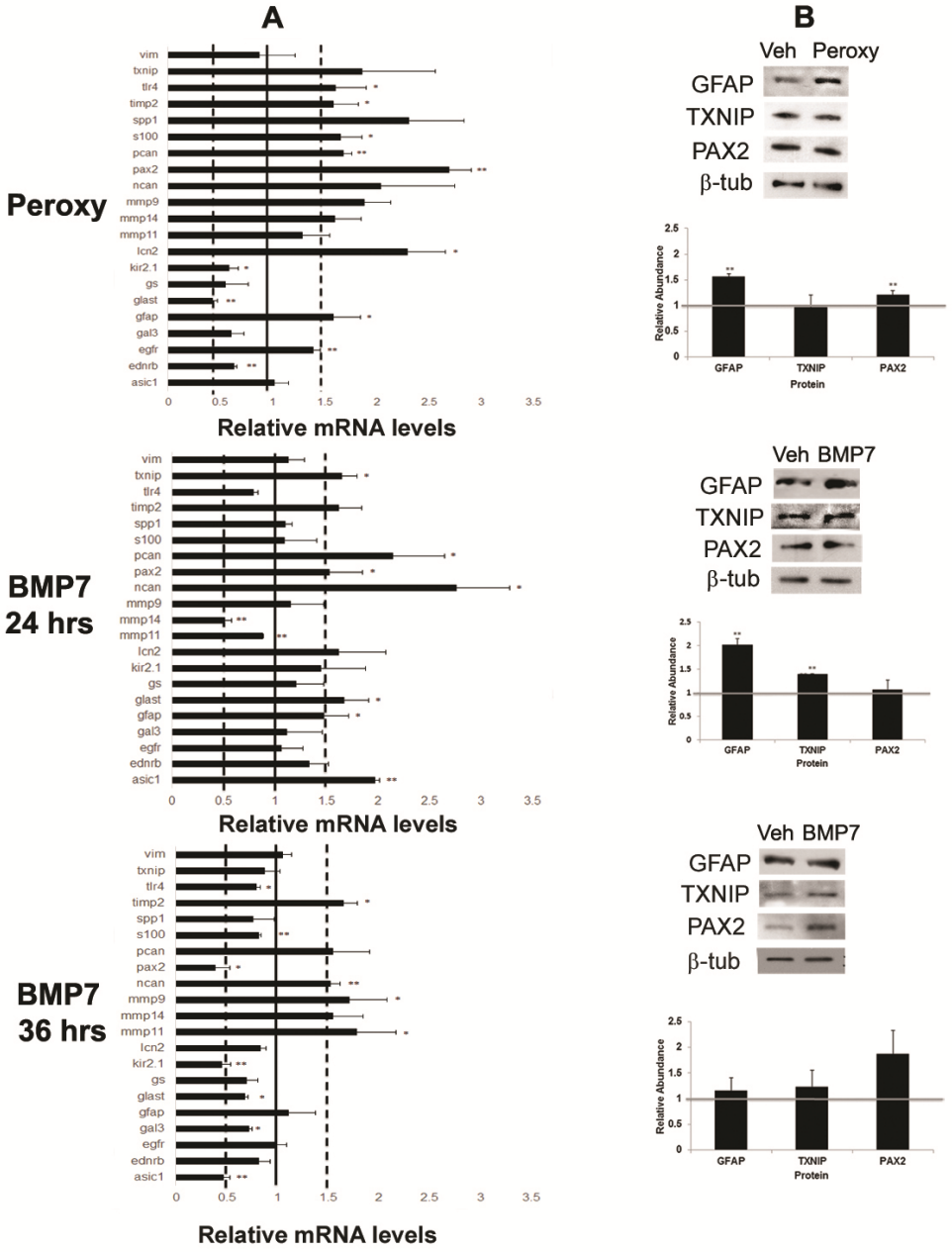

Fig. 2.3. Bone morphogenetic protein 7 (BMP7) treatment of retinal astrocyte cells increases markers of glial scar formation (Continued on next page).

Fig. 2.3. Bone morphogenetic protein 7 (BMP7) treatment of retinal astrocyte cells increases markers of glial scar formation. A: Expression patterns for a panel of markers associated with reactive gliosis were compared in murine retinal astrocytes treated with sodium peroxynitrite or BMP7 for 24 or 36 h. Values represented are means +/− SEM. Unpaired t test was performed between the control and treated groups with $*$ denoting a p value<0.05 and $**$ denoting a p value<0.005. Any change above or below 1.0 indicates a change relative to control values. Peroxynitrite-treated cells showed statistically significant increases above 1.5-fold in mRNA levels of *Pax2*, *Lcn2*, *Mmp9*, *Pcan*, *S100β*, *Tlr4*, *Timp2* and *Gfap*. Decreases in mRNA levels below 0.5-fold were noted for *Glast* in peroxynitrite-treated cells. In comparison, 24 h of BMP treatment led to a modest increase above the 1.5-fold level in *Ncan*, *Pcan*, *Asic1*, *Glast*, *Txnip*, *Pax2*, and *Gfap* mRNA levels. By 36 h post BMP7-addition, Gfap levels had returned to baseline and *Asic1*, *Kir2.1*, and *Pax2* mRNA levels were reduced in comparison to vehicle-treated cells. Levels of *Mmp11, Timp2*, and *Ncan* were still increased in comparison to vehicle-treated cells. B: Western blot analysis was performed for GFAP, TXNIP, and PAX2, with β-TUBULIN used as a loading control. Densitometric data shown are means +/− SEM of 3 trials. Unpaired t test was performed between the control and treated groups with $*$ denoting a p value<0.05 and $**$ denoting a p value<0.005. Densitometric analysis of the blots showed a statistically significant increase in protein levels of GFAP in the peroxynitrite and 24 h BMP7 treatments. Significant increases in levels of PAX2 and TXNIP was observed in the peroxynitrite and 24 h BMP7 treatments, respectively. No statistically significant change was observed in the 36 h BMP7 treatment.

that met the 0.5 threshold and was a statistically significant change in comparison to vehicle-treated cells (Figure 2.3A). Western blotting was used to assess the levels of a subset of proteins in vehicle- and BMP-treated cells. A statistically significant increase in protein levels of GFAP and TXNIP protein was noted for BMP7-treated cells compared to vehicle-treated cells at 24 h post-treatment (Figure 2.3B).

However, there were no detectable differences in the levels of TXNIP or PAX2 at 24h (Figure 2.3). Cells treated with BMP7 for 36 h showed changes in levels of a slightly different cohort of mRNAs; *Mmp11, Timp2, Ncan*, and *Mmp9* were modestly increased, while *Asic1, Kir2.1* and *Pax2* were decreased slightly (Figure 2.3B). By western blotting there were small but statistically insignificant increases in GFAP, TXNIP and PAX2 (Figure 2.3).

Similar to the retinal astrocyte cultures, treatment of the Müller glial cell line MIO-M1 with peroxynitrite also led to increases in some of the markers in the reactive gliosis panel (Figure 2.4). Western blots showed a modest increase in protein levels of GFAP and S100β; however, no change was noted in PAX2 expression (Figure 2.4). Treatment of MIO-M1 cells with BMP7 yielded similar, but slightly different changes in mRNA levels following treatment for 24 or 36 h. At 24 h, *Gfap* and *Pax2* mRNA levels were increased in comparison to control vehicle-treated cells above the 1.5-fold threshold, while there was a decrease in *Txnip, Gal3, Lcn2* and *Mmp9* levels below the 0.5-fold threshold (Figure 2.4).

Western blotting showed statistically significant changes in GFAP, S100β, and TXNIP protein levels in comparison to controls; however increases in PAX2 were not statistically significant (Figure 2.4B). Treatment of cells with BMP7 for 36 h yielded increases in *Gfap* and *Tlr4* mRNA levels in comparison to control cultures and a decrease in secreted phosphoprotein 1 (*Spp1*; Figure 2.4B). By western blot, densitometric analysis showed a statistically significant decrease in PAX2 levels and no significant changes in GFAP, S100β, or TXNIP levels in comparison to vehicle-treated cells (Figure 2.4B).

To determine if treatment of cells with another BMP family member, BMP4, led to similar changes in reactive gliosis markers, retinal astrocytes and MIO-M1 cells were treated with BMP4 for 24 or 36 h, and changes in mRNA levels were assessed by RT-qPCR. Overall there were fewer statistically significant changes in BMP4-treated cells at or over the level of 1.5 fold increase or 0.5-fold decrease in comparison to vehicle-treated cells in both retinal astrocytes and MIO-M1 cells (Figure 2.5). In retinal astrocytes, *Txnip* and *Gs* were increased more than 1.5 fold over control and were statistically significant. Only *Mmp9* showed a decrease in comparison to control at 24 h post-treatment. In comparison, at the 36 h time point only a decrease in Mmp9 was statistically significant and reached the 0.5-fold level. In the MIO-M1 cells only *Asic1* and *Spp1* were up-regulated at least 1.5 fold over levels of control mRNA at 24 h post-addition. Further, at the 36 h time point a statistically significant increase at the 1.5-fold level in endothelin receptor type B (*Ednrb*) and *Asic1* were the only increases noted at 36 h post-addition of BMP4.

2.3.4 Intravitreal injection of bone morphogenetic protein 7 induces reactive gliosis

To further explore the role of BMP7 in reactive gliosis, wild type adult mouse eyes underwent intravitreal injections of vehicle or BMP7. To determine the BMP signaling cascade in BMP7 mediated gliosis, the vehicle- and BMP7-injected retinas were

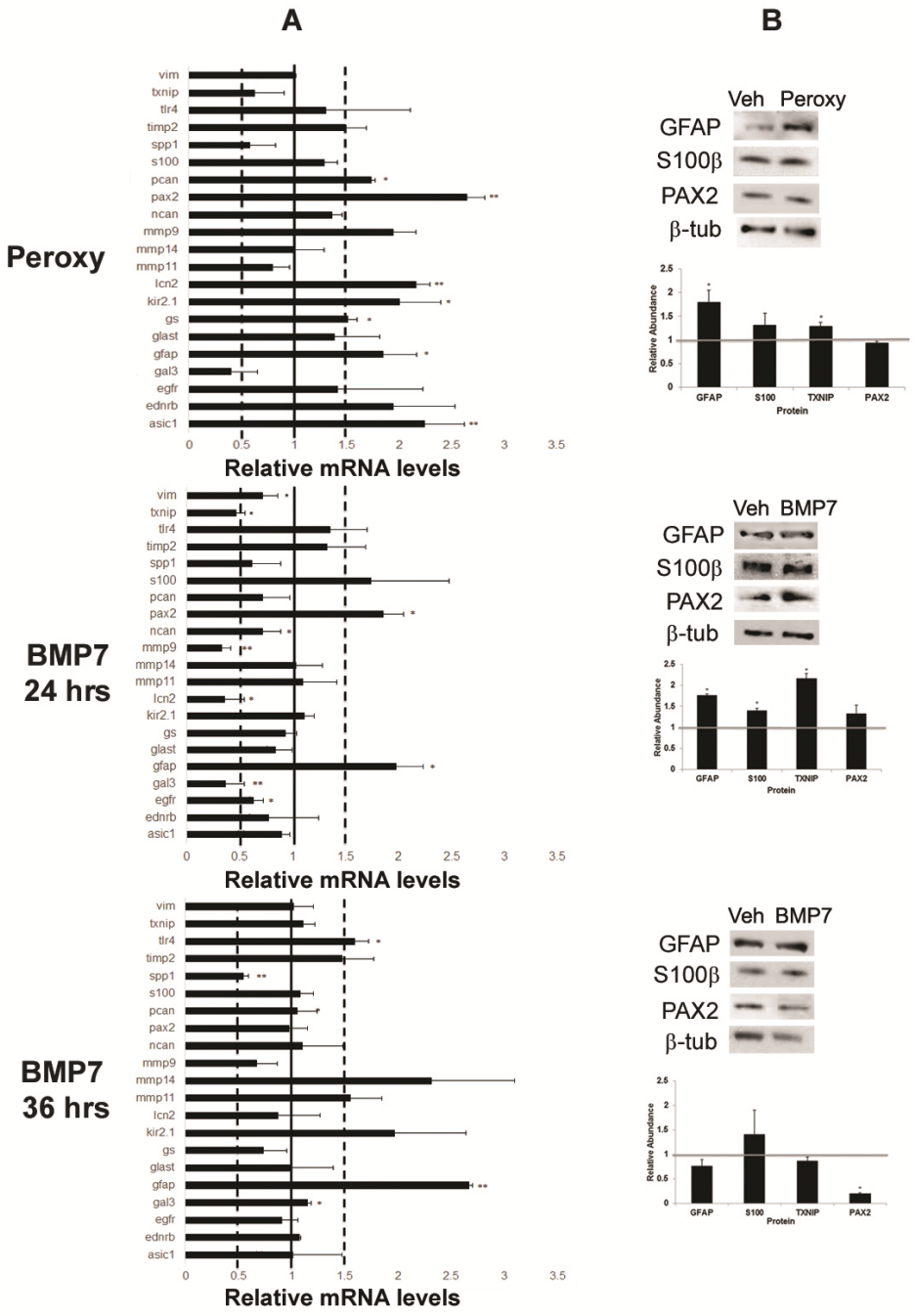

Fig. 2. 4. Bone morphogenetic protein 7 (BMP7) treatment of MIO-M1 Müller glial cell line increases glial fibrillary acidic protein (GFAP) expression (Continued on next page).

Fig. 2.4. Bone morphogenetic protein 7 (BMP7) treatment of MIO-M1 Müller glial cell line increases glial fibrillary acidic protein (GFAP) expression. A: Expression patterns for a panel of markers associated with reactive gliosis were compared in human MIO-M1 Müller glial cells treated with sodium peroxynitrite, or BMP7 for 24 or 36 h. For each experimental treatment, cells were treated with vehicle, sodium peroxynitrite, or BMP7 and real-time quantitative PCR (RT-qPCR) was undertaken. Values represented are means +/–SEM. Unpaired t test was performed between the control and treated groups with * denoting a p value<0.05 and ** denoting a p value<0.005. Any change above or below 1.0 indicates a change relative to control values. BMP7-treated MIO-M1 cells showed a statistically significant increase above the 1.5-fold level in *Pax2, Asic1, Lcn2, Kir2.1, Gfap*, and *Pcan* in comparison to vehicle-treated cells. Twenty-four hours following BMP7 addition, the MIO-M1 cells only showed a statistically significant increase above the 1.5-fold level in *Gfap* and *Pax2*, and a decrease in *Txnip, Gal3, Lcn2*, and *Mmp9*. At the 36 h time point *Gfap*, and *Tlr4* levels of mRNA were increased above the 1.5-fold level in comparison to vehicle-treated cells and *Spp1* was decreased. B: western blot analysis was performed for GFAP, S100β, TXNIP, and PAX2, with β-TUBULIN used as a loading control. Densitometric data shown are means+/–SEM of 3 trials.Unpaired t test was performed between the control and treated groups with $*$ denoting a p value<0.05 and $**$ denoting a p value<0.005. Densitometric analysis of the blots showed a statistically significant increase in protein levels of GFAP and TXNIP in the peroxynitrite treatment. A significant increase in levels of GFAP, S100β, and TXNIP was observed in the 24 h BMP7 treatment, while a significant decrease was observed in PAX2 levels in the 36 h bmp7 treatment.

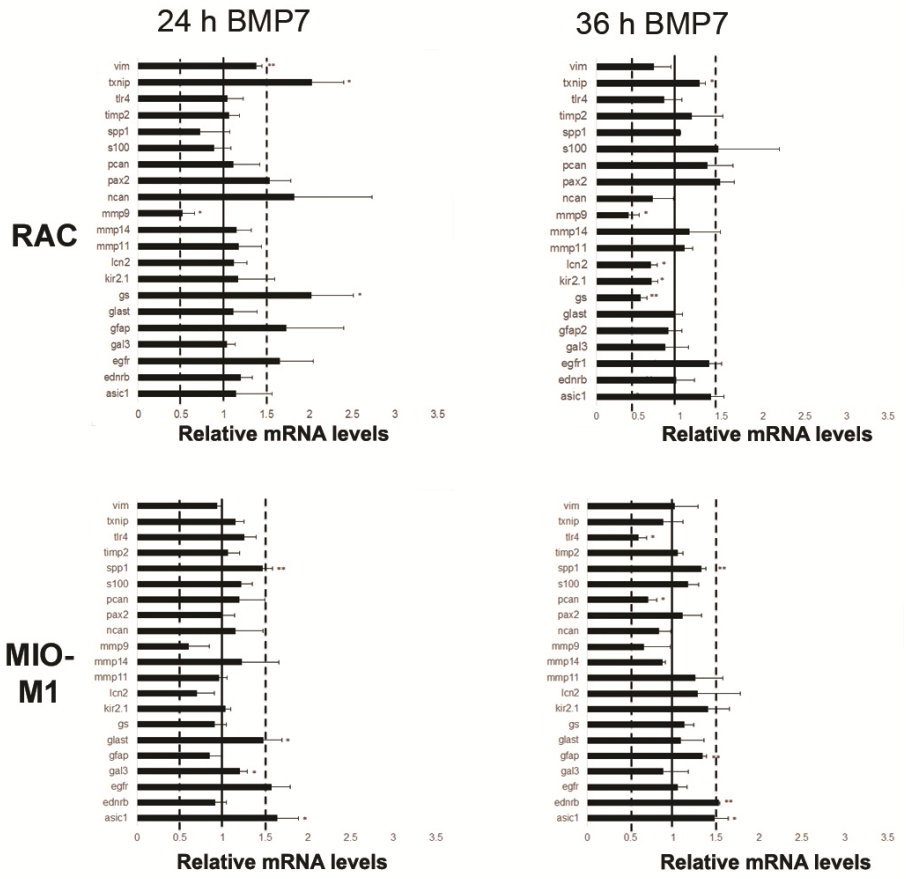

Fig. 2.5. Retinal astrocytes and MIO-M1 cells show an attenuated response to bone morphogenetic protein 4 (BMP4). Retinal astrocytes (RAC) and MIO-M1 cells were treated with BMP4 and mRNA isolates from samples treated for 24 h or 36 h were subjected to real-time quantitative PCR (RT-qPCR) using the reactive gliosis panel established in previous experiments. Values represented are means +/–SEM. Unpaired t test was performed between the control and treated groups with $*$ denoting a p value<0.05 and $**$ denoting a p value<0.005. At 24 h, retinal astrocytes treated with BMP4 showed statistically significant increase above the 1.5-fold level in *Txnip* and *GS* in comparison to controls, as well as a decrease in *Mmp9*. By 36 h, statistically significant decreases in *GS* and *Mmp9* in comparison to vehicle were noted. Similarly, MIO-M1 cells treated showed small changes in *Asic1, Glast* and *Spp1*, following 24 h of BMP4 treatment. At 36 h, increases above 1.5-fold in *Ednrb* and *Asic1* in comparison to controls were noted.

colabeled with SOX2 and phospho-SMAD 1/5/8 (Figure 2.6) or phospho-TAK1 (Figure 2.7). While the vehicle-injected retina showed little or no phospho-SMAD and SOX2 co-label, the BMP7 injected retinas showed an increased colabel for phospho-SMAD 1/5/8 and the Müller glial marker SOX2 (Figure 2.6). Co-label was also performed for SOX2 and phospho-TAK1 to determine activation of the BMP-MAPK non-canonical signaling cascade. The vehicle-injected retina showed phospho-TAK1 label primarily in the ganglion cell layer, while the BMP7-injected retina showed an increase in the phospho-TAK1 label in the inner nuclear layer and an increase in co-label with SOX2 (Figure 2.7).

Further, retinas at 3 and 7 days after injection were examined using RT-qPCR, immunofluorescence, and Western blot analysis. Three days following injection, the only statistically significant changes that reached threshold was a decrease in *Pax2* and *Gal3* mRNA levels (Figure 2.8A). At the 7 day time point, however, statistically significant increases in mRNA levels above threshold were observed for *Txnip, Glast, Mmp9, Lcn2, Gs, Kir2.1,* and *Mmp14* (Figure 2.8 A). There were also several decreases noted at 7days after injection; *Tlr4, Pax2*, and *Egfr*. Immunohistochemistry on sections through injected retinas at 3 days post-injection revealed no readily apparent changes in GFAP, S100β or NCAN in BMP7-injected retinas as compared to vehicle-injected (Figure 2.8B). In contrast, there was a marked increase in GFAP, S100β and NCAN in BMP7-injected retinas when compared with their control counterparts (Figure 2.8B). By western blot, there were small but significant increases in S100β and TXNIP at 3 days post-injection in BMP7-injected retinas and, while there were increases in GFAP, S100β and TXNIP at 7 days post-injection in BMP-injected retina, none of the changes were statistically significant (Figure 2.8C).

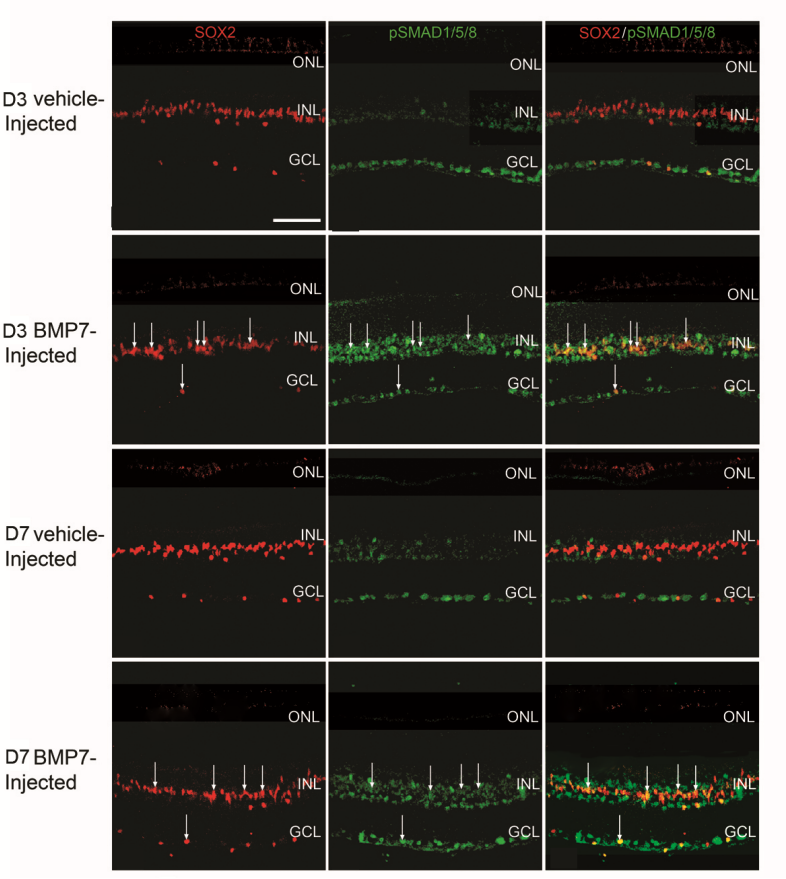

Fig. 2.6. Canonical bone morphogenetic protein (BMP) signaling is activated in the Müller glia in BMP7 injected murine eyes. Sections of retina from adult mouse eyes injected with vehicle or BMP7 and harvested 3 or 7 days after injections were double-labeled with antibodies against phospho-SMAD1/5/8 (green) and the nuclear marker sex determining region Y box 2 (SOX2; red) which labels Müller glia, retinal astrocytes and cholinergic amacrine cells. While the vehicle-injected control showed phospho-SMAD 1/5/8 labeled cells primarily localized in the ganglion cell layer (GCL), with little or no co-label with the SOX2 (+) cells, in the D3 and D7 BMP7-injected retinas, phospho-SMAD1/5/8 label was also detectable in the inner nuclear layer (arrows INL). A sub population of the cells in the INL which were positive for phospho-SMAD1/5/8 were also SOX2 positive. n=3 different retinas for each immunolabel. Scale Bar A=50 μm applies to all panels.

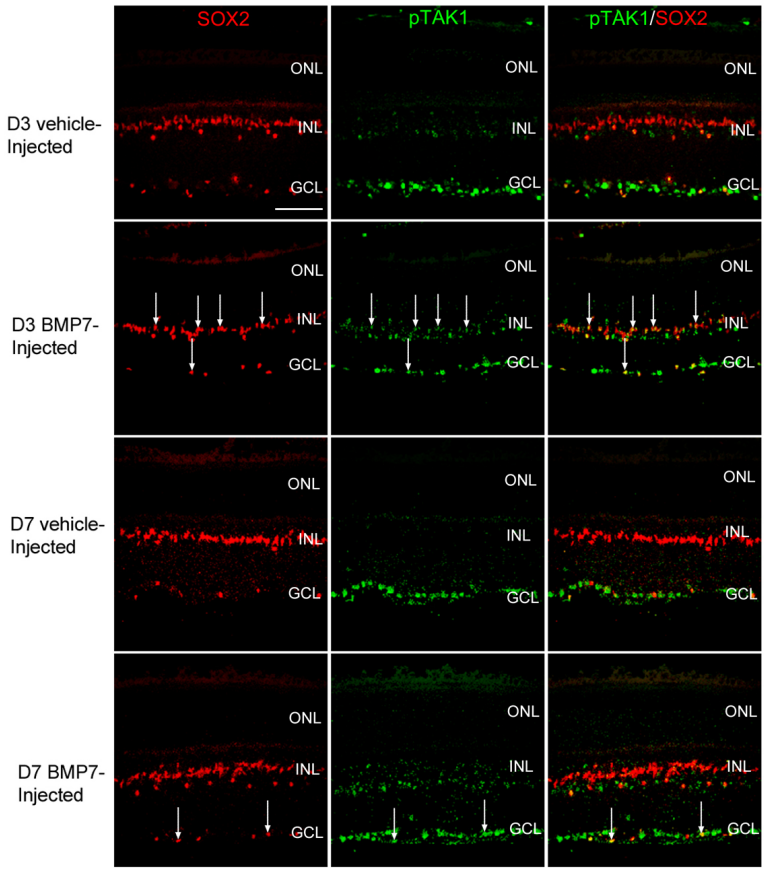

Fig. 2.7. Non-canonical bone morphogenetic protein (BMP) signaling mediated via Transforming Growth Factor-β activated kinase (TAK) is upregulated in the Müller glia in BMP7 injected murine eyes. Retinal sections from mouse eyes processed 3 and 7 days following injection with either vehicle or BMP7 were co-labeled with antibodies against phospho-TAK1 (green) and Müller glial marker sex determining region Y box 2 (SOX2; red) . The vehicle injected control retinas for 3 and 7 days (D3 and D7 respectively) showed phospho-TAK1 label primarily cells in the ganglion cell layer (GCL), with no phospho-TAK1 labeling in the iner nuclear layer (INL) or outer nuclear layer (ONL). SOX2 (+) reinal astrocytes were observed in the GCL, however very little co-expression was observed with phospho-TAK1 in the vehicle injected retinas. The BMP7-injected retinas did show an increase in phospho-TAK1 expression in the INL, showing a comparatively higher expression in the BMP7-injected retina at 3 days than at 7 days. A subpopulation of the SOX2 (+) in the GCL and INL were co-labeled with phospho-TAK1 in the BMP7-injected retinas (arrows). n=3 different retinas for each immunolabel. Scale Bar A=50 μm applies to all panels.

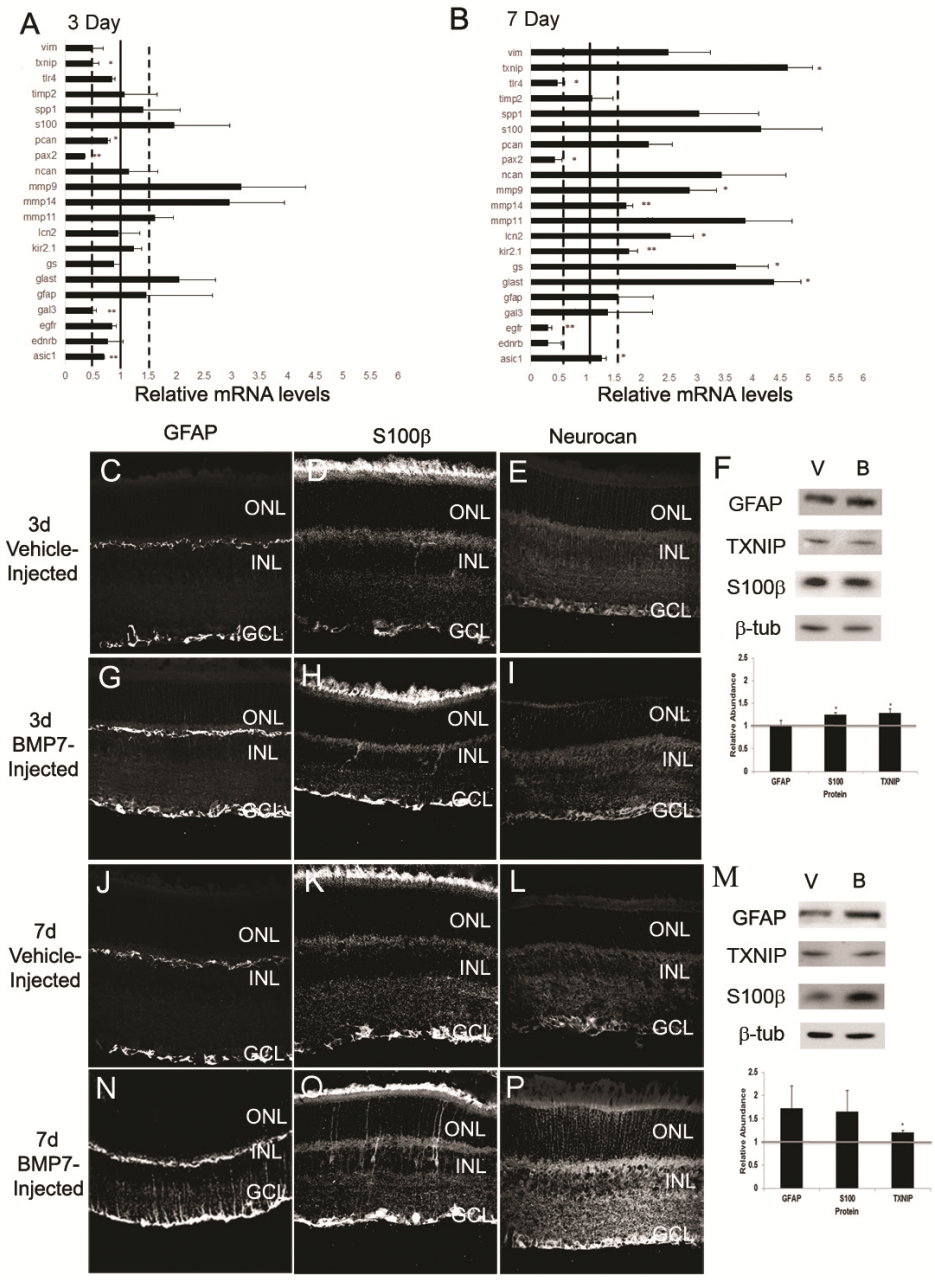

Fig. 2.8. Intravitreal injection of bone morphogenetic protein 7 (BMP7) into murine eyes leads to reactive gliosis (Continued on next page).

Fig. 2.8. Intravitreal injection of bone morphogenetic protein 7 (BMP7) into murine eyes leads to reactive gliosis. A: RNA from adult eyes injected with vehicle or BMP7 was isolated 3 and 7 days following injections and real time quantitative PCR (RT-qPCR) was performed using the reactive gliosis panel described in previous figures. Values represented are means+/ −SEM. At 3 days following injection, there was a significant decrease in *Pax2* and *Gal3*. In contrast, by 7 days following injection there were significant increases in *Txnip, Glast, GS, Mmp9, Lcn2, Kir2.1*, and *Mmp14* and decreases in *Tlr4, Pax2*, and *Egfr*. B: Immunolabel of retinas from 3 day and 7 day vehicle and BMP7-injected eyes for a subset of the gliosis markers. To confirm some of the changes seen at the mRNA level, eyes injected with vehicle or BMP7 were fixed 3 or 7 days after injection and immunolabeled for GFAP, S100β, or NEUROCAN (NCAN). At 3 days following injection, GFAP, S100β and NCAN immunolabel looks similar in vehicle- and BMP7-injected eyes. In contrast, by 7 days, sections immunolabeled for GFAP, S100β, and NCAN showed an increase in labeling in BMP7-injected eyes in comparison to vehicle-injected. C: western blot analysis was performed for GFAP, TXNIP, S100β, and PAX2, with β-TUBULIN used as a loading control. Densitometric analysis of the blots showed a statistical increase in protein levels of S100β at the 3 day stage. While there did appear to be an increase in GFAP, S100β, and TXNIP at 7 days following injection in the BMP7-treated retinas as compared to vehicle-injected, none of the changes in protein levels was statistically significant. Scale bar C=50 μm applies to C–P.

2.4 Discussion

Our findings indicate that the BMP7 pathway plays a role in triggering and/or maintaining reactive gliosis in the retina. The glial cells of the retina express the BMP receptors (BMPR1A, BMPR1B and ALK2). While the downstream components for the canonical and non-canonical signaling pathways are present in the retina, only the SMADs appeared to be present in the retinal glia prior to BMP7 injection. Following injection, both activated SMADs and TAK1 were present, indicating that TAK1 had been upregulated following injection. Treatment of retinal astrocyte cells and Müller glial cells *in vitro* with BMP7 regulated various reactive gliosis markers. The profile of gliosis markers regulated due to exposure to BMP7 was similar, although not identical, to that observed due to exposure to peroxynitrite. Injection of BMP7 into mouse retina also triggered a reactive gliosis response. Incubation of cells with BMP4, however, showed no significant increase or decrease in the levels of the gliosis markers.

2.4.1 Regulation of glutamine synthetase during reactive gliosis

Reactive gliosis is a common and a complex response observed following neural injury [119]. One response typical of Müller cells undergoing gliosis is a change in levels of glutamine synthesis, the enzyme critical for glutamate-glutamine cycling in the nervous system. Under normal circumstances within the retina, GS prevents the excitotoxic effects of glutamate and is necessary for ammonium detoxification [21]. In the retina, GS is widely expressed in the astrocytes and Müller glial cells [120]. Levels of GS are exquisitely regulated by injury in an injury- or disease-state manner. For instance, expression of GS is downregulated in diseases states in which photoreceptors (the major source of glutamate in the retina) degenerate [121, 122]. However, in disease states where the presence of GS is necessary to detoxify the retina when high levels of ammonia, glutamate, or glutamate agonists are present (such as hepatic retinopathy or following kainic acid injection), expression levels of the enzyme

increase [123,124]. Finally, levels of GS can remain stable in some injury and diseases states including diabetic retinopathy and following nerve crush [125,126]. In the studies presented here, GS levels increased following addition of BMP7 *in vitro* and *in vivo*, suggesting that the BMP7 addition mimics situations where there is an increase in glutamate or NH4+ concentrations in the retina. Further studies will be necessary to determine if differential regulation of BMP7 occurs in a disease-dependent manner.

2.4.2 Bone morphogenetic protein 7 triggers reactive gliosis via the SMAD and the transforming growth factor-β activated kinase pathway

Reactive gliosis encompasses a wide range of responses ranging from hypertrophy to regulation of transporter channels and enzymes, as well as cell migration, proliferation and de-differentiation [43]. The triggers for these different molecular and functional responses vary with the injury or disease state. Many growth factors have been implicated in regulating one or more of the changes associated with gliosis. For instance, EGF has been associated with Müller glial proliferation, FGF2 with the scarring response, and CNTF with GFAP upregulation [104,108]. Further, inflammation is also a commonly observed response during gliosis. Factors such as TNF-α and CNTF have been known to play a role in inflammatory response of reactive gliosis, while TNF-α and some of the interleukins are also known to induce proliferative reactive gliosis [68,127,128].

BMPs have also been associated with various changes that occur during reactive gliosis; however many of the studies to date have focused on the role of the BMPs following injury to the spinal cord [77,81,129]. Initial studies indicated that BMP signaling increased at the site of spinal cord lesions and treatment of astrocytes *in vitro* with BMPs 4 or 7 increased expression of chondroitin sulfate proteoglycans typically associated with glial scars [77]. Further, inhibition of BMPs following spinal

cord injury leads to a decrease in chondroitin sulfate proteoglycans and an increase in the ability of axons to regenerate over time [77, 129]. Similarly, knockout studies for two of the Type 1 BMP receptors have shown that BMPR1A is critical in the hypertrophy response that occurs early in reactive gliosis and BMPR1B is critical for some aspects of the scarring response. Little is known about the role of BMPs in injury or disease within the retina and/or optic nerve. Detailed descriptions of the expression patterns of the BMPs, BMP receptors, and several BMP binding proteins have been described in developing and adult optic nerve, optic nerve head and trabecular meshwork [111, 130, 131]. An increase in BMP signaling within the trabecular meshwork has been implicated in blocking TGF -β driven changes in gene expression [132–134]. Finally, BMP stimulation downstream of EGF signaling has recently been implicated in Müller glial cell proliferation [135].

In the studies detailed here, we showed that the Müller glial cells express BMPR1A, BMPR1B, and ALK2 receptors. While it is probable that astrocytes are also expressing the receptors, due to the intensity of the label in the ganglion cell and inner limiting membrane area we were unable to ascertain this for certain. BMP7 preferentially binds ALK2 receptor and transduces signal via SMAD 1/5/8 [73]. To determine BMP signaling in the retinas, we first analyzed expression and glial localization of the canonical and non-canonical BMP signaling components: SMAD, TAK and FRAP. While co-label showed SMAD and TAK to be localized with Müller glia, with SMAD comparatively to be more than TAK, FRAP showed no localization (Figure 2.2). Analysis of the activated phosphorylated forms of SMAD (phospho-SMAD) and TAK (phospho-TAK) revealed that there is an activation of both in the BMP7-injected retinas (Figure 2.6 and Figure 2.7).

Apart from the glial cells, several other cells also showed positive label for both phospho-SMAD and phospho-TAK. This upregulated BMP signaling in both macroglial and other cells of the retina suggests that BMP7 can regulate gliosis either by directly acting on the retinal glia or indirectly by regulating other retinal cells.

In comparison to BMP7, treatments with BMP4 did not appear to induce gliosis in retinal astrocytes or Müller cells *in vitro*. While BMP4 has been shown to have a neuroprotective effect when injected prior to a toxic insult, BMP7 was not shown to have the same protective effect [69]. The differential response of retinal neurons and macroglia to BMP4 and 7 is indicative of the involvement of different signaling pathways, but further study is necessary in order to elucidate the mechanism of this differential response.

2.4.3 Differences in response patterns

Apart from growth factors, various molecular factors such as adenosine tri-phosphate (ATP), nitric oxide (NO) etc. can also trigger reactive gliosis [43]. Although role of specific factors have been implicated in certain aspects of gliosis such as GFAP, vimentin and neurofilament expression [69, 136], there does not seem to be a clear correlation between the various gliosis markers and its regulators. GFAP is used as the standard indicative for gliosis. However, it and other markers such as GS, MMPs and others have been shown to be regulated differentially depending on the stress they are subjected to [121, 126, 137, 138]. In this study, RT-qPCR analysis of RNA from BMP7-injected retinal tissue compared to the RNA prepared from treated retinal astrocytes and Müller glial cells showed a greater deviation from their respective control treatments (Figure 2.3, Figure 2.4, and Figure 2.8). This could be attributed to the fact that the cells *in vitro* represented a pure population of cells, while the retinal tissue represented a mixed population of macroglia, microglia, neurons, as

well as components of the vasculature. We also observed differences in the profile of regulated genes between the sodium peroxynitrite and BMP7 treated cells. This observation is consistent with the idea that various factors are responsible for driving specific aspects of the gliosis response [3, 69, 102].

In addition to differential expression between peroxynitrite and BMP7 treatments *in vitro*, as well as *in vivo* versus *in vitro* responses, we also noted that there were substantial differences between the regulation of various markers at the mRNA and protein level. The asymmetry has also been noted by other investigators who have compared mRNA and protein levels, indicating that there may be multiple levels of regulation involved in gliosis [76, 139–142]. Although mRNA levels showed increased regulation both *in vivo* and *in vitro*, a similar change was not detected at the protein level. mRNA translation and protein levels are regulated in the cell by a number of systems: regulation of mRNA localization and translational repression mediated by RNA binding proteins, regulation via micro RNAs, ubiquitin proteasome system as well as changes in protein stability [143, 144]. Here we do not observe a linear correlation between the mRNA and protein levels in the gliosis models analyzed. We, thus, hypothesize that protein is regulated at the mRNA translation level, mediated either by RNA binding proteins or by micro RNAs. Furthermore, protein stability may also be regulated in BMP7 mediated gliosis leading to differences in mRNA and protein levels. mRNA binding protein such as cytoplasmic polyadenylation element binding protein (CPEB) has been previously shown to upregulated in the gliosis [145]. One of the downstream targets of the TAK mediated BMP cascade is the p38-MAPK [73, 146]. p38-MAPK can regulate the phosphorylation, and thereby, activation of CPEB [145]. Micro RNAs (miRNAs) are small 22-25 nucleotide long non coding RNA which play an important role in cell fate and development. miRNAs have been found which are specific to the nervous system and also to the retina, and BMPs have also been shown to regulate miRNA levels [147–150]. Further, regulation of miRNAs have also been observed in astrocytes following injury in the spinal

cord [151]. The miRNAs bind to their target RNA and can either direct it to degradation or can repress translation. Competing endogenous RNA (ceRNA) interaction mediated by miRNA which can target more than mRNA has been previously reported in diabetic retinopathy in RPE cells [152]. Similar interactions may also be prevalent in the glial cells leading to translational regulation.

In this study, we observe a more severe response in gliosis *in vivo* as compared to *in vitro*. Immunohistochemistry for BMP receptors in mouse retina showed a large population of neuronal cells other than Müller glia and retinal astrocytes to also express them. Thus, binding of BMP7 to receptors in these cells and also to Müller glia, could amplify the gliosis signal leading to a comparatively severe response in the mouse retina.

2.4.4 Extracellular matrix and reactive gliosis

One of the responses seen during reactive gliosis is extracellular matrix modifications. These changes in the matrix are primarily due to the regulation of MMPs, which remove extracellular matrix molecules, and the regeneration-inhibiting chondroitin sulfate, ultimately leading to the formation of a glial scar [43, 153]. The formation of the scar serves to protect the injured site while also preventing axonal regrowth [110].We observe here an increase in RNA levels of extracellular matrix molecules such as *Ncan, Pcan* and *Mmps*, both *in vivo* and *in vitro* (Figure 2.3, Figure 2.4 and Figure 2.8). Furthermore, immunohistochemistry of the BMP7 injected mouse retina also showed an increase in localization of NCAN in the inner nuclear layers of the retina (Figure 2.8). Other members of the TGF-β family have been previously shown to increase proteoglycan production in reactive glial cells [103].

We observe here an increase in NCAN at the 7 day stage when compared to the earlier 3 day time point, a result similar to a previous study [103]. Further study is necessary to determine if the effects of BMPs on the extracellular matrix production are direct or indirect.

3. MICROGLIA ACTIVATION IS ESSENTIAL FOR BMP7-MEDIATED RETINAL REACTIVE GLIOSIS

3.1 Introduction

The mammalian retina consists of at least two distinct glial populations. The macroglia, which includes Müller glia and retinal astrocytes, and the microglia. The Müller glia are the primary glial cells found in the retina, having their nucleus in the inner nuclear layer (INL) with processes extending from the inner limiting membrane at the vitreal border to the outer limiting membrane at the base of photoreceptor inner segments [11]. Retinal astrocytes migrate into the retina from the optic nerve and reside in the nerve fiber layer [154]. The microglia are the resident macrophages found scattered through all the retinal layers [33]. The retina of some species also contain oligodendrocytes and another glial-like cell type, known as the non-astrocytic inner retinal glia-like (NIRG) cells, that reside in the INL of the chick retina [79, 155].

Müller glial cells and retinal astrocytes are essential for maintaining retinal homeostasis. Any injury or disease leading to retinal damage or disruption of the homeostasis triggers the glial cells to become active, a response termed reactive gliosis. Reactive gliosis has been observed in all retinal disease and injury models including glaucoma, age related macular degeneration, and diabetic retinopathy [42, 46, 78, 156]. Reactive gliosis is characterized by hypertrophy, altered function brought about by changes in expression of proteins such as glutamine synthetase (GS), S100β, extracellular matrix proteins, chondroitin sulphate proteoglycans (CSPG), matrix metalloproteinases (MMP), and an increase in growth factors such as ciliary neurotrophic factor (CNTF), leukemia inhibitory factor (LIF), and vascular endothelial growth factor (VEGF) [41, 157]. Multiple factors can trigger gliosis, including the bone mor-

phogenetic proteins (BMPs) [65, 81, 158]. Recent evidence from the Belecky-Adams laboratory showed that BMP7 triggered gliosis in both the Müller glia and astrocytes of the mouse retina; however, the mechanism by which BMP7 triggers gliosis is unknown [157].

The BMPs are growth factors that belong to the transforming growth factor beta (TGF-β) superfamily. BMP signaling is initiated following the binding of the ligand to serine threonine kinase receptors. This leads to the activation of the receptors and the subsequent phosphorylation and activation of downstream signaling components. In the canonical pathway, the BMP signals by phosphorylation and activation of downstream receptor SMADs (RSMADs). The RSMADs form a dimer with the co-SMAD (SMAD4) and are shuttled to the nucleus to regulate transcription. BMP can also mediate the activation of a non-canonical pathway referred to as the BMP mitogen -activated protein kinase pathway (BMP-MAPK). In the BMP-MAPK pathway, the receptors recruit the X-linked inhibitor of apoptosis (XIAP) to a complex containing TAB1 and TAK1, thereby activating TAK1. TAK1 then activates downstream kinases, eventually activating NF-κB, p38 and JNK MAPKs [73, 75]. In the CNS, BMP regulation has been observed in various diseases and injury models, such as spinal cord injuries, axonal damage and ischemia [77,158,159]. In the retina, upregulation of BMPs and their signaling components are observed in the photo-damaged retina injury model and in diabetic retinopathy [133, 160, 161].

Microglia are the innate immune cells of the retina. In their resting state, the microglia act as sentinels, extending their processes throughout the retina. In the mouse retina, the microglia are initially found in the ganglion cell layer, entering the retina from the ciliary marginal zone and vitreous. By post natal day 7, the microglia spread to the rest of retinal layers, finally resting in the plexiform layers [162]. Upon receiving signals from injured or dying cells, the microglial cells become activated: they retract their processes, undergo an increase in cellular area, become amoeboid in

shape, and migrate to the area of injury or disease to phagocytize cellular debris and metabolic products [31, 163]. Stimuli such as neuronal loss or damage, inflammation and nerve degeneration, activate the microglia into a motile effector cell with altered morphological characteristics [164, 165].

Microglial activation has been observed in all retinal diseases, including diabetic retinopathy, age related macular degeneration, glaucoma and models of retinal pathologies. In addition to the morphological changes following activation, microglia also induce a change in production of various cytokines such as interleukin 1 beta (IL-1β), IL-6 and interferon gamma (IFN-γ), chemokines such as regulated on activation, normal T cell expressed and secreted (RANTES), monocyte chemotactic protein 1 (MCP1); growth factors such as colony stimulating factor (CSF) and VEGF, and various scavenger receptors and antigen presenting molecules such as the scavenger receptor A (SR-A) and major histocompatibility complex (MHC), respectively / [33, 54]. Furthermore, research has revealed that activated microglia can be further classified into the following phenotypes: the M1 or pro-inflammatory phenotype, and the M2 or the anti-inflammatory phenotype [55, 166]. Polarization to the M1 phenotype, following exposure to factors such as lipopolysaccharide (LPS) and IFN-γ, the microglia upregulate pro-inflammatory factors such as IL-1β, tumor necrosis factor alpha (TNF-α), inducible nitric oxide synthase (iNOS), SRs and MHC-II [167, 168]. The M2 phenotype plays a role in the resolution of the inflammation and tissue remodeling. This phenotype is induced by factors such as IL-4 and IL-10 or through the maturation of the M1 cells. This phenotype was characterized by an upregulation of markers such as arginase-1 (Arg-1) and mannose receptor (Mr), cytokines such as IL-10, IL-13 and growth factors such as TGF-β and VEGF [167, 169].

Signals from neurons and macroglia, such as fractalkine, neurotransmitters and neurotrophins help keep the glial population in the quiescent state [42, 170]. Activation of the glial cells has been found to be mediated by similar stimuli *in vitro* and in

retinal disease models *in vivo* [42, 164, 171, 172]. Cytokines and other inflammatory markers such as TNF-α, iNOS, CNTF and LIF are not only regulated during gliosis, but are also factors known to act on the glial cells and regulate gliosis [68, 160, 173]. Activated microglia are known to regulate Müller cell activity directly, regulating cell morphology, proliferation and gene expression [59, 165]. Activated microglia can also regulate the generation of Müller glia-derived progenitors [174]. Here we provide evidence that supports the hypothesis that BMP7 indirectly triggers gliosis by activating the pro-inflammatory state of retinal microglia.

3.2 Methods

3.2.1 Cell culture

Mouse retinal astrocytes were isolated in the Sheibani lab and maintained as previously described in [116, 157]. Microglial cells were isolated from retinas of newborn (P0-P4) immortomouse back crossed into C57BL/6J as described in [175] with some modifications. Briefly, the retinas were placed in a solution of Trypsin/EDTA (5 ml; 0.25% trypsin and 1 mM EDTA; ThermoFisher Scientific) and incubated at 37°C for 5 min. Following incubation, the samples were triturated by pipette, and 5 ml of DMEM with 10% FBS was added to stop trypsin activity. The digested tissue was centrifuged for 5 min at 400xg at room temperature, the supernatant was carefully aspirated, the pellet re-suspended in the microglia medium [a 1:1 mixture of DMEM: F12 (ThermoFisher Scientific) containing 10% FBS, and 44 U/ml of interferon-γ (R&D Systems, Minneapolis, MN)], plated on a single well of a 6-well plate, and incubated in a tissue culture incubator at 33°C and 5% CO_2. The cells were allowed to grow for 1-2 weeks and fed every 3-4 days until nearly confluent. The medium was then removed from the plate and rinsed with PBS containing 0.04% EDTA. The plate was then incubated with 2 ml of PBS containing 0.04% EDTA and placed on a multipurpose rotator at 100 rpm at room temperature for 20-30 min. The supernatant was

collected in a 15 ml tube containing 3 ml of DMEM with 10% FBS and centrifuged at 400xg for 5 min. The detached cells were then re-plated in the microglia medium, allowed to reach confluence, and expanded into 60 mm dishes. The purity of the microglial cultures was inspected by immunocytochemical staining and flowcytometric analysis for F4/80 (eBiosciences; San Diego, CA) and keratin sulfate (Seikagaku Corporation; Jersey City, NJ). The purity of culture was nearly 95% using FACS and immunostaining analysis. Astrocytes and microglia were grown in tissue culture dishes (BD Falcon) in an incubator with 5% CO_2 at 33°C, and passaged every 5-7 days using trypsin-EDTA and the medium changed every 3-4 days. Cells were treated with 1μl/ml vehicle (4mM HCL with 0.1%BSA), 100 ng/ml of mouse bone morphogenetic protein 7 (BMP7; R&D systems), 300 ng/ml mouse interferon-gamma (IFN-γ; R&D systems) or 100 ng/ml LPS (Sigma). Medium from microglial cells incubated with BMP7 or vehicle (conditioned medium) for 24 hour (h) was used to treat retinal astrocytes. The conditioned medium was added to the retinal astrocytes medium at 25% concentration in the presence of DMSO or 2.5 μM ALK2/ALK3/ALK6 inhibitor LDN193189 (Cuny et al. 2008). The retinal astrocytes were allowed to grow for 24 h, after which cells were harvested for RNA isolation and RT-qPCR analysis.

3.2.2 Experimental groups

Experiments were carried out in 4 - 8 weeks old male C57BL/6J. All procedures were in accordance with the guidelines set by the Institutional Animal Care and Use Committee (IACUC) at the school of science IUPUI (protocol number SC230R). For BMP7 injection studies, n=8 mice were used with the left eye injected with the vehicle and the right eye injected with BMP7. For the PLX studies, two groups of mice were considered, the age matched control chow group (n=12) and the PLX group (n=12), kept on PLX chow diet. For the PLX BMP7 injection studies, two groups of mice were considered: the age matched control group (n=12) and the PLX group

(n=12), kept on the PLX diet. Both the groups were injected with the vehicle control in the left eye and BMP7 in the right eye. P30 VE-YFP mice (n=3), which express YFP in endothelial cells, generated by crossing a line of mice containing an enhanced yellow fluorescent protein (YFP) with a floxed stop sequence upstream of the YFP (B6.129X1-Gt(ROSA)26Sortm1(EYFP)Cos/J; strain number 006148 Jackson laboratory) [176] with the VE-cadherin-cre line (B6.FVB-Tg(Cdh5-cre)7Mlia/J; stock number 006137 Jackson laboratory) (Alva et al. 2006), were used for immunofluorescence experiments determining PU.1 co-localization in the retina.

3.2.3 Intraocular Injections

Postnatal day 30 (P30) C57BL/6J mice were anaesthetized with ketamine and xylazine cocktail. Mice were injected intravitreally with 1 μl of vehicle (4mM HCL with 0.1%BSA) or 1 μl BMP7 (20 ng/μl) as previously stated in [157]. Intraocular injections were performed using a manual microsyringe (World precision instruments) and pulled glass micropipettes.

3.2.4 Microglia Ablation

C57BL/6J mice were kept on chow feed containing 1200 ppm PLX5622 (PLX; Plexxikon Inc.) for up to 21 days, starting at P30. Eyes were harvested at 7, 14 and 21 days following start of the PLX diet for assessment of loss of microglia. The control mice were kept on the control chow supplied by Plexxikon Inc. To determine if loss of microglial cells affected BMP7-mediated gliosis, mice were maintained on PLX chow for the entirety of the experiment. In some animals, eyes were injected with 1μl vehicle (4mM HCL with 0.1%BSA) or 1μl (20ng/μl) BMP7 14 days following treatment with PLX, and eyes were harvested and processed 3 and 7 days post-injection.

3.2.5 Tissue Processing

Eyes from euthanized C57BL/6J mice were enucleated, washed in PBS, and either fixed in 4% paraformaldehyde (PFA) for immunofluorescence (IF) or dissected to isolate retina for preparation of RNA and/or protein. For IF analysis, enucleated eyes were washed and fixed in 4% PFA, incubated in ascending series of sucrose and frozen in a sucrose OCT solution as previously described [157] Thick sections (12 μm) were cut using Leica CM3050S cryostat onto Superfrost Plus slides (ThermoScientific) and stored at -80°C until use. Retinas from enucleated eyes were isolated as previously described [157]. Isolated retinas were immediately processed for RNA isolation using RNeasy kit (Qiagen).

3.2.6 RT-qPCR

Reverse transcriptase-quantitative polymerase chain reaction (RT-qPCR) was performed to detect changes in markers associated with gliosis and inflammation as previously described [157]. The primers for RT-qPCR analysis are listed in Table 2.2. Included in this table is the accession number of each gene, the sequence of each primer, product length, and calculated efficiency of each primer. Primers used for assessing changes in inflammation are listed in Table 3.1. RT-qPCR was performed using SYBR green master mix (Roche) with the reactions carried out in the LighCycler480 system (Roche). The change in RNA levels was measured using the $2^{-\delta\delta Ct}$ method, where Ct is the crossing threshold / crossing point (Cp) value. Relative RNA levels were calculated using the geometric means from the Ct value derived from three housekeeping genes: *β- 2 Microglobulin (β2m), succinate dehydrogenase complex subunit A (Sdha)* and *signal recognition particle 14kDa (Srp14)*. A no template control was also tested for each marker.

Table 3.1.
List of RT-qPCR primers

Gene	**Primer**	**Sequence**	**Length (bp)**
Ccl5	Forward	TGCCCACGTCAAGGAGTATTT	111
	Reverse	ACCCACTTCTTCTCTGGGTTG	
Cd45	Forward	TGACCATGGGTTTGTGGCTC	134
	Reverse	TTGAGGCAGAAGAAGGGCAT	
Cd68	Forward	AAGGGGGCTCTTGGGAACTA	139
	Reverse	AAGCCCTCTTTAAGCCCCAC	
Csf1	Forward	ACCAAGAACTGCAACAACAGC	91
	Reverse	GGGTGGCTTTAGGGTACAGG	
Iba1	Forward	ACGAACCCTCTGATGTGGTC	118
	Reverse	TGAGGAGGACTGGCTGACTT	
Il-1β	Forward	TGTCTGAAGCAGCTATGGCAA	141
	Reverse	GACAGCCCAGGTCAAAGGTT	
Il-6	Forward	ACTTCACAAGTCGGAGGCTT	111
	Reverse	TGCAAGTGCATCATCGTTGT	
Ifn-α	Forward	CAAGCCATCCCTGTCCTGAG	131
	Reverse	TCATTGAGCTGCTGGTGGAG	
Ifn-γ	Forward	CAACAGCAAGGCGAAAAAGGA	90
	Reverse	AGCTCATTGAATGCTTGGCG	
Irf8	Forward	CGGATATGCCGCCTATGACA	73
	Reverse	CTTGCCCCCGTAGTAGAAGC	
Gm-csf	Forward	AGTCGTCTCTAACGAGTTCTCC	178
	Reverse	AACTTGTGTTTCACAGTCCGTT	
Sdha	Forward	GGACAGGCCACTCACTCTTAC	130
	Reverse	CACAGTGCAATGACACCACG	
Srp14	Forward	CCTCGAGCCCGCAGAAAA	134
	Reverse	CGTCCATGTTGGCTCTCAGT	
Thbs1	Forward	GCCACAGTTCCTGATGGTGA	149
	Reverse	TTGAGGCTGTCACAGGAACG	
Thbs2	Forward	GGGAGGACTCAGACCTGGAT	105
	Reverse	CGGAATTTGGCAGTTTGGGG	
Tnf-α	Forward	TAGCCCACGTCGTAGCAAAC	136
	Reverse	ACAAGGTACAACCCATCGGC	
Vegf	Forward	ACTGGACCCTGGCTTTACTG	74
	Reverse	CTCTCCTTCTGTCGTGGGTG	

3.2.7 Immunofluorescence

Frozen tissue sections were labeled as previously described in [157]. Antigen retrieval was performed by using 1% sodium dodecyl sulfate (SDS) in 0.01M PBS (5 min at room temperature) or by heat antigen retrieval method. Briefly, sections were washed with 1X PBS, post-fixed with 4% PFA, permeabilized with methanol. Sections were then incubated in 10mM sodium citrate buffer at 65°C for 45 min, allowed to cool at room temperature (RT) for 20 min, rinsed in deionized (DI) water 3X and washed in PBS once. To reduce autofluorescence, slides were then incubated 1% sodium borohydride in PBS for 2 mins at RT. Slides were then blocked with 10% serum (goat or donkey) in 1XPBS with 0.25%TritonX-100 for 1 h followed by primary antibody diluted in blocking buffer overnight at 4°C. Slides were then incubated with Dylight conjugated secondary antibodies (1:800; Jackson Immunoresearch) or Alexa flour (1:500; Invitrogen) conjugated secondary for 1 h at RT in the dark, washed with 1X PBS, incubated with Hoechst staining solution (2 μg/ml in PBS) and then mounted with Aqua Polymount (Polysciences).

Biotin-streptavidin amplification was done by incubating slides with biotinylated antibody (1:500; Vector Labs) for 1 h at RT followed by Dylight conjugated to streptavidin (1:100; Vector Labs) for 1 h at RT, in lieu of Dylight or Alexa flour conjugated secondary antibodies. For co-labeling involving primary antibodies made in the same host, tyramide signal amplification was performed as per manufacturers protocol (Perkin Elmer). For primary antibodies made in mouse, reagents from the mouse on mouse kit (Vector Labs) were used for blocking and primary antibody dilution. Labeled slides were imaged using Olympus Fluoview FV 1000. Antibodies used for immunofluorescence are listed in Table 3.2.

Cell counts were performed using the cell counter plugin of ImageJ. 40x images (n=9) of retinal sections labeled with SOX9, CALBINDIN, CHX10 and BRN3A and 60X

image of retinal flatmounts (n=8) labeled for G α TRANSDUCIN were used for cell count analysis. Retinal thickness was measured on cross section of retina 200 μm away from the optic nerve.

3.2.8 Western Blotting

Extraction of proteins from retinal tissue was performed using lysis buffer as previously described in [157]. Briefly, retinal tissue was homogenized in PBS and centrifuged at 13,000 rpm, 4°C for 10 min. The supernatant was discarded and the pellet incubated with lysis buffer (150mM NaCl, 50mMTris pH 8.0, 2mM EDTA, 5μl TritonX-100; 100mM PMSF and protease inhibitor cocktail, RPI corp.) for 20 min at 4°C. The samples were centrifuged at 13,000 rpm, 4°C for 10 min and total protein was estimated using BCA protein assay kit (ThermoScientific).

Forty μg of protein was loaded onto 4-20% SDS precast gels (Expedeon), placed in a Biorad gel run apparatus and run at 150V for 1 h. Proteins were transferred onto a PVDF membrane, which was blocked with a 5% milk in tris buffered saline tween 20 (TBST) at RT for 1 h on a shaker. The blots were incubated with primary antibody diluted TBST at 4°C overnight on a shaker. The following day, the blots were washed in TBST and incubated with HRP conjugated secondary diluted 1:5000 in TBST for 1 h at RT. Blots were washed in TBST, incubated with super signal west femto chemiluminescent substrate (ThermoScientific) and visualized on x-ray film. β-TUBULIN was used as a loading control and the concentrations of antibodies used are listed in Table 3.2.

Table 3.2.
List of antibodies used

Antibody	**Company**	**IHC concentration**	**Flatmount concentration**	**Western blot concentration**
BRN3A	Chemicon	1:250		
CALBINDIN	Sigma	1:250		
GFAP	Dako (polyclonal)	1:250	1:100	
GFAP	Dako (monoclonal)			1:1000
GαT	SantaCruz		1:100	
IBA1	Wako	1:500	1:250	
NEUROCAN	R&D	1:100		
PU.1	Cell signaling	1:100		
phosphoSMAD 1/5/8	Cell Signaling	1:50		
phosphoTAK1	Abcam	1:500		
S100β	Abcam	1:300		1:1000
CHX10	Exalpha	1:500		
SOX2	SantaCruz	1:250		
SOX9	Millipore	1:500		
TXNIP	SantaCruz			1:250

3.2.9 ELISA

Enzyme linked immunosorbent assay (ELISA) for IFN-γ was performed on media from treated cells *in vitro* or from whole mouse retina protein lysates using the mouse IFN-γ ELISA kit (Cat # ENEM1001, ThermoScientific) as per manufacturers protocol.

3.2.10 Retinal Flatmounts

Preparation of retinal flatmounts and immunolabeling was done as described in [177]. Briefly, enucleated eyes were washed in 1X PBS, fixed in 4%PFA for 15 min, transferred to 2X PBS on ice for 10 min followed by retina isolation. Four to five radial incisions were made in the retina to create a petal shape. Excess PBS was absorbed and retinas were transferred to cold methanol (-20°C) for 20 mins. The tissue was washed with 1X PBS and blocked in Perm/Block solution (1XPBS, 0.3% TritonX-100, 0.2% bovine serum albumin and 5% donkey or goat serum). Tissue was then washed in PBSTX (1XPBS, 0.3%TritonX-100) and incubated with primary antibody (Table 3.2) overnight at 4°C. On the following day, the tissue was washed in PBSTX, incubated with secondary antibody, washed, incubated with Hoechst solution and mounted onto a slide with Aqua Polymount (Polysciences, Inc). Labeled slides were imaged using Olympus Fluoview FV 1000.

Morphological analysis of labeled microglia (n=4 per timepoint) for changes in area and number of branches was performed using the Scholl analysis plugin in Fiji image analysis software (Ferreira et al. 2014). Briefly, the flatmount image was loaded on to the Fiji software and converted to binary. To calculate the area of the cell, the "Measure plugin was selected from the Analyze options. To determine number of branches, a center of analysis was defined via the straight line method. This line was drawn from the center of the cell to the end of the longest branch to define a

valid Startup ROI. The program was run on the default parameters with the starting radius set at 10 pixels.

3.2.11 Statistical Analysis

Statistical analysis was performed via unpaired Studentss t-test using SPSS software (IBM) between control/vehicle and treated groups for RT-qPCR, cell counts and microglia morphology. RT-qPCR and densitometries from PLX and control mice injected with vehicle or BMP7 was analyzed via one way ANOVA with Tukeys test for post hoc analysis. $p<0.05$ were considered to be statistically significant.

3.3 Results

3.3.1 BMP signaling in retinal microglia

Previous studies have shown that BMP7 triggers reactive gliosis of the retinal macroglia. Both the canonical as well as the non-canonical BMP-MAPK pathways were active in the retinal Müller cells and astrocytes following BMP7 treatment (Dharmarajan et al. 2014). However, the mechanism by which BMP7 triggered gliosis remains unclear. To determine if any of these pathways were activated in the microglia of control- or BMP7-treated retina, double-label immunohistochemistry was performed using antibodies to phospho SMAD 1/5/9 (pSMAD), phospho TAK1 (pTAK1), and PU.1 on adult retinas following intravitreal injection of vehicle- or BMP7- (Figure 3.1). In both vehicle- (Figure 3.1A–D) and BMP7-treated retinas (Figure 3.1E–H), sections showed nuclear co-labelling with PU.1 and pSMAD. In contrast, pTAK1 was localized primarily to the nuclei of GCL of vehicle-injected retinas with no apparent co-localization with PU.1 (Figure 3.1I–L), but co-labeled PU.1+ cells in the BMP7-treated retinas, in addition to other cells in the INL and GCL (Figure 3.1M–P).

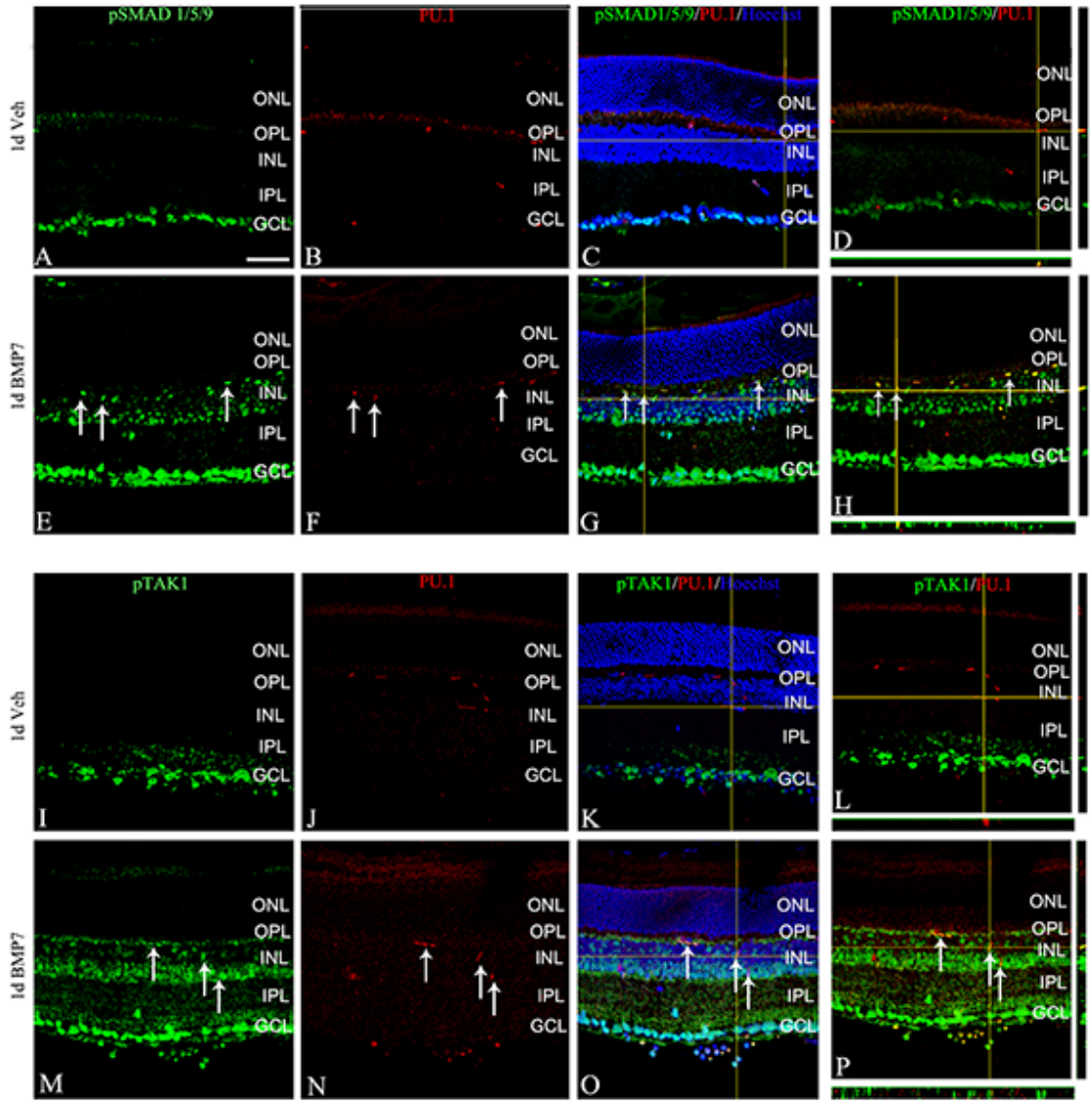

Fig. 3.1. pSMAD and pTAK1 are localized to retinal microglia (Continued on next page).

There was also a striking increase in the localization of pTAK1 in the both inner and outer plexiform layers of BMP7-treated retinas that was not apparent in vehicle-treated retinas (Figure 3.1M–P). Retinal sections were also co-labeled with IBA1 and pTAK1 or pSMAD to show localization in microglia (Figure 3.2). Negative controls showed no label (Figure 3.3).

Fig. 3.1. pSMAD and pTAK1 are localized to retinal microglia. Retinal sections from P30 mouse injected with vehicle or BMP7 24 h post-injection were double-labeled with antibodies that label microglial nuclei (PU.1) and phospho SMAD 1/5/9 (pSMAD; A–H) or phospho TAK1 (pTAK1; I–P). Thin plane confocal microscopy images with y,z (strips to right of the panel) and x,z planes (strips at the bottom of the panels) shown in (D), (H), (L), and (P). pSMAD-labeled cells were primarily found in the GCL in the vehicle-treated retina, with some co-localization with the nuclear microglial marker PU.1 (A–D). The BMP7-injected retina had an increase in pSMAD expression in the INL as well as substantial co-localization with PU.1 (E–H). In contrast, vehicle-injected retina showed pTAK1 expression in the GCL with little to no PU.1 co-localization (I–L), while the BMP7-injected retinas showed increased levels of pTAK1 levels in the INL, as well as significant co-localization with PU.1 (M–P). Magnification bar in A=50 μm, for images (A–P).

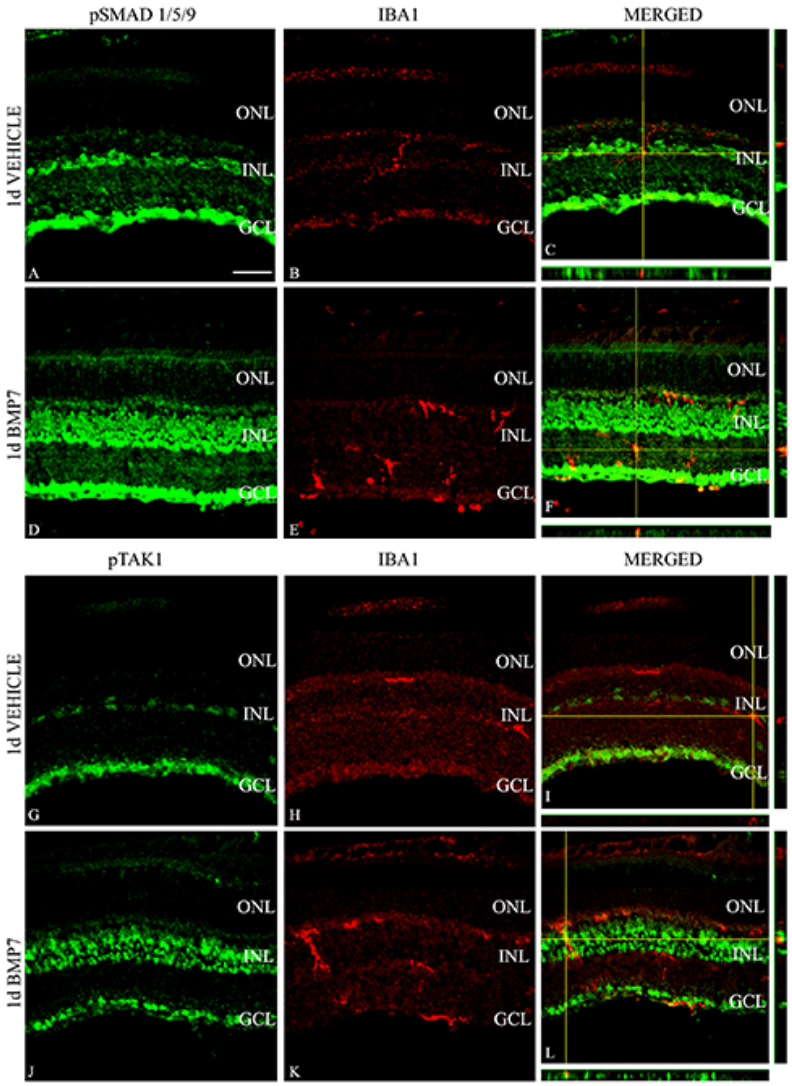

Fig. 3.2. Expression of BMP signaling molecules in microglia in vehicle and BMP7-injected retinas (Continued on next page).

Fig. 3.2. Expression of BMP signaling molecules in microglia in vehicle and BMP7-injected retinas.Retinal sections from P30 mouse injected with vehicle or BMP7 24 h postinjection were double-labeled with antibodies that labels microglia cytoplasm (IBA1) and phospho SMAD 1/5/9 (pSMAD; A–F) or phospho TAK1 (pTAK1; G–L). Thin plane confocal microscopy images with y,z (strips to right of the panel) and x,z planes (strips at the bottom of the panels) shown in C, F, I and L. pSMAD-labeled cells were primarily found in the GCL in the vehicle-treated retina, with some co-localization with the cytoplasmic microglial marker IBA1 (A–C). The BMP7-injected retina had an increase in pSMAD expression in the INL as well as substantial co-localization with IBA1 (D–F). Vehicle-injected retina showed pTAK1 expression in the GCL with little to no IBA1 co-localization (G–I), while the BMP7-injected retinas showed increased levels of pTAK1 levels in the INL, as well as significant co-localization with IBA1 (J–L). Magnification bar in A=50 μm, for images (A–L).

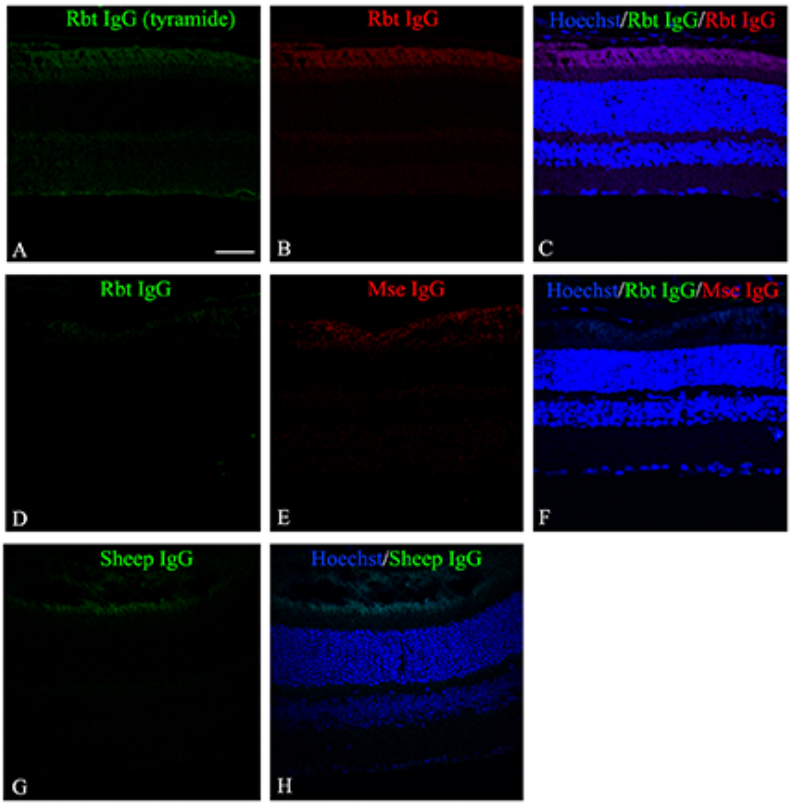

Fig. 3.3. Negative control of immunofluorescence labels. Retinal sections from P30 mouse labeled with rabbit immunoglobulin G (Rbt IgG; A–C, D, F), mouse IgG (Mse IgG; E, F), and sheep IgG (G, H) to determine background fluorescence. Images of sections labeled with the nuclear stain, Hoechst merged with the images of green and red channels are shown in C and F. Panels A–C represent sections, which were labeled with IgG following the procedure used for tyramide amplification when using two antibodies for the same species. Images in D–F represent sections co-labeled with rabbit and mouse IgG. Images A–C are negative controls for Figure 3.1 and Figure 3.2. Images D–F are negative controls for sections labeled with GFAP, S100β, CALBINDIN, BRN3A, CHX10, SOX9, and IBA1. Images G and H are negative control sections for NCAN-labeled slides. Magnification bar in A=50 μm, for all panels.

3.3.2 BMP7 induces inflammatory changes *in vivo*

To determine whether BMP7 regulated inflammatory signals that could then either trigger or enhance the gliosis response, BMP7-treated retinas were analyzed for mRNA levels of pro-inflammatory markers (Figure 3.4A). For the analyses of mRNA levels, values plotted in graphs were all relative to control levels which were set to a value of 1.0; hence, increases in mRNA levels in comparison to controls are bars above a level of 1.0, while a decrease is represented by bars below the level of 1.0. Three days post-injection, increases of 1.5-fold or more in mRNA levels of *Tnf-α, Il-1β* and *Ifn-γ* were present. However, larger increases were evident in multiple factors 7 days post-injection, including *Gm-Csf, Csf, Ifn-α, Ifn-γ, Il-6, Vegf, thrombospondins-1 and-2 (Thbs1 and Thbs2)* and *Cd68*. We also observed more than a two-fold increase in microglial marker *Iba1* and *Irf8*, markers for activated microglia.

To determine if the increases in pro-inflammatory markers present in BMP7-treated retinas were mediated by retinal microglial cells, the effect of BMP7 treatment on isolated mouse retinal microglial cells *in vitro* was observed using RT-qPCR. mRNA levels were investigated in microglial cells incubated with vehicle or BMP7 for 3, 6, 12, or 24 h (Figure 3.4B). Again, changes in mRNA levels relative to controls were plotted, where a value of 1.0 indicates levels of control mRNA. Following 3 h of incubation with BMP7, only levels of *Ifn-γ* were 1.5-fold greater, whereas at 6 h the average mRNA levels of *Gm-csf, Ifn-γ, Csf1, Tnf-α* and *Il-6* and *Cd68* were increased to 1.5-fold above control or greater (Figure 3.4B). By 24 h of incubation, many of the molecules levels were decreased in comparison to the 6 h time point; however, Ifn-γ and Thbs2 were increased in comparison to control and 6 h mRNA levels. As a positive control for inflammation, microglia were incubated with LPS for 3 h (Figure 3.4C). To determine if the changes in RNA levels are being translated to protein, we determined IFN-γ levels by an ELISA using medium from microglial cells incubated with BMP7 for 24 h and whole retinal lysates from mice treated with vehicle

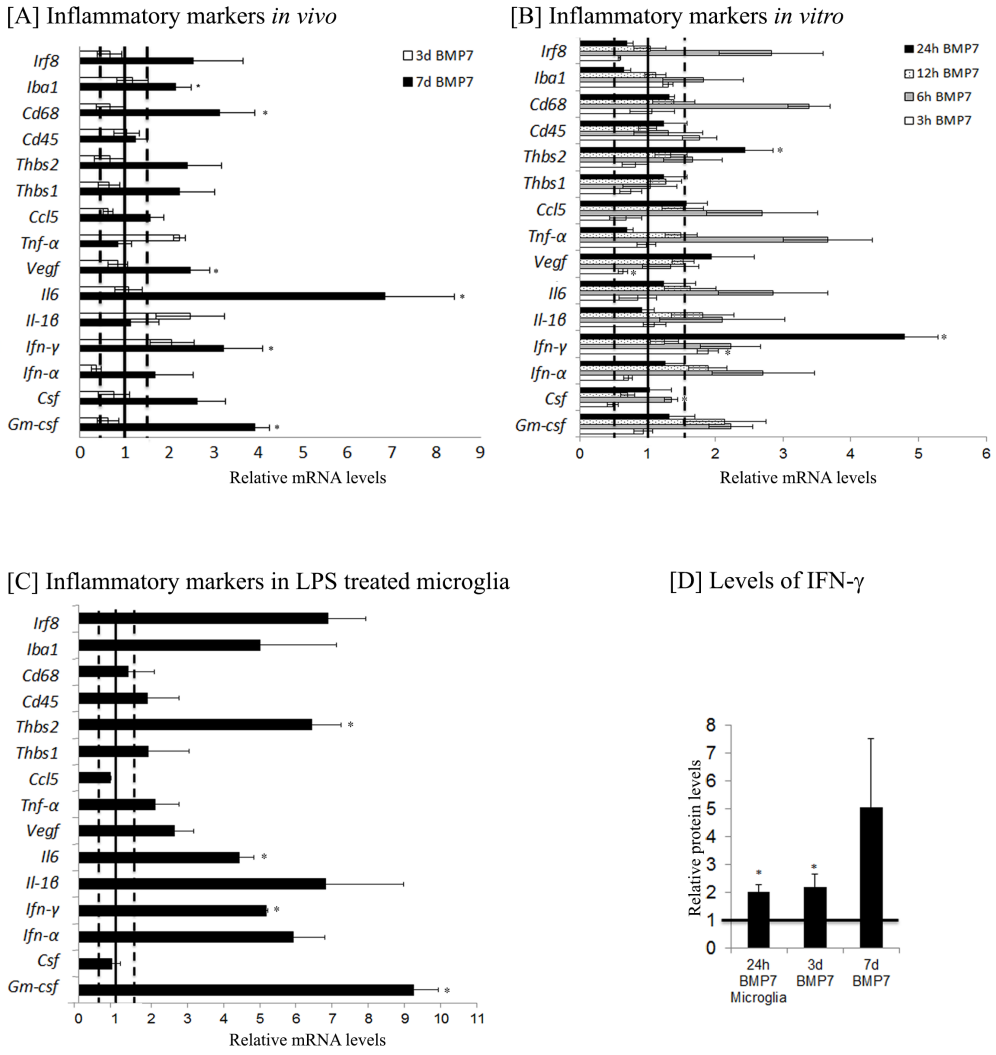

Fig. 3. 4. BMP7 injection triggers inflammatory changes in the mouse retina (Continued on next page).

Fig. 3.4. BMP7 injection triggers inflammatory changes in the mouse retina. Expression levels of a panel of pro-inflammatory markers were analyzed by RT-qPCR in RNA samples from mouse retina injected with vehicle or BMP7, harvested 3 and 7 days post-injection (A). At 3 days post-BMP7 injection, about a 2-fold increase in RNA levels, relative to the vehicle controls, was observed in levels of *Ifn-γ, Tnf-α*, and *Il-1β*. Seven days post-BMP7 injection, 2-fold increase in levels was observed in *Csf, Vegf, Thbs1*, and *Thbs2*, and greater than 3-fold increase in *Gm-csf, Ifn-γ, Il6*, and *CD68* RNA levels relative to the vehicle-injected control. Mouse retinal microglial cells treated with BMP7 for 3, 6, 12, and 24 h were also analyzed for changes in RNA levels of inflammatory markers (B), with LPS treatment used as a positive control (C). *In vitro* treatments showed a significant increase in Ifn-γ levels at the 3-h time point. At 6 h post-BMP7 treatment, mRNA levels of *Gm-csf, Ifn-γ, Csf, Tnfα, Il-6* and *Cd68* were increased to 1.5-fold or greater. By 12 h, we observed no significant differences between BMP7 and vehicle-treated samples. At the 24-h time point, however, we observed significant increases in the levels of *Ifn-γ* and *Thbs*. The LPS-treated microglia showed a relative increase in most of the markers, with significant increases observed in levels of *m-csf, Ifn-γ, Il-6* and *Thbs2* (C). Protein levels of IFN-γ was also determined via ELISA (D). We observed a 2-fold increase in levels in medium from microglial cells incubated with BMP7 for 24 h and in protein from whole retinal tissue from mice injected with BMP7 for 3 days, when compared to their respective vehicle control. Protein from 7 days BMP7-injected retina showed a 5-fold increase in protein levels compared to the vehicle control. Data shown in graphs represent relative expression levels of RNA or protein of BMP7 or LPS-treated samples to their respective vehicle control. Bars above a level of 1.0 (solid black line) represent an increase in mRNA levels while bars below the level of 1.0 represent a decrease in mRNA levels relative to the corresponding vehicle control. Statistical analysis was performed by unpaired Students t-test. Significant difference from the respective vehicle controls $*$ =p value <0.05.

or BMP7 (Figure 3.4D). Values plotted in graph are relative to the respective vehicle controls; hence, increases in mRNA levels in comparison to controls are bars above a level of 1.0, while bars below the level of 1.0 represent a decrease. We observed a two-fold increase in the IFN-γ protein levels in the astrocytes and microglial cell medium, and a five-fold increase in IFN-γ protein level was detected in retinal lysates 7 days post-treatment with BMP7 compared with vehicle.

Changes in morphological characteristics of microglia following control and BMP7 treatments were subsequently investigated. It has been reported by other investigators that activated microglia increase in area with an increase in branch points (Kreutzberg 1996). Retinal flatmounts of 1 day BMP7- and vehicle-treated retinas were labeled with IBA1 and analyzed for average cell area and number of branch points in cellular processes (Figure 3.5A, B). Graphs show relative changes in the area and number of branches (Median intersections output from the Sholl analysis). Morphological analysis revealed that the BMP7-treated retinas contained microglia with a larger area in comparison to vehicle-treated retinas, and a decrease in the number of branches (Figure 3.5C).

3.3.3 Activated microglia secrete factors that induce gliosis

We have observed that BMP7 is able to activate retinal microglia *in vitro* and *in vivo* (Figure 3.4 and 3.5, respectively). To determine if microglia secrete factors that trigger reactive gliosis *in vitro*, we used conditioned medium obtained from mouse microglia cultures treated with vehicle (vehicle conditioned media) or BMP7 (BMP7 conditioned media) for 24 h, and used for treatment of mouse retinal astrocytes (Figure 3.6B, C, D). Graphs represent mRNA levels in astrocyte cultures treated with BMP7 conditioned media relative to cultures treated with vehicle conditioned media; pretreated with DMSO or LDN193189. Retinal astrocyte cells were incubated

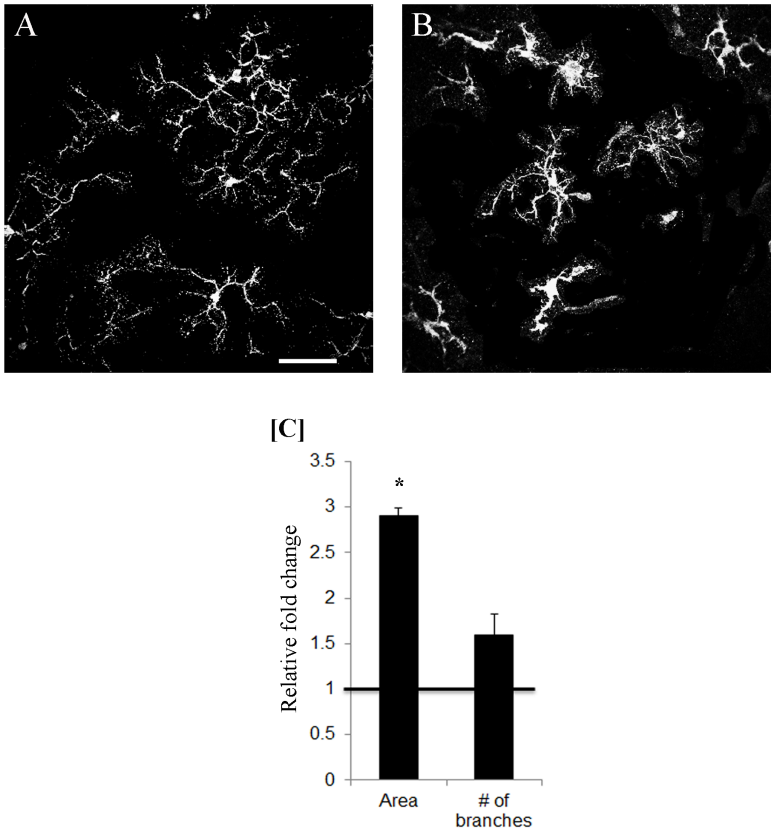

Fig. 3.5. BMP7 alters microglial morphology. Retinal flatmounts from 1 day BMP7- and vehicle-injected retina were labeled for IBA1 (A, B) and analyzed for morphological changes. An increase in the area of the microglia was observed when compared to the vehicle control (C). Number of branches and branch length were also assessed for the treated cells, and increase in the number of branches was observed with a decrease in the branch length of the cells incubated with LPS or BMP7 when compared to the vehicle control (C). Data shown in c represent relative change in area and number of branches in BMP7-treated samples to the vehicle control. Bars above a level of 1.0 (solid black line) represent an increase while bars below the level of 1.0 represent a decrease in the parameter measured, relative to the corresponding vehicle control. Statistical analysis was performed by unpaired Students t-test. Significant difference from the respective vehicle controls $*$ =p value <0.05. Magnification bar in A=50 μm, for images (A, B).

for 24 h with microglial cell conditioned medium and were assessed for changes in markers associated with gliosis. To reduce the possibility that the BMP7 added to the microglial medium might directly affect the astrocytes, an inhibitor of BMP receptors, LDN193189 was added to the conditioned medium (Figure 3.6D). RT-qPCR analysis showed a statistically significant increase in expression of gliosis markers *Gfap, S100β, Gs, Egfr* and *Pcan* 1.5-fold above that of astrocyte cells treated with DMSO and vehicle-treated conditioned media (Figure 3.6B). When BMP inhibitor was added to the astrocyte medium prior to addition of conditioned medium from microglia, statistically significant increases were detected in *Gfap, Gs, S100β, Egfr* and *Tlr4* (Figure 3.6D). Treatment of retinal astrocytes with DMSO or LDN alone, or with conditioned media in presence of DMSO were used as experimental controls (Figure 3.6A, C). We did not observe any changes when cells were treated with LDN alone (Figure 3.6A). Treatment of retinal astrocytes with conditioned media in presence from DMSO showed similar changes in expression as cells treated with conditioned media alone (Figure 3.6C).

3.3.4 PLX ablates retinal microglia

To further investigate the role of microglia in BMP7-mediated gliosis, a means to ablate microglial cells within the retina was sought. Previous reports have shown colony stimulating factor receptor 1 (CSFR1) inhibitor, PLX3397, to selectively ablate microglia in the brain (Elmore et al. 2014). We have used a variant of the drug, PLX5622, supplied by Plexxikon Inc. in chow form to determine its effect on retinal microglia. Starting at postnatal day 30, mice were switched to control chow or chow containing 1200 ppm PLX. The mice continued treatment with the inhibitor-laced chow until sacrificed 7, 14, or 21 days later. Retinal flatmounts from control and PLX mice were isolated 7, 14 and 21 days, and labeled for IBA1 and GFAP (Figure 3.7). Although no apparent change in GFAP was observed (Figure 3.7B–E), there

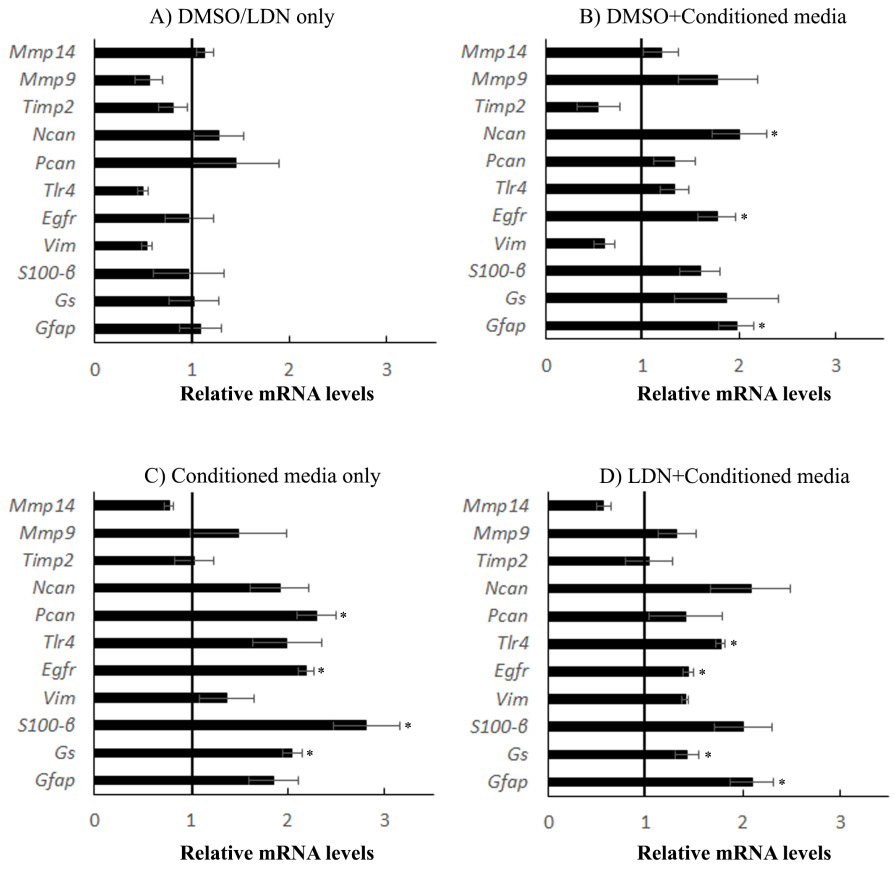

Fig. 3.6. Activated microglia secrete factors that trigger retinal gliosis. Conditioned medium from microglial cells incubated with BMP7 or vehicle for 24 h was added to the medium of the retinal astrocytes, directly or pretreated with LDN193189 (C, D). RNA was isolated from these cells 24 h posttreatment and analyzed via RT-qPCR for a panel of gliosis markers. Statistically significant increase in levels of *Gfap, Gs, S100β, Pcan, Egfr* and *Tlr4* was observed in astrocytes incubated with conditioned medium added directly or pretreated with LDN193189 (C, D). Cells treated with DMSO (carrier for LDN193189) or LDN only (A) or cells pretreated with DMSO and conditioned medium from BMP7 or vehicle-treated microglia (B) were used as experimental controls. Data shown in graphs represent relative expression levels of RNA in retinal astrocyte cells treated with LDN193189 relative to DMSO (A) or with conditioned media from BMP7-treated microglial cells relative to retinal astrocyte cells treated with conditioned media from vehicle-treated microglia (B–D). Statistical analysis was performed by unpaired Students t-test. Significant difference from the respective vehicle controls $*$ = p value <0.05.

was a clear decrease in the number of IBA1+ cells 7 days after starting the PLX diet, and IBA1 immunoreactivity was completely lost by 14 days (Figure 3.7F–M). Retinal tissue sections from these mice were also analyzed for ganglion cells (BRN3A), bipolar cells (CHX10), Müller glia (SOX9) and horizontal cells (CALBINDIN) (Figure 3.7A–D, F–I). Cell counts for labeled cells showed no statistically significant change between the control and PLX treated mice (Figure 3.8K). Retinal flatmounts of PLX and vehicle treated retinas were also labeled with Gα transducin to label photoreceptors (Figure 3.8E, J). Cell count of labeled images showed no statistically significant change in cell numbers (Figure 3.8L). Thickness of retinal sections of the control and PLX treated mice also showed no change (Figure 3.8M).

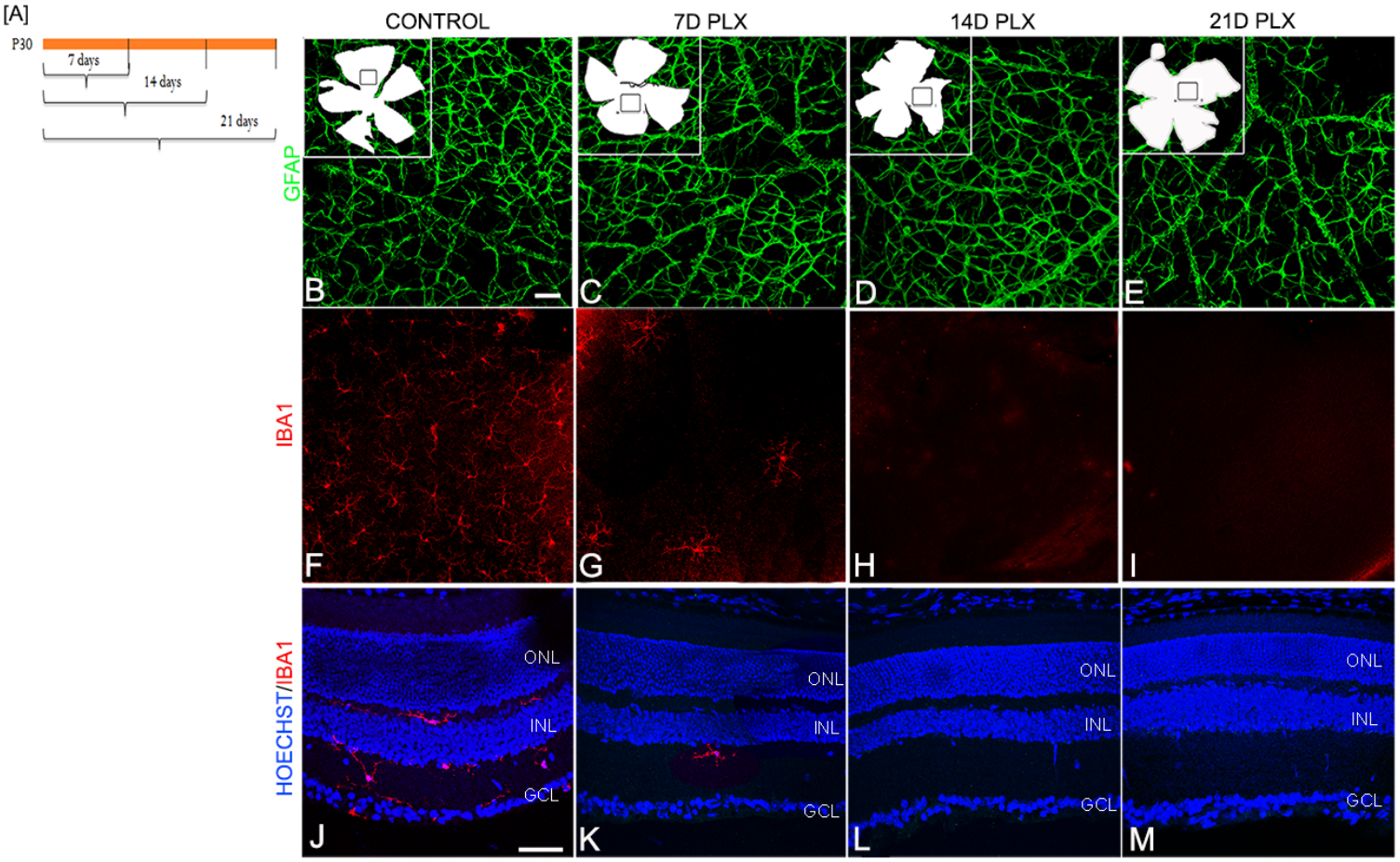

Fig. 3.7. PLX ablates microglia in the retina (Continued on next page)

Fig. 3.7. PLX ablates microglia in the retina. Mice were fed with chow-containing PLX or vehicle dye to determine ablation of microglia in the retina. a Schematic describing the time points for which the mice were fed with chow-containing PLX, following which eyes were harvested. Retinal flatmounts prepared from the eyes harvested at 7, 14, and 21 days were labeled for GFAP or IBA1 (B–I). Insets in B–E indicate the flatmount outline and from where the images (B–I) was taken. While GFAP did not show any difference between the stages examine (B–E), there was a significant decrease in IBA1 label in mice kept on PLX diet for 7 days (F, G). By 14 days, no IBA1 label was found in the retinal flatmount and this absence persisted into the 21-day time point (H, I). Retinal sections control and PLX-treated mice labeled for IBA1 to show loss of microglia in the deeper layers of the retina (J–M). Magnification bar in B=50 μm, for images B–I. Magnification bar in J=50 μm, for images J–M.

3.3.5 Microglial ablation reduces BMP7-mediated gliosis

To determine if microglia were involved in BMP7-mediated gliosis response, mice with ablated microglia (PLX mice) were injected intravitreally with vehicle or BMP7, and mRNA levels of pro-inflammatory markers or gliosis-related molecules were determined by RT-qPCR 7 days (d) post-injection. As in previous graphs, levels of mRNA are relative to levels in the respective vehicle-treated mice. Mice kept on control chow and treated with BMP7 showed an increase in levels of inflammatory markers including *Gm-csf, Ifn-γ, Il-6* and *Iba1*, and gliosis markers including *Vim, Gfap, Egfr, Mmp9, Lcn2* and *Txnip* (Figure 3.9A, B). Analysis of inflammatory markers of mice on PLX chow and treated with BMP7 via RT-qPCR also showed only modest increases in levels of *Il-1β* and *Vegf* compared to vehicle control (Figure 3.9B). mRNA levels of *Gm-csf, Ifn-γ, Il-6, Cd68* and *Iba1* dropped drastically when microglia were not present (Figure 3.9B). RT-qPCR analysis of PLX mice 7 d post-BMP7 treatment showed no increase in mRNA levels of gliosis markers compared to the PLX vehicle controls (Figure 3.9A). Markers indicative of gliosis were further investigated by examining patterns of immunoreactivity for GFAP, S100β, and NCAN (Fig. 3.9A, B). Three days following vehicle or BMP7 injection, the PLX mice showed similar levels of GFAP and S100β label in control and PLX mice (Figure 3.10 A(a, b, d, e, g, h, j, k)). However, 7 d post-injection, the PLX mice showed decreased GFAP and S100β label in BMP7-injected PLX retinas (Figure 3.10B (j, k)), when compared to the control BMP7-injected retinas (Fig. 3.9B (d, e)). NCAN immunofluorescence label did not diminish following PLX treatment in comparison to controls at either 3 d (Figure 3.10A (f, l)) or 7 d post-injection (Figure 3.10B (f, l)). Moreover, levels of NCAN were increased in vehicle-injected eyes at both 3 and 7 d of PLX-treated mice in comparison to vehicle-injected eyes of control-treated mice (compare Fig A (c and i) and Fig B (c and i)), supporting a potential role for microglia in extracellular matrix remodeling. Gliosis markers showed similar label in uninjected mice in comparison to the 3 day and 7 day vehicle injected mice (Figure 3.11). Protein levels

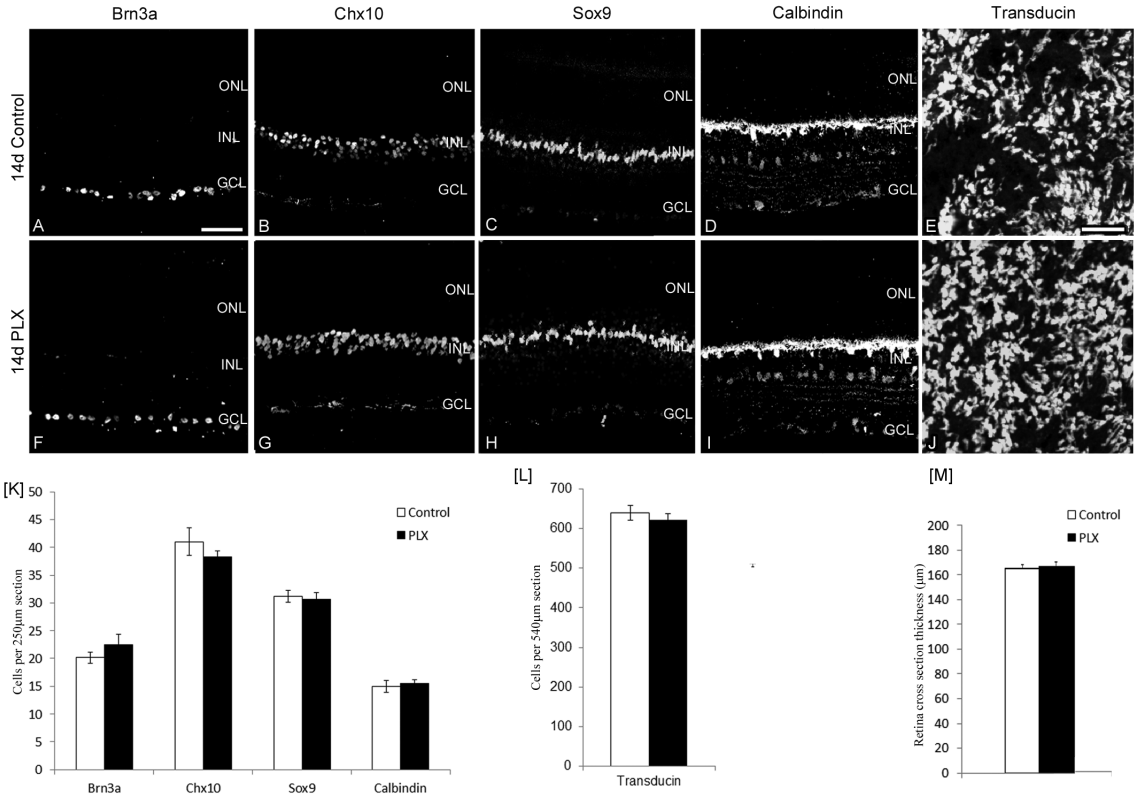

Fig. 3.8. PLX ablates microglia without affecting other retinal cells. Retinal sections from mice kept on the PLX or vehicle chow diet for 14 days were labeled for ganglion cells (BRN3A; A, F), bipolar cells (CHX10; B, G), Müller glia (SOX9; C, H), and horizontal cells (CALBINDIN; D, I). Cell counts of images for the labeled markers (n=8) showed no difference between the control and PLX-treated mice (K; Images taken were within 200 μm from the optic nerve). 60 images of retinal flatmounts of PLX and control-treated mice were labeled for Gα transducin (E, J). Cell counts showed no difference in the two treatments (L). Retinal thickness was also assessed in control and PLX retinas and showed no difference (M). Magnification bar in a=50 μm, for images (A–D, F–I). Magnification bar in E=10 μm, for images (E, J)

of gliosis markers GFAP, S100β, and TXNIP were also quantified using western blot (Figure 3.12).

3.4 Discussion

Our lab previously showed that BMP7 is able to trigger reactive gliosis in the retina. Here we show that the Müller cell gliosis triggered by BMP7 is an indirect effect resulting from microglial activation to a pro-inflammatory state. Following exposure to BMP7, microglia upregulated at least two molecules, IFN-γ and IL-6, both of which have been shown in previous studies to trigger gliosis (Lee et al. 1993; Yong et al. 1991; Corbin et al. 1996; Chakrabarty et al. 2010; Chiang et al. 1994). The CSFR1 inhibitor PLX was used to specifically target and ablate retinal microglia without affecting numbers of other retinal cells, in order to show that the BMP7 triggers gliosis through microglial activation. We observed that BMP7 injection into retinas lacking microglia produced an abated inflammatory response and a complete loss of gliosis, suggesting an important role for the microglia in mediating the gliosis response.

3.4.1 BMP pathway in retinal disease

BMPs have been previously shown to be regulated in injury and disease models of the CNS and retina [111, 129, 161, 178]. The BMP receptors type 1A and 1B regulate hypertrophic and scarring responses of astrocytes following spinal cord injury [81]. In the retina, BMP signaling components phospho SMAD 1/5/8, have also been shown to be upregulated following NMDA induced injury and promote retinal ganglion cells survival [78]. We observed an increase in pTAK1 label in IBA labeled cells in the retina, as well as in other cells of the inner nuclear layer. Increases in expression of pTAK1 in neurons has been previously reported in the brain following cerebral ischemia and is known to be expressed in axonal arbors of sensory neurons [179, 180]. BMPs have also been shown to be important in retinal cell proliferation and regen-

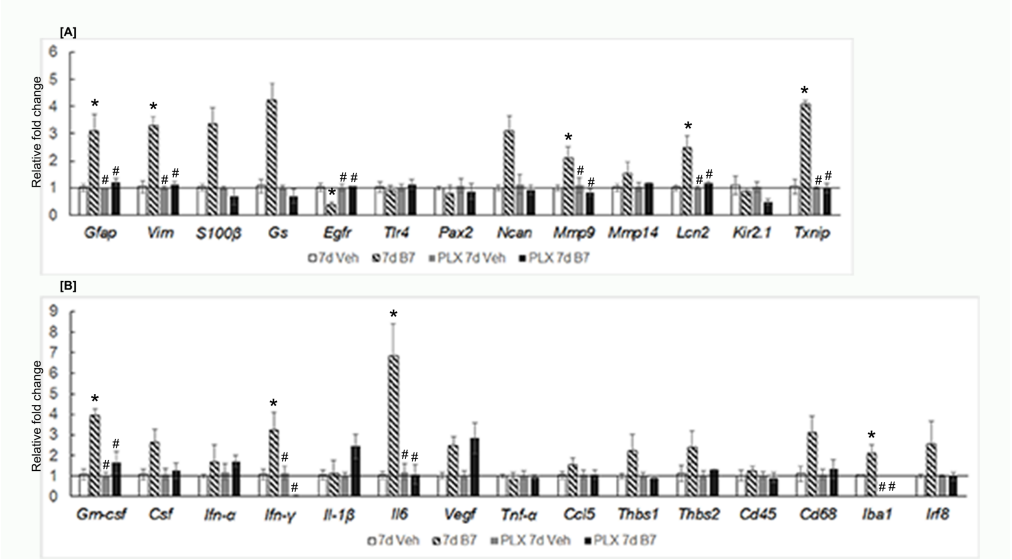

Fig. 3.9. Effect of BMP7 is diminished in the absence of microgliaRNA levels. BMP7 or vehicle was injected intravitreally into the eyes of mice kept on regular chow or PLX chow and harvested 7 days postinjection. RNA isolated from the retina were analyzed via RT-qPCR for changes in levels of inflammatory markers (A) and gliosis markers (B). Mice kept on the control chow and injected with BMP7 showed a relative increase by 2-fold or greater of inflammatory markers: *Gm-csf, Csf, Ifn-γ, Il-6, Vegf, Thbs1, Thbs2* and *CD68* (B). Gliosis markers *Gfap, Vim, S100β, Gs, Ncan, Mmp9, Lcn2* and *Txnip* showed a 2-fold increase or more in these mice (A). Data shown in graphs (A, B) represent relative expression levels of RNA in mouse retina to the respective vehicle treatments. Bars above a level of 1.0 (solid black line) represent an increase in mRNA levels while bars below the level of 1.0 represent a decrease in mRNA levels relative to the corresponding vehicle control. Mice kept on the PLX chow and injected with BMP7 showed a 2-fold increase in inflammatory markers *Il-1β* and *Vegf*, while all the gliosis markers showed relatively unchanged RNA levels (A, B). Statistical analysis was performed by one way ANOVA with post hoc Tukey's test. Significant difference from vehicle-injected control mice $*$ =p value <0.05. Significant difference from BMP7 injected control mice # =p value <0.05.

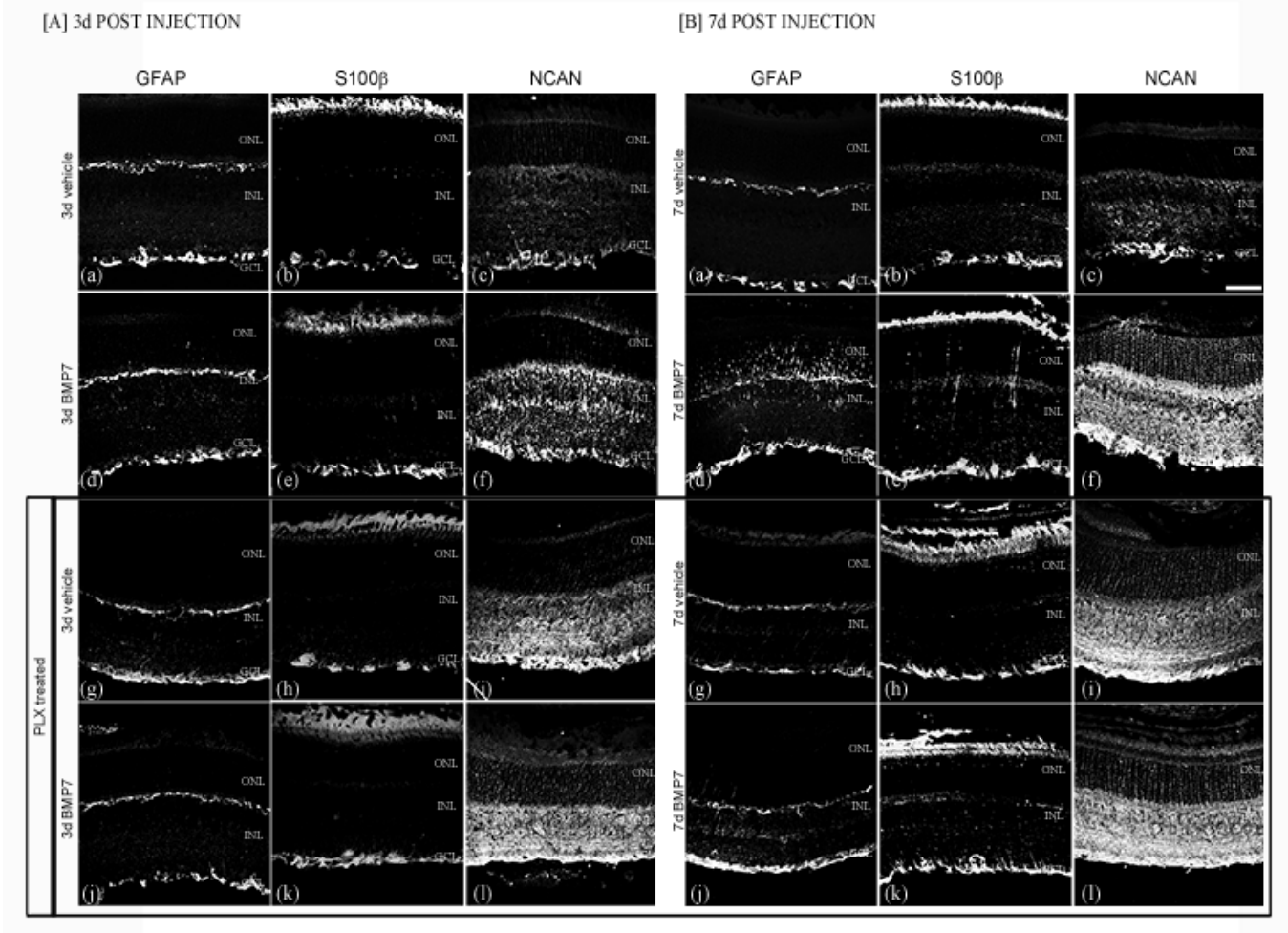

Fig. 3. 10. Effect of BMP7 on gliosis in absence of microglialocalization of gliosis markers (Continued on next page).

Fig. 3.10. Effect of BMP7 on gliosis in absence of microglialocalization of gliosis markers. Mouse retinal sections from eyes injected with vehicle or BMP7 were labeled for gliosis markers GFAP (A, B (a, d, g, j)), S100β (A, B (b, e, h, k)), and NCAN (A, B (c, f, j, l)). Mice kept on the PLX diet did not show an increase in label for the gliosis markers GFAP and S100β BMP7 or vehicle-injected retina 3 and 7 days postinjection (A, B (g, h, j, k)). NCAN label appeared to be similar in the BMP7 injected and the respective age-matched vehicle controls in mice kept on the PLX chow (A, B (i, l)). Mice kept on the control chow and injected with BMP7 clearly showed an increase in GFAP, S100β and NCAN levels 7 days postinjection, when compared to their respective vehicle control (B (a–f)). Three days postinjection, there is an increase in GFAP and NCAN label in BMP7-injected retinas in comparison to the respective vehicle control-injected retinas (A (a, c, d, f)). When comparing mice kept on control chow or the PLX chow, there is an increase in GFAP and S100β label in the mice kept on control chow in comparison to the mice kept on the PLX chow, 7 days post BMP7 injection (B (d, e, j, k)). GFAP and S100β label in mice kept on control chow and PLX chow appears to be similar in the BMP7-injected retinas, 3 days postinjection (A (d, e, j, k)).

eration in the chick retina [181]. Ueki and Reh (2013) showed that SMAD upregulation was essential in mediating EGF dependent Müller glial cell proliferation in the mouse [135]. The presence of BMPs in disease states is consistent with a potential role for them playing a role in retinal gliosis.

3.4.2 Activated microglia drive retinal gliosis

We had previously reported that BMP7 was able to trigger gliosis in retinal glia *in vitro* and *in vivo*. However, we observed a higher response in the *in vivo* model, which suggested there may be other cells involved in this response. Microglia are the resident macrophages in the retina. Similar to the macro glia, these cells also undergo activation. Their activation has been observed in various disease and injury

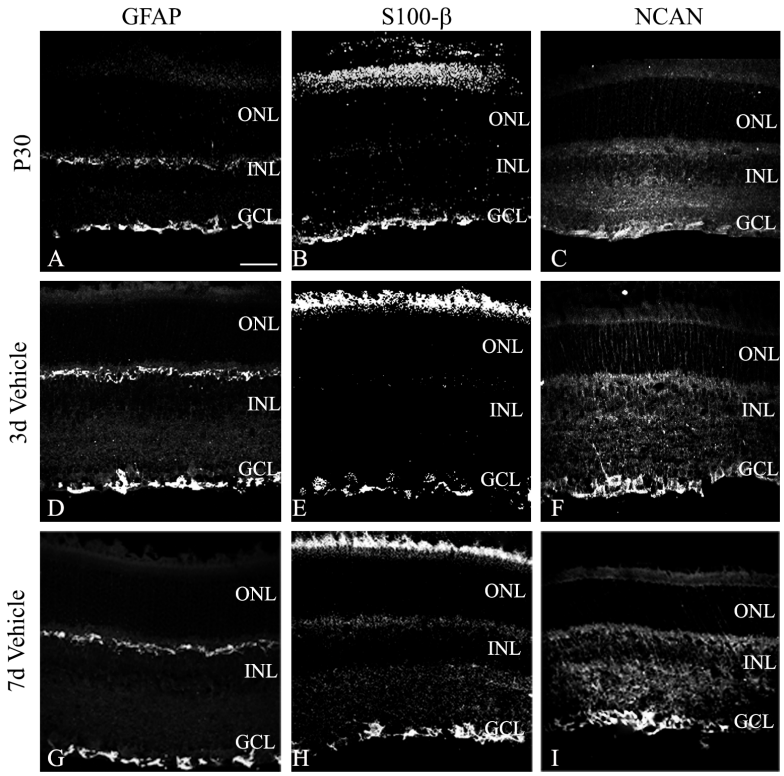

Fig. 3.11. IF label of retinas for GFAP, S-100-β, and NCAN in P30 uninjected and 3 and 7 days vehicle-injected retinas.Retinal sections from uninjected P30 mouse, vehicle-injected P30 mouse, obtained 3 and 7 days post-injection, labeled for GFAP (A, D, G), S100β (B, E, H), and NCAN (C, F, I). Label for all three markers appears to be similar in the uninjected and the vehicle-injected retinas. Magnification bar in A=50 μm, for images A–I.

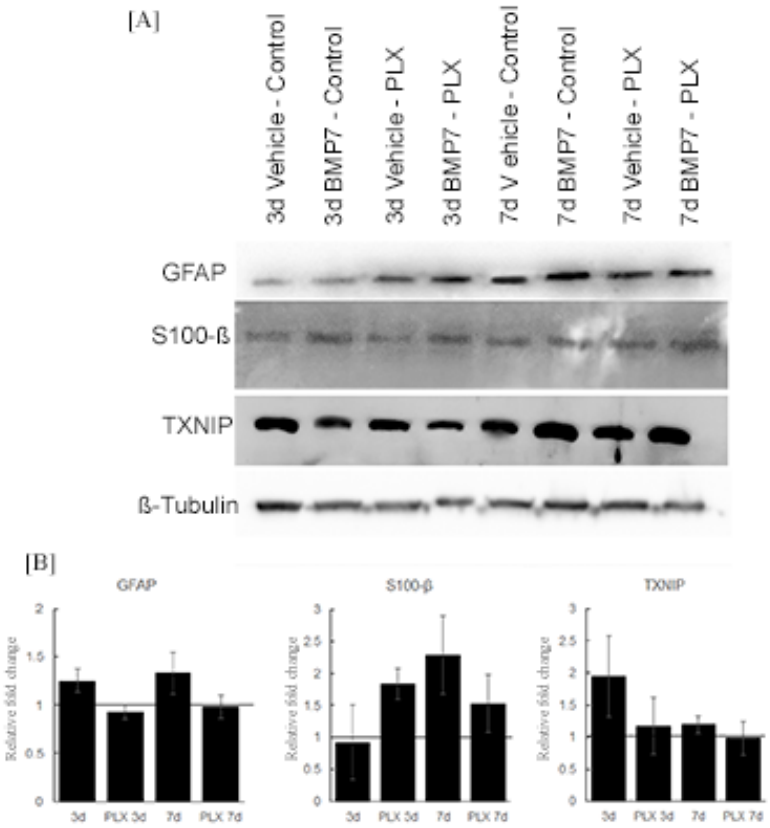

Fig. 3.12. Protein levels in PLX-treated mice. Protein isolated from control and PLX-treated mice injected with vehicle or BMP7 changes in protein levels of gliosis markers GFAP, S100β, and TXNIP, with β-TUBULIN used as a loading control.GFAP showed elevated levels in the BMP7-injected control mice, while PLX mice had GFAP levels similar to the vehicle injection. S100β was elevated in the 3 and 7 days BMP7-injected PLX mice as well as in the 7 days BMP7-injected control mice, compared to the respective vehicle controls. TXNIP levels did not change in the control and PLX mice injected with vehicle or BMP7 3 days post-injection. Seven days post-injection, TXNIP levels did increase in the control BMP-injected mice, while no such change was observed in the PLX mice. No statistical significance was observed in the densitometric analysis (B) of blots from (A).

models, such as, retinitis pigmentosa, diabetic retinopathy, retinal detachment and glaucoma [182–186]. Activated microglia change morphology from a ramified cell to an amoeboid cell, along with changes in expression of cell surface markers, such as the cluster of differentiation molecule 11b (CD11b), CD68, major histocompatibility complexes (MHC), scavenger receptors, TLR, and secreted actors such as RANTES, interferon, interleukins and TNFα. These changes serve to enhance the phagocytic effect of the microglial cells as well as the cytotoxic effect on injured cells and foreign pathogen [31, 187]. Müller glia also undergo activation following disruption retinal homeostasis. The reactive Müller glia hypertrophy and upregulate expression of various growth factors, reactive oxygen species scavengers, protect neurons from excitotoxicity and in some organisms, can regenerate retinal neurons. These changes serve to protect the damaged retina. However, gliosis can also have detrimental effects by remodeling the extracellular matrix and due to loss of normal glial functions which are necessary for normal neuronal activity [42, 46].

The retinal astrocytes and Müller glial cells exhibit similar responses to injury, such as hypertrophy, upregulation of GFAP, VIMENTIN and GS, as observed in rat models of retinal detachment and retinitis pigmentosa [124, 188, 189]. However, research has also revealed that there are differences in the response of the two cells types. GFAP upregulation was observed in Müller glia and not in the astrocytes in rats subjected to episcleral vein cauterization [190]. Similarly, upregulation of GFAP was observed in the Müller glial cells in retina subjected to laser induced ocular hypertension, while the astrocytes of the contralateral control eyes also exhibited an increase in GFAP and a change in the area covered by the astrocytes [191, 192]. The differences observed may suggest distinct functional roles for the astrocytes and Müller glia, which cooperate to restore retinal homeostasis.

Here we observed a decreased gliosis response in the retina following BMP7 treatment in mice lacking microglia. We used a novel CSF1R inhibitor (PLX) to selectively ab-

late microglia. Following microglial ablation, mice were treated with BMP7 to assess gliosis in the retina. The inclusion of the inhibitor in the chow allowed its continual application over a longer period of time, enabling the maintenance of a microglia-free environment in the retina in which we could test the role of the microglia in BMP7-mediated gliosis. Without continual application of the inhibitor, microglia could repopulate the retina from one of two sources: 1) bone marrow-derived stem cells can penetrate the blood-brain barrier and differentiate into microglia, or 2) residential microglia can proliferate and replace lost cells (Elmore et al. 2015; Jin et al. 2016). The two sources of microglia are not equivalent; residential microglia primarily give rise to microglia that display an M1 inflammatory phenotype, whereas the bone marrow-derived cells give rise to microglia with an M2 anti-inflammatory phenotype [193]. At any rate, in order for us to test the role of BMP7 in indirectly triggering gliosis, we had to maintain a microglial-free environment for the duration of the experiments.

3.4.3 BMP and inflammation

Activation of microglia and macroglia have been studied in various models. While there are differences in the responses of the two glial populations, they do exhibit similarities. These include regulation of inflammatory markers, regulation of antigen presentation complexes, various factors such as IFN-γ, TNF-α, and toll like receptor (TLR) [33, 42, 172]. While several different factors have been shown to regulate macrophage and microglia activation, the effect of BMPs is still not completely characterized [59, 165, 174, 194]. BMP6 regulates expression of inflammatory markers such as IL-6, IL-1β and nitric oxide synthase in macrophages [195–197]. In addition, more recent studies indicate that BMP exposure particularly leads to the M2 or anti-inflammatory phenotype of the macrophages promoting tissue repair [198–201]. Microglia are descendants of immature macrophages and are thought to act as macrophages in disease and injury states [202]. In our studies, BMP7 in-

creased the pro-inflammatory state of the microglia. Further studies are necessary to determine if all microglia respond to BMP7 by increasing pro-inflammatory markers or if this is a response unique to certain populations of microglia.

In this study, we observed that microglia showed an upregulation of inflammatory markers in response to BMP7 treatment, indicative of activation. Furthermore, in the PLX treated mice, the gliosis response was subdued in comparison to control BMP7 treated retinas, suggesting that microglia are an essential mediator of retinal gliosis. These results support our hypothesis that microglia are activated by BMP7, which in turn regulate factors causing Müller cell gliosis.

In the PLX-treated mice (both vehicle and BMP7-injected), we also observe an increase in neurocan levels in the retina. Müller glia secrete MMPs that regulate neurocan levels in the extracellular matrix. In addition, microglia also secrete these enzymes [203, 204]. Their upregulation has been observed in the CNS during inflammation in various injury models. Furthermore, microglia derived factors such as TNF-α have also been shown to regulate MMP expression by the Müller glia [205]. Thus, we propose that the lack of microglia in the retina contributes to the increase in neurocan by regulating MMP levels either directly or indirectly by regulating Müller glia.

Comparing the mRNA and protein levels in the control and PLX injected retinas, we observed a difference in expression patterns (Figure 3.7). Although the mRNA levels of S100β and TXNIP was reduced in the BMP7-injected PLX mice, we did not observe a similar change at the protein level. Non-correlation between mRNA and protein levels has been noted in other studies [140, 142, 206, 207]. mRNA translation and protein stability in the cell is regulated by multiple systems including, by micro RNAs (miRNAs), mRNA localization translational repression and protein stability [144, 207]. miRNAs have been previously reported to be regulated in neural tissue

under conditions of stress [151,208,209]. Furthermore, BMPs can regulate translation by regulating cytoplasmic polyadenylation element binding protein (CPEB) via the TAK pathway [145, 210]. Further studies will be required to determine what pathway(s) mediate this non-correlation between the mRNA and protein levels.

3.4.4 Microglia release inflammatory factors prior to formation of gliosis

We observed a decrease in expression of GFAP and S100β in mice kept on the PLX diet and treated with BMP7. BMP7-treatment also revealed decreased RNA levels of gliosis and inflammatory markers in PLX mice when compared to the mice kept on the normal diet. Previously, it has been reported that microglia respond early to changes in microenvironment and become activated. Bosco et. al showed that microglia become activated early in the retina, prior to any increases in the intra-ocular pressure (IOP) in the DBA/2J mice [164]. Similarly, early activation of microglia has also been observed and implicated in progression of Parkinsons disease [211]. Furthermore, in the ocular hypertension mouse model studied in Gallego et. al 2012, the authors, suggest that upregulation of MHC-II in microglia in the controlateral eye regulated the morphological changes of retinal astrocytes [192]. Thus, we propose that microglia respond to the BMP7 first and become activated. These activated microglia upregulate factors, which in turn can trigger Müller cell gliosis. Consistent with this notion our findings indicate the IFN-γ and other inflammatory factors were upregulated as early as 3 h following incubation of microglial cells with BMP7 *in vitro*, and these levels were further increased 6, 12 and 24 h post-incubation with BMP7. In contrast, factors associated with gliosis do not begin to increase until 3 d *in vivo*, with most markers increasing after 7 days.

3.4.5 Potential factors regulating microglia mediated activation of Müller glia

Previous studies looking into microglia and macroglia interactions have revealed several secreted as well as membrane bound factors which could activate the macroglia, such as IL-1β, IL-18, TGF-β and TNF-α [31, 59, 212]. Morphological changes and increases in RNA levels of inflammatory markers in the microglia following BMP7 treatment indicate activation of the microglia. We observed in our analysis that RNA levels of Ifn-γ, Il-6, Vegf and Thbs1 to be greater following Müller glia activation. Previously, Cotinet et.al 1997 and Goureau 1994 showed that IFN-γ can trigger Müller glia to regulate TNF-α and nitric oxide (NO) [67, 213]. Similarly, IL-6 has been shown to induce Müller glia derived progenitor cells in the injured zebrafish and chick retina [70, 174]. We propose that BMP7 causes activation of microglia, which leads to upregulation of factors such as IFN-γ and IL-6, which in turn trigger Müller cell gliosis.

Our findings indicated an important role for microglia in Müller cell gliosis in the murine retina. However, the mechanism and potential factors that play a role in microglia and Müller glia interactions are not known. Future studies will aim to identify the potential role of IFN-γ and IL-6, upregulated by BMP7 in the retina, in microglia function and gliosis.

4. ROLE OF AMOT-YAP SIGNALING IN REGULATION OF GLIOSIS

4.1 Introduction

Gliosis has been shown to involve a wide range of factors and pathways including TGF-β, CNTF, LIF, Wnt and Notch. While gliosis is observed in all retinal injury and disease models, studies have revealed different factors to be involved in its regulation. In diabetic retinopathy, hyperglycemia can induce factors such as VEGF and inflammatory factors such as TNF-α and IL from the Müller glia, which lead to the activation of the glial cells and disease pathology, particularly by activating ERK signaling in the Müller glia [214–216]. ERK signaling is also regulated during ischemia and leads to Müller cell gliosis. In retinal detatchment, FGF2 and endothelin-2 (ET-2) are known to regulate gliosis [217, 218]. In retinitis pigmentosa and similar photoreceptor injury models, TGF-β, CNTF and FGF regulate the gliosis response in the retina [219–222]. Although many secreted factors are known to trigger gliosis, it is not clear if these factors trigger gliosis through separate pathways or if they trigger the activation of a common pathway which regulates gliosis.

The Hippo pathway, which mediates tissue homeostasis by regulating proliferation, growth and differentiation, has been shown to interact with pathways involved in gliosis activation such as the Wnt, TGF-β, BMP and Notch. While, the Hippo pathway has been identified as a regulator proliferation and differentiation in progenitors in the zebrafish retina, its role in Müller glia activation has not been investigated.

The effector protein of the Hippo pathway is the yes activated protein (YAP). Activation of the Hippo pathway leads to phosphorylation and activation of the core

kinases (MST1/2 and LATS1/2), which then phosphorylate YAP, leading to degradation, ubiquitination or cytoplasmic retention. The unphosphorylated YAP, in a complex with transcriptional co-activator with PDZ binding motif (TAZ), is translocated to the nucleus and binds to the transcription co-factor transcriptional enhancer associated domain (TEAD) to bring about activation of genes associated with proliferation, cell cycle progression and inhibition of apoptosis [84].

The Hippo pathway is regulated by cell-cell and cell-ECM contact via Rho GTPases, growth factors via G-protein coupled receptors, cell polarity proteins including angiomotins (AMOTs) as well as stress signals. Cell interaction with ECM as well as low cell density induce YAP/TAZ nuclear localization by inhibiting phosphorylation of LATS kinases [223, 224]. Alternatively, at high cell density, the core kinases are phosphorylated preventing the nuclear localization of YAP [225, 226]. Similarly mechanical signals such as stretching also regulate the hippo pathway through F-actin, directly by phosphorylating kinases MST and LATS or indirectly via GPCRs [86]. Growth factors regulate the hippo pathway by inhibiting phosphorylation of LATS, through activation of GPCRs (example Wnts) or through phosphatidyl inositol 3-kinase (PI3K; example EGF) [227,228]. Tight junction and adherens junction proteins such as α-catenin, NF2, protein tyrosine phosphatase-1 and angiomotins (AMOTs) also regulate YAP localization by regulating the kinases or by directly binding YAP and sequestering it to the cytoplasm [59, 229, 230].

Angiomotins (AMOTs) are a family of cytosolic proteins found in tight junctional complexes. The PPxY motif and WW domain in the AMOTs and YAP, respectively, mediate the interaction of the two proteins, binding AMOTs with YAP. This localizes YAP to the tight junctions thereby inhibiting the Hippo pathway. The AMOT family consists of AMOT, which includes isomers AMOT p130 and the N terminal truncated version AMOT p80, AMOT like 1 and AMOT like 2. The AMOT p80 is the dominant negative form of AMOT and binds to AMOT p130, preventing the cy-

toplasmic localization of the AMOT p130 YAP complexes [231–233]. Thus, AMOTs are important mediators of the cell-cell interaction cues to the Hippo pathway. Here we hypothesize that AMOTs are down regulated during gliosis in the Müller glia, leading to nuclear localization of YAP, which in turn regulates the hypertrophic and proliferative gliosis responses. Furthermore, YAP in the retinal glia interacts with transcription factors such as STATs, SMADs and β-catenin, which are downstream of factors such as CNTF, TGF/BMP and Wnts, respectively, and regulate the gliosis response.

4.2 Methods

4.2.1 Cell culture

Mouse retinal astrocytes were isolated and maintained as previously described in [116]. Confluent cell culture plates were treated with 0.1μg/ml YAP/TEAD inhibitor, verteporfin (VP) or 1μl/ml DMSO. Cells allowed to grow for 24 h following which RNA was isolated from the cells and subsequently used for RT-qPCR analysis.

4.2.2 Intraocular injections

Postnatal day 30 (P30) C57BL/6J mice were anesthetized with ketamine/xylazine cocktail and injected intravitreally with 1 μl 20ng/μl VP in one eye and 1μl/ml DMSO in the contralateral eye or 1μl 150ng/μl IFN-γ and 1μl PBS in the contralateral eye. Mice were also co-injected with 1μl 150ng/μl IFN-γ and 1 μl 20ng/μl VP or 1μl PBS and 1μl/ml DMSO in the contralateral eye. Injections were performed using a manual microsyringe and pulled glass micropipettes as previously described in [234].

4.2.3 Tissue processing and immunofluorescence

Eyes from euthanized C57BL/6J mice were enucleated, washed in PBS, and either fixed in 4% paraformaldehyde (PFA) for immunofluorescence (IF) or dissected to isolate the retina for preparation of RNA and/or protein. For IF analysis, enucleated eyes were washed and fixed in 4% PFA, incubated in ascending series of sucrose, and frozen in a sucrose OCT solution as previously described in Dharmarajan et al., 2014. Thick sections (12 μm) were cut using Leica CM3050S cryostat onto Superfrost Plus slides (ThermoScientific) and stored at 80°C until use. Frozen sections were labeled as previously described in (Dharmarajan et al. 2017). Briefly, sections were fixed in 4% PFA for 20 mins, followed by permeabilization in methanol for 10 mins. Slides were washed in 1x PBS and blocked in 0.25% triton x 100 PBS with 10% serum (donkey or goat) for 1 h at room temperature (RT). Slides were incubated with primary antibody (YAP 1:500, abcam; GFAP 1:250, dako; GLUTAMINE SYNTHETASE 1:300, Millipore; SOX9 1:300, santa cruz; S100β 1:300, abcam; AMOT 1:500, Dr.Clarke Wells laboratory, IUSM) diluted in blocking buffer overnight at 4°C, washed in PBS and incubated with secondary antibody diluted in PBS for 1 h at RT in dark. The slides were then washed in PBS, incubated with hoecsht nuclear staining solution for 5 min at RT in dark and mounted with aqua polymount.

4.2.4 Western blotting

Extraction of proteins from retinal tissue was performed using RIPA lysis buffer as previously described. Total protein was estimated using the BCA protein assay kit and 40μg of total protein was loaded onto a 4-20% SDS precast gel and transferred to a PVDF membrane, as previously described. Membrane blots were blocked in 5% milk in TBST for 1 h at RT on a shaker and incubated with primary antibody (AMOT 1:500; AMOTL1 1:500; β-TUBULIN 1:1000, Sigma; GFAP 1:1000, Dako; S100β 1:1000, Abcam; GS 1:1000, Millipore) diluted in blocking buffer at 4°C overnight. The blots were washed in TBST, incubated with secondary antibody for 1 h at RT,

washed in TBST, incubated with super signal femto chemiluminescent substrate and visualized on x-ray films.

4.2.5 RT-qPCR

RT-qPCR was performed using Sybr green master mix in the LightCycler 480 system (Roche). Change in RNA levels was measured using the $2^{-\delta\delta Ct}$ method, where CT is the crossing threshold value. Delta CT values were calculated by subtracting the geometric mean of three housekeeping genes (*β- 2 Microglobulin (β2m), succinate dehydrogenase complex subunit A (Sdha)*, and *signal recognition particle 14 kDa (Srp14)*) from the average CT value of the target gene. A no template control was also used during each run. The primers used for analysis include gliosis markers included in Table 2.2 as well as downstream targets of YAP/TEAD signaling (Table 4.1).

Table 4.1.
List of RT-qPCR primers

Gene	**Primer**	**Sequence**	**Length (bp)**
Edn1	Forward	GGCCCAAAGTACCATGCAGA	127
	Reverse	TGCTATTGCTGATGGCCTCC	
Kif14	Forward	GGGAGCAAGCTCTGTGTTCT	110
	Reverse	GGTCTCCAGCCCAGAGTCTA	
Ets1	Forward	GCCCGACTCTCACCATCATCA	102
	Reverse	AGCTTTCAAGGCTTGGGACA	
Ets2	Forward	ATGCTGTGTAACCTCGGCAA	95
	Reverse	CCGCGTTGAGGTGAGAGTTT	
Myc	Forward	CGCGATCAGCTCTCCTGAAA	84
	Reverse	GCTGTACGGAGTCGTAGTCG	

4.3 Results

4.3.1 AMOTs and YAP are expressed in the glial cells in the retina

As a first step in determining if AMOTs and YAP may be critical to the gliosis response, sections through adult murine retinas were co-labeled with antibodies that label Müller glia and retinal astrocyte cells (SOX9 or glutamine synthetase; GS) and YAP or AMOT (Figure 4.1). Both YAP and AMOT co-labeled with glial cell markers in the adult retina. While YAP showed nuclear co-localization, AMOT label was cytoplasmic. YAP co-labeled with the nuclear Müller glia marker SOX2 (Figure 4.1 A–C). AMOT showed cytoplasmic distribution and co-labeled with the glial cytoplasmic marker, GS (Figure 4.1D–F).

YAP label was restricted to the inner nuclear layer where Müller cell nuclei reside, while AMOT co-expressed with retina Müller cell processes that span the width of the retina and potentially the retinal astrocytes in the nerve fiber layer.

4.3.2 AMOT and YAP upregulated during IFN-γ induces gliosis

Preliminary data from the Wells lab had shown that a luciferase construct under the regulation of the AMOT promoter, showed increased activity following exposure to IFN-γ and IL6 in HEK293 cells (unpublished data). Thus, the first step was to determine the changes induced in the retina following exposure to IFN-γ. Samples of eyes injected with IFN-γ were assessed for changes in gliosis markers via immunofluorescence or RT-qPCR (Figure 4.2). Immunofluorescence label for gliosis markers GFAP and S100-β was greater in the IFN-γ injected retinas as compared to the 4 d PBS (vehicle for IFN-γ) injected retina (Figure 4.2A–F). Label for the gliosis markers was greater 4 d following IFN-γ injection when compared to 1 d post IFN-γ injection (Figure 4.2B, C, E, F). RT-qPCR was performed for a subset of gliosis markers using

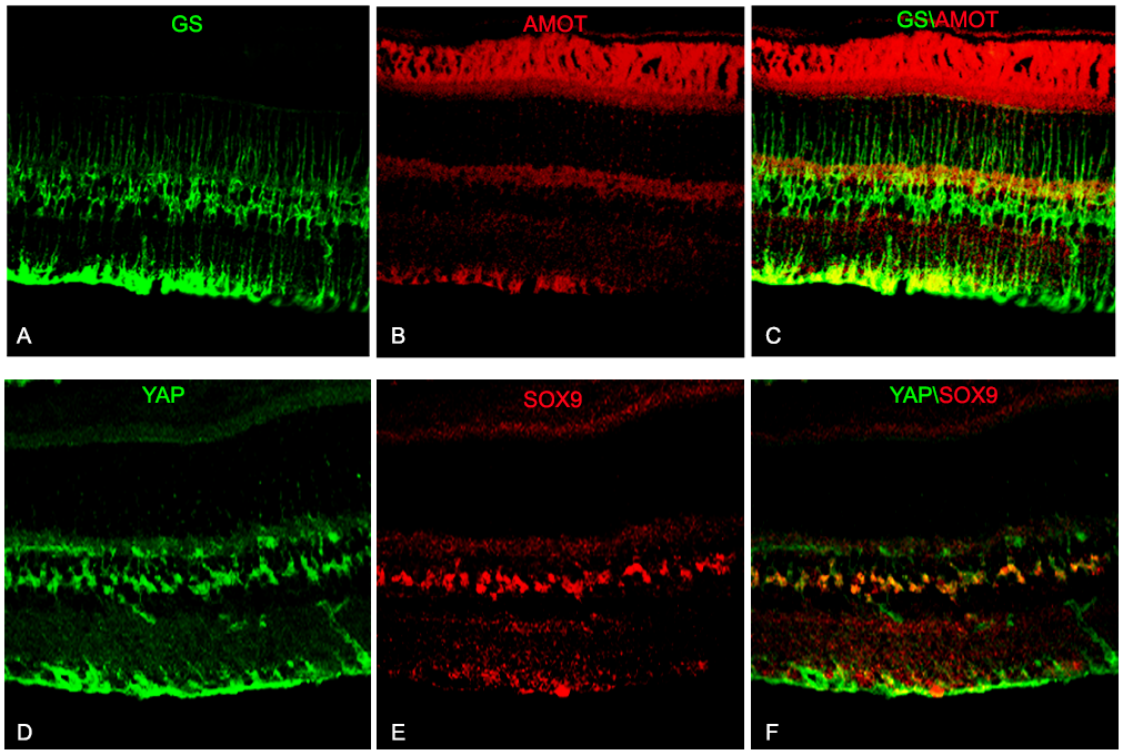

Fig. 4.1. AMOT and YAP expression in the murine retina. Retinal sections labeled with antibodies against YAP and SOX9 (A–C) and AMOT and GS (D–F). Merged images indicate co-localization of YAP with the nuclear marker for glial cells, while AMOT colocalization with GS suggests cytoplasmic localization in the retinal glia. Magnification bar in A=50 μm, for all panels.

RNA from 4 d IFN-γ or PBS injected retinas. A relative increase in RNA levels of gliosis markers *Gfap, S100-β, Tlr4, Egfr* and *Ncan* was observed in the IFN-γ injected retinas.

Protein levels of AMOT and YAP were also assessed in retinas injected with IFN-γ or vehicle. Immunofluorescence label revealed an upregulation of AMOT in the ganglion cell layer and nerve fiber layer in the IFN-γ injected retinas (Figure 4.3 A–C), no visible change was observed in the localization of the YAP in the retinal glia (Figure 4.3

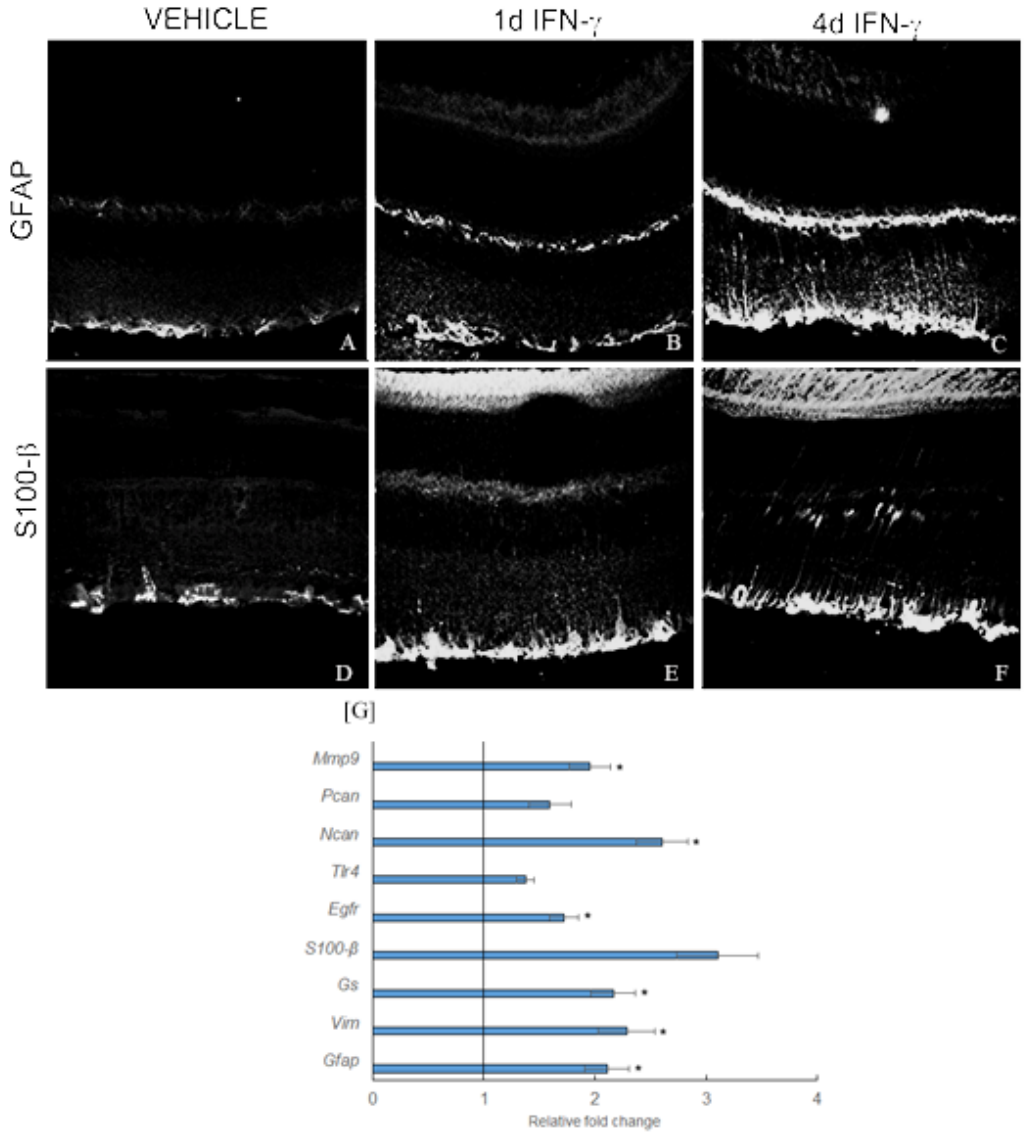

Fig. 4.2. IFN-γ upregulates gliosis markers in the retina. Retinal sections from P30 mice injected with vehicle or IFN-γ were labeled for gliosis markers (A–F) or analyzed for a subset of gliosis markers via RT-qPCR (G). Immunofluorescence label of injected retinas showed an increase in label for GFAP and S100-β in the IFN-γ injected retinas, compared to the vehicle injected retinas.RT-qPCR anaysis of RNA from IFN-γ injected retinas revealed an increase in levels of *Gfap, S100-β, Tlr4, Egfr* and *Ncan* relative to RNA from the vehicle injected retinas. Magnification bar in A=50 μm, for panels A–F.

D–F). Western blot analysis was performed to determine changes in AMOT and YAP protein levels during gliosis using the IFN-γ injected retinas. Protein levels of p80 and p130 isoforms of the AMOT was upregulated in the IFN-γ injected retina when compared to the vehicle injected retina (Figure 4.3 G). Furthermore, AMOTL1 also showed an increase in the IFN-γ injected retina (Figure 4.3 G). YAP levels were also upregulated in the IFN-γ injected retina (Figure 4.3 H).

4.3.3 Verteporfin treatment decreases RNA levels of YAP/TEAD downstream targets

Verteporfin (VP), a small molecule inhibitor that prevents YAP from binding to TEAD and thereby regulate target gene expression, was used to inhibit YAP signaling in the glial cells. Mouse eyes were injected intravitreally with 20, 50 or 100 ng/μl VP and assessed for changes in the YAP downstream targets via RT-qPCR to determine the efficacy of the inhibitor (Figure 4.4). 4d post treatment, a decrease in four out of the five YAP downstream targets was observed in the mouse retina treated with 50ng/μl when compared to the DMSO (vehicle) treated cells. In mice treated with 20ng/μl significant decrease in the RNA levels of *Edn1, Ets1* and *Ets2* was observed, while in eyes injected with 100ng/μl VP, we observed significant decreases in *Edn1* and *Ets1*.

4.3.4 Effect of IFN-γ on retinal gliosis in presence of verteporfin

To determine if YAP inhibition can regulate gliosis, adult mice were injected with 1μłof 150ng/μl IFN-γ followed by an injection with 1μl of 20ng/μl or 50ng/μl verteporfin. Samples were isolated from the injected eyes 4 d post injection and analyzed via RT-qPCR (Figure 4.5) for changes associated with gliosis. RT-qPCR analysis revealed an increase in RNA levels of *Gfap, Vim, Gs, S100-β, Ncan* and *Mmp9* in the presence or

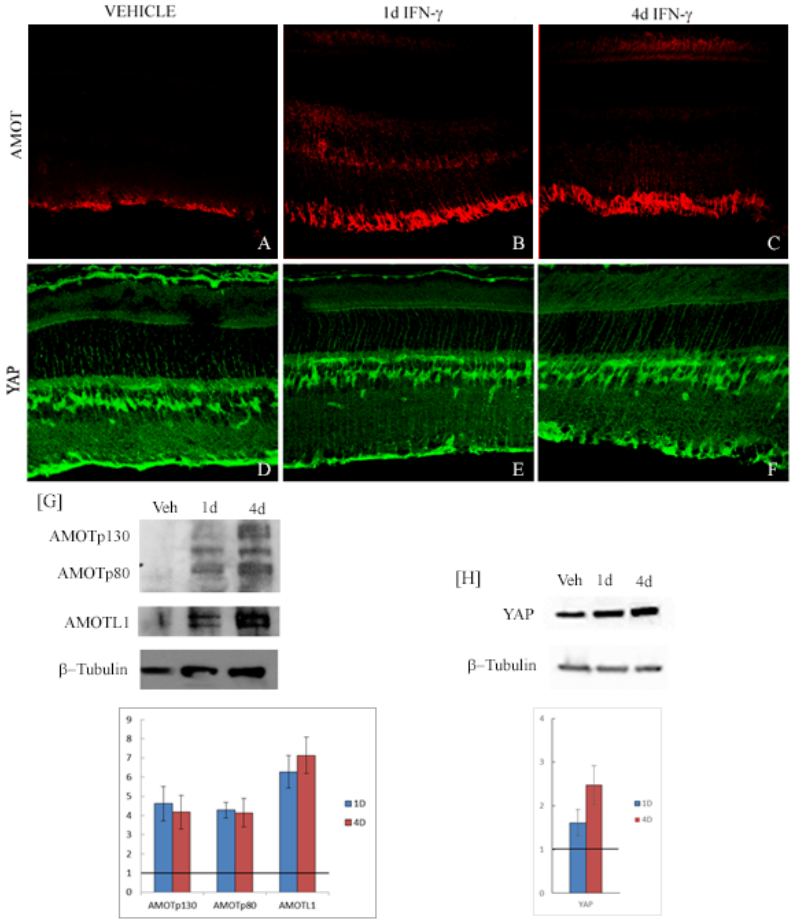

Fig. 4.3. IFN-γ upregulates AMOT and YAP in the retina. Retinal sections from P30 mice injected with vehicle or IFN-γ were AMOT (A - C) and YAP (D - F). AMOT levels were upregulated in the ganglion cell layer and nerve fiber layers in the 1 and 4 d IFN-γ injected retinas compared to the vehicle injected retinas. Changes in the protein levels were also quantified via western blot. β-TUBULIN was used as aloading control for the western blots. Densitometric analysis of blots revelaed an increase in AMOT levels in the IFN-γ injected retinas relative to the vehicle injected retina. Upregulation of AMOTp80, AMOTp130 and AMOTL1 were similar in the 1d and 4d IFN-γ injected retinas. YAP levels were upregulated by about 2 fold in the 4d IFN-γ injected retinas, while only a 1.5 fold increase was observed in the 1d IFN-γ injected retinas. Magnification bar in A=50 μm, for panels A–F.

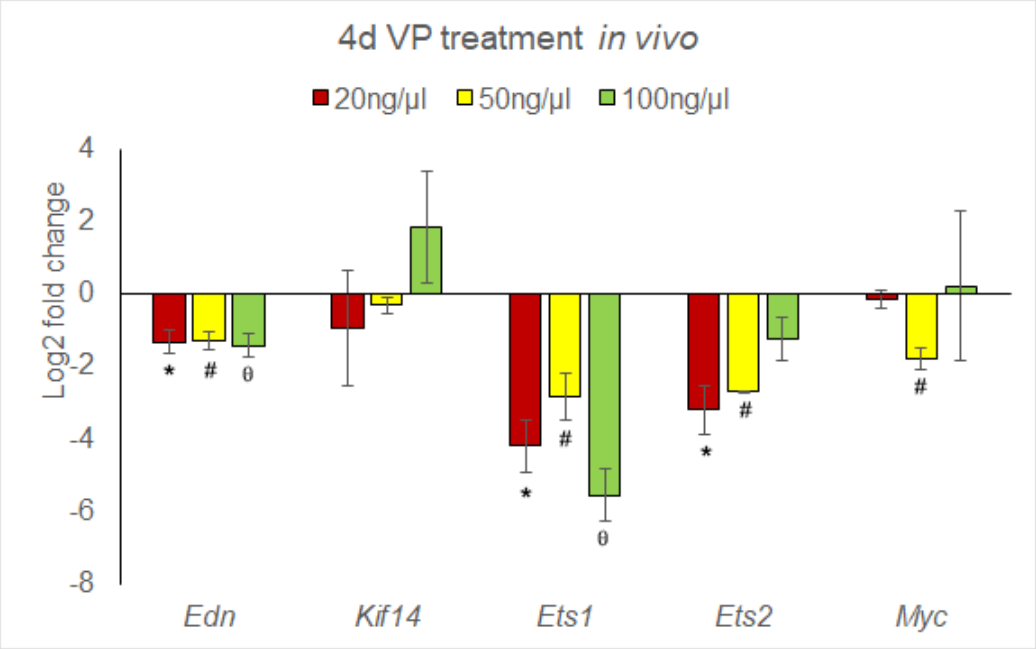

Fig. 4.4. Verteporfin downregulates RNA levels of downstream YAP targets. Adult mice injected intravitreally with different concentrations of verteporfin compared with the vehicle controls analyzed for downstream YAP target via RT-qPCR. Graphs represent a log2 fold change in the RNA levels of eyes injected with verteporfin relative to the vehicle injected control eyes. Statistical analysis was performed by unpaired Students t test. $*$, # and θ represent a p value <0.05 between the 20ng/μl, 50ng/μl and 100ng/μl inhibitor injected eyes and their respective vehicle controls. A significant decrease in *Edn1* and *Ets1* was observed in the three concentrations tested. Additionally, *Ets2* was decreased in eyes injected with 20ng/μl and 50ng/μl of verteporfin and *Myc* was decreased in the eyes injected with 50ng/μl of the inhibitor.

absence of verteporfin in the IFN-γ injected retinas (Figure 4.5). However, Vim RNA level was upregulated following VP treatment. Furthermore, RNA levels of *Tlr4, Egfr* and extracellular matrix markers *Ncan* and *Pcan* were decreased following 20ng/μl VP treatment, while *Gs, S100-β, Egfr, Pcan* and *Mmp9* were decreased in the eyes co-injected with IFN-γ and 50ng/μl of VP.

4.4 Discussion

This study revealed that AMOT and YAP are expressed in the macroglial cells in the retina. While AMOT expression was observed in the Müller glial fibers and retinal astrocytes, YAP was expressed in the nuclei of Müller glia. The increase in AMOT and YAP levels correlated with increase in gliosis markers in the retina. Furthermore, inhibiting YAP/TEAD binding decreased RNA levels of ECM markers in IFN-γ injected retinas, but did not return *Vimentin* and *GFAP* to normal levels.

In the murine retina, we observed that AMOT and YAP were expressed in the glial cells. In the eye, the Hippo pathway has been known to regulate eye development by regulating proliferation and inhibiting apoptosis of the retinal progenitors to generate sufficient cells prior to differentiation [235]. YAP knockout has associated with reduced eye size [236]. Furthermore, the Hippo pathway also regulates patterning of the retina. Activation of the Hippo pathway prevents nuclear localization of YAP, allowing the transcription factor Rx1 to activate photoreceptor genes Otx2, Otx5 and Crx [237]. Downregulation of the Hippo pathway leads to the nuclear localization of the YAP analog in drosophila, Yki, leading to proliferation of retinal progenitors and activation of Wg which prevents pre mature differentiation of the retinal cells [238]. The significance of YAP has also been established in differentiation of glial cells. Huang et al. 2016 demonstrated that nuclear YAP stabilizes pSMAD in neural stem cells, promoting astrocyte differentiation [223, 239]. YAP overexpression maintained the stem cells in a proliferative state, while neuronal differentiation was rescued by

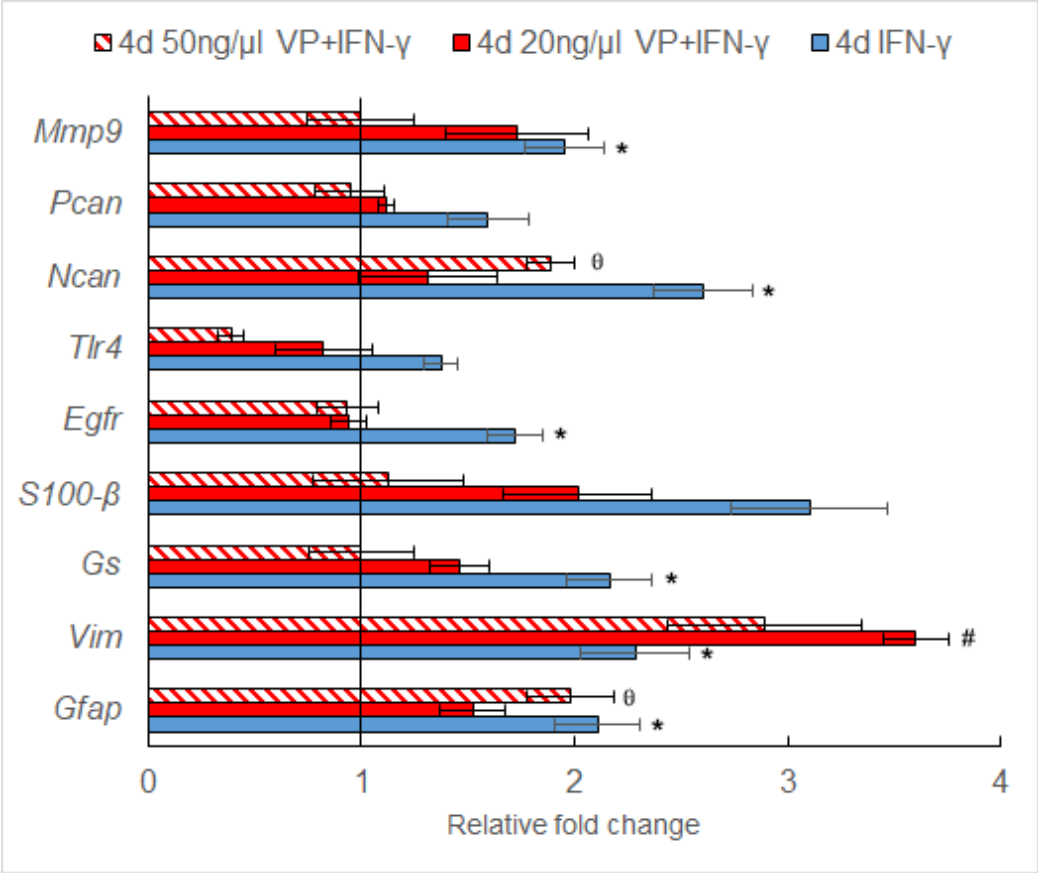

Fig. 4.5. Inhibition of YAP in IFN-γ injected retina. RT-qPCR of RNA from samples co-injected with verteporfin and IFN-γ or vehicle were analyzed for gliosis markers. Graphs represented are fold change in treatments relative the vehicle and verteporfin co-injected samples. RNA from IFN-γ injected retinas showed a two fold increase in levels of *Gfap, Vim, Gs, S100-β* and *Ncan*. In the presence of the inhibitor, RNA levels of *Vim* was upregulated in the 20 and 50 ng/μl verteporfin injected retinas. *S100-β* and *Mmp9* were also elevated over two fold in the retinas injected with IFN-γ and 20ng/μl verteporfin, while *Gfap* and *Ncan* was upregulated in the in the retinas injected with IFN-γ and 50ng/μl verteporfin.

knockdown of Gli2. While YAP can regulate the proliferation of progenitor and stem cells in various tissues and organs including the retina and brain, its role in regulating the regenerative potential of Müller glia is yet unexplored. The regenerative activity of Müller glia is limited in mammals although treatment with factors such as CNTF and FGF have been shown to induce proliferation in the Müller glia in the mouse retina. However, in lower vertebrates such as zebrafish Müller glia have been shown to undergo proliferation and de-differentiate into retinal neurons [240, 241]. Thus, regulation of YAP/Hippo pathway could be the underlying mechanism mediating the regenerative potential of Müller glia.

Regulation of Hippo pathway has been observed following injury in the skin and intestinal tissues. YAP regulates TGF-β signaling in skin fibroblasts following injury and mediate wound healing. Knockdown of YAP and its co-factor TAZ lead to an increase in the wound closure time indicating its importance in injury response in the skin [242]. Similarly, YAP overexpression has been shown to inhibit growth and regeneration of the intestine in mouse by regulating Wnt signaling [243]. The regenerative and proliferative properties of the Hippo/YAP signaling could be indicative of a role for this pathway in regulating the gliosis response following injury or disease. Glial cell activation has been associated with activation of signaling pathways such as TGF-β, Wnt, Notch, CNTF and inflammatory markers such as IFN-γ and TNF-α. YAP mediated stabilization of SMAD, a downstream component of the TGF-β signaling has been reported in the retina, intestine, liver and skin fibroblasts. Hippo mediated regulation of Notch and Wnt signaling has also been described in the intestine and liver, respectively. Furthermore, recent reports have described YAP regulation during gliosis [239, 244].

While we observed an increase in AMOT and YAP expression following treatment with IFN-γ, Huang Z et al., 2016 observed an increase in YAP in mouse brain astrocytes following treatment with CNTF and IFN-β. Furthermore, YAP was found

to interact with phospho-STAT3 and induced expression of SOCS3 to inhibit inflammatory response, with YAP knockout astrocytes displaying a hyper inflammatory response. Hamon A et al., 2017 re-affirmed the expression we observed in our studies. Using a mouse model for retinal degeneration (rd10), they showed that YAP and its co-transcription factor TEAD are expressed in the Müller glia and that they are upregulated in the diseased retina [244]. Furthmore, downstream targets of the Hippo/YAP pathway such as Cyr61 and Ctgf have also been observed to be upregulated in models of retinitis pigmentosa, diabetic retinopathy and glaucoma.

Another related response we observe is an increase in the expression of AMOTs in the retina during gliosis. Two different isoforms of AMOTs (AMOTp130 and AMOTp80 lacking an N terminal domain) are known to be expressed along with AMOT like1 (AMOTL1) and AMOT like 2 (AMOTL2). While AMOTp130, AMOTL1 and AMOTL2 have been shown to interact with YAP and localize it to the cytoplasm, AMOTp80 which lacks the N-terminal domain serves as a dominant negative form inhibiting the AMOT interaction with YAP [231]. In the retina, AMOTp80 is known to mediate endothelial cell migration during angiogenesis, while AMOTp130 mediated stabilization and maturation of the retinal vasculature [245,246]. Here we observe an increase in the levels of both isoforms of AMOT. We propose that AMOTs expressed in the glial are also involved in stabilizing the Müller glia and maintaining cell-cell contacts. During gliosis, AMOTp80 oligomerizes with AMOTp130 disrupting Müller glia stabilization and making the cell conducive for the changes of gliosis. Furthermore, this interaction removes the inhibition on YAP, which is translocated to the nucleus and can further regulate the gliosis response. However, it will be important to further explore the interactions of AMOTs in the retinal glia.

Our experiments where mice were injected with a YAP/TEAD inhibitor revealed a decrease in RNA levels of some of the gliosis markers following IFN-γ treatment. However, *Gfap, Vim* and *S100β* levels were similar to the IFN-γ injected retinas

not treated with verteporfin. It has been previously mentioned that YAP binds to its target genes through association with co-factors, primarily TEAD. However, research has revealed that YAP can also bind with other co-factors such as SMAD and β-catenin to mediate gene regulation. While its interaction with TEAD has been inhibited, its interaction with other co-factors could also be involved in regulation of gliosis. Thus, it will be essential to examine AMOT YAP interactions, protein modification to YAP as well as the co-transcription factors which can interact with nuclear YAP in the retinal glia.

5. DISCUSSION

The changes caused due to gliosis has been described as having both beneficial and detrimental effects on the surrounding tissue. While it was initially described as inhibitory to the neural tissue due to scarring, proliferation and inflammatory responses, knockout studies revealed that gliosis is essential to limit the spread of lesion following injury to neurons [43]. Changes during the early phases of gliosis such as hypertrophy, upregulation of glutamate uptake, increased reactive oxygen species scavengers and water and ion uptake have been shown to be essential in limiting the spread of injury in the tissue [43]. Gliosis also leads to increase in release of factors such as BDNF and FGF which are essential for neuronal survival. However, prolonged gliosis can lead formation of glial scars which prevent axon regeneration, an increase in the inflammatory response, disruption of normal functions which otherwise help in maintaining tissue homogeneity as well as alter the barrier functions of the associated blood vessels causing further damage to the tissue [42].

The activated microglia mediated inflammatory changes is essential in responding to early injury/disease states, however, like gliosis, long term activation of the microglia can have detrimental effects on the tissue [14]. The activated microglia have been proposed to exhibit two functionally distinct phenotypes: the M1 or pro-inflammatory phenotype and the M2 or anti-inflammatory phenotype. While the two classes of activated microglia are distinguished on the factors secreted/markers expressed, research suggests that microglia transition from an initial M1 phenotype to the M2 phenotype before returning to its resting state. The early response of the microglia is essential as it signals migration of the microglia to the injury site, increase phagocytosis and debris clearance, and recruiting more microglia to aid in damage limitation. The transition of microglia from this state to a M2 phenotype leads to increase in signals

which aid in neuronal survival, ECM remodeling and decrease of the pro-inflammatory signals [55]. Similar to the gliosis response of the macroglia, prolonged activation of the microglia leads to an increase in pro-inflammatory signals which can in turn lead to further tissue damage as well as activation of the macroglia.

In the retina, gliosis is observed in all diseases and injuries. Triggers identified so far include reactive oxygen species such as NO, physical stress or injury, increased neurotransmitter release from neurons, leaky blood vessels as well as inflammatory factors. *In vitro* studies as well as various model organisms have revealed that factors such as CNTF, LIF, EGF and TNF-α are regulated during gliosis. While several factors have been identified, the underlying mechanism regulating gliosis is still not clearly understood. How the various triggers identified in different disease and injury models bring about certain similar gliosis responses is essential to understanding approaches to tissue repair. Furthermore, being able to delineate between the detrimental and beneficial changes of the glial cells will aid in tissue regeneration.

In this study we have identified BMP7 as one of the triggers of gliosis in the retina. To determine this effect we developed a panel of markers encompassing a wide range of changes previously reported by other researchers. RT-qPCR data from our initial studies indicate that while BMP7can trigger gliosis in the retina glia, prolonged exposure to BMP7 may be involved in regulating the extracellular matrix remodeling. While we do observe an increase in RNA and protein levels of the inhibitory CSPG neurocan, we also do observe an increase in RNA levels of MMPs as well as tissue inhibitors of MMPs. Regulation of CSPGs via SMAD signaling in astrocytes has been described by [77, 247]. The CSPGs have also been shown to be regulated by non-canonical TGF-β signaling in rat cortical astrocytes via the PI3K-AKT-mTOR signaling pathway [72]. In our experiments with BMP7 treatments, we observed an increase in phospho SMAD levels as well as increase in the expression of phospho TAK in the retinal glia. Similarly, MMPs are also regulated by SMADs and other

transcription factors such as STATs and NF-κB [248]. Thus, further studies looking into regulation of the BMP signaling mechanism, its effect on other growth factors and inflammatory factors will help provide a better understanding of extracellular matrix remodeling.

While the glial cells are essential in formation of the blood retinal barrier, activation of the retinal glia leads to barrier breakdown due to loss of gap junctions and signaling between the glia and the cells of the vasculature [42, 102]. Alternatively hyperglycemia, hypoxia, oxidative stress and inflammatory signals also affect the cells of the vasculature leading to dysfunction of the blood vessels and increased leakage, in turn leading to gliosis [45]. BRB disruption has been described in several retinal injury/disease models and can also lead to extravasation of macrophages into the retina, which can exacerbate the inflammatory response and compound the gliosis response. The resident macrophages of the retina are the microglial cells, which also undergo activation in retinal disease and injury state. Activation of the microglia has been described in various models of retinal diseases including glaucoma, diabetic retinopathy, AMD and RP, where these cells induce secretion of inflammatory cytokines and chemokines [125]. The factors secreted by the activated microglia such as TNF-α, IFN-γ and IL have been shown to regulate gliosis in the Müller glia and retinal astrocytes (Karlstetter et al. 2015). Müller glial cells regulate the resting state of microglia through ATP secretion [165]. In a model of retinal degeneration, microglia-Müller glia interaction mediates the release of neurotrophic factors bFGF and GDNF to enhance neuronal survival [194]. Wang et al., 2011 further demonstrated that activated microglia induce Müller glia to express inflammatory cytokines and chemokines to maintain the microglia in an activated state as well as mediate microglia migration to the injury site [59]. We have demonstrated in our studies that microglia, along with the Müller glia, respond to BMP7 stimulation and undergo activation upregulating expression of various inflammatory cytokines. Decrease in expression of gliosis markers following ablation of microglia strengthens the importance of microglia in

regulating the gliosis response. Inflammatory cytokines upregulated by microglia following disruption of retinal homeostasis could be essential in regulating the gliosis response.

We propose that BMP7 is able to regulate gliosis via the following pathways: BMP7 triggers upregulation of factors and markers associated with gliosis in the macroglia. It leads to an increase in BMP7 secretion from the Müller glia in an autocrine manner to trigger further gliosis. BMP7 could also upregulated secreted factors such as LIF, which has been shown by other researchers to trigger gliosis. Simultaneously, the BMP7 activates the retinal microglia. The activated microglia upregulate factors such as GM-CSF, IFN-γ and IL-6. These factors recruit more microglia and activate them. Furthermore, factors such as IFN-γ and IL-6 could also trigger gliosis and prolong the gliosis response in the retina (Figure 5.1). Inhibition of signaling between the glial populations could serve to develop therapeutic approaches to treat retinal injuries/ diseases. By intervening at the appropriate time by ablating the microglia and/or inhibiting signals from microglia, prolonged gliosis and/inflammatory response can be curtailed which can potentially help in neuronal survival and an improved recovery of retinal function.

We have described previously the different growth factors regulated in the various retinal injury and disease models. Whether there is a common underlying pathway which regulates a somewhat similar gliosis response in the different injury conditions is not known. The Hippo pathway could be a central pathway linking the gliosis response in various conditions as crosstalk with other pathways such as TGF-β, CNTF, and TNF-α and the Hippo pathway has been established. In the various retinal diseases such as glaucoma, AMD, retinal degeneration and diabetic retinopathy, different factors or group of factors have been determined to play a role in regulation gliosis and progression of the diseased phenotype (see introduction). However, in all diseases, upregulation of GFAP has been observed starting at a particular stage of disease

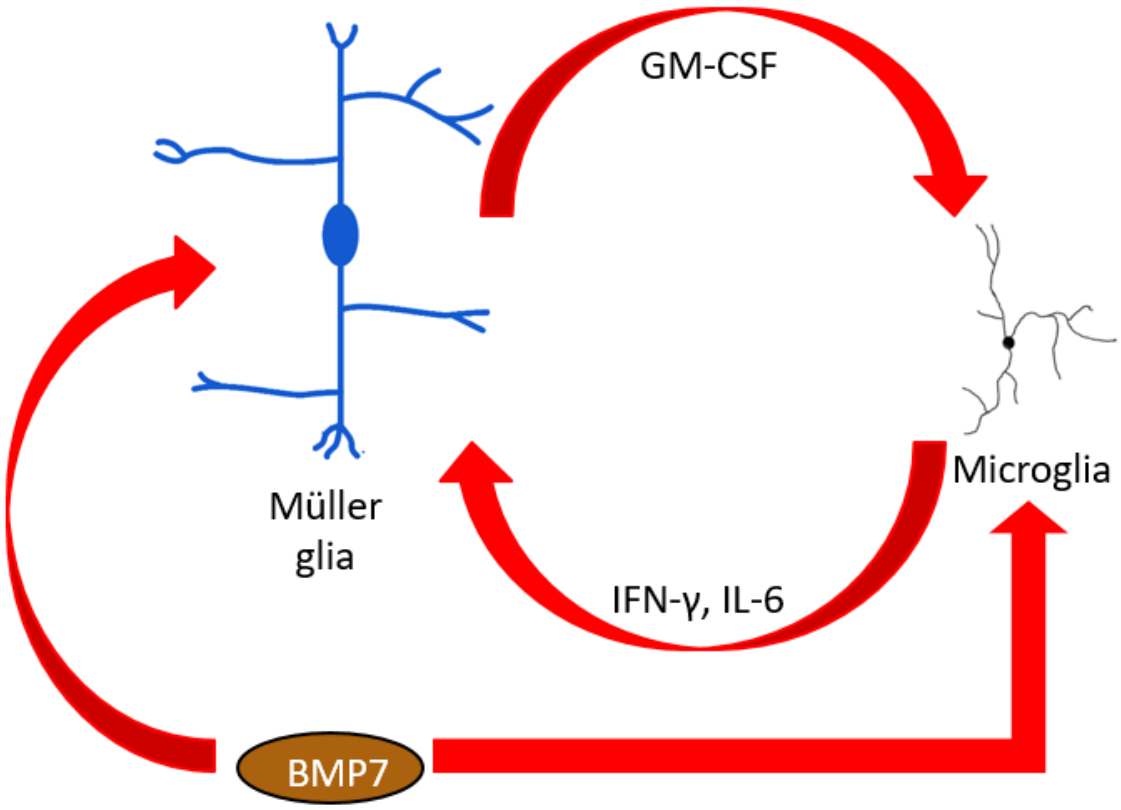

Fig. 5.1. Proposed model of BMP7 mediated regulation of retinal gliosis. BMP7 triggers a response in the Müller glia as well as microglia leading to secretion of factors such as IFN-γ, IL-6 and GMCSF. These factors could potentially mediate the gliosis response following BMP7 treatments.

progression. Other common changes include increase in expression of inflammatory markers, upregulation of neuroprotective factors and factors which regulate the blood retina barrier properties. Transcription factors such as SMAD, STAT and NF-κB are known to regulate the genes associated with gliosis such as GFAP, vimentin, Kir4.1 and interleukins. This suggests one of two possibilities for the common regulatory events of gliosis influenced by different factors: 1) regulation of non-canonical signaling via growth factors leading to activation of multiple transcription factors which leads to similar change;.for example, BMP signaling which can signal via SMADs or non-canonically via TAK leading to activation of p38/MAPK signaling to regulate

target genes, and 2) a common pathway activated by the different stresses that can trigger gliosis. The Hippo pathway can be regulated by growth factors, physical stress as well as factors such as ATP [249]. While regulation of Hippo pathway has been shown to be important in regulating retinal progenitor cell fate, its expression in the mature retina is not known. The results from this study as well as recently published data from Muriel Perrons lab show that AMOTs, YAP and TEADs are co-localized to the retinal glia [244]. Furthermore, regulation of Hippo-YAP signaling was observed in this study in retinas where gliosis was induced by IFN-γ injection, as well as in Hamon et al., 2017 mouse model of retinal degeneration. While we observed that inhibition of YAP/TEAD association decreased RNA levels of extracellular matrix molecules following IFN-γ treatment in the retina, Huang et al., 2016 observed that YAP knockout in development lef to hyperactivation of inflammatory response in primary brain astrocyte cultures [250].

We observe in the mouse retina that most of the YAP is localized in the nucleus of the Müller glia in wild type and the IFN- induced gliosis retinas. Furthermore, mammalian Müller glia exhibit proliferation in vitro or in show limited proliferation in the mouse retina [244]. This could be suggestive of a different role for YAP in the Müller glia. We propose that YAP in the murine retina serves as the common factor linking the response of the Müller glia to various gliosis inducing factors such as Wnts, TGF-β and IFN-γ (Figure 5.2). However, further studies need to be carried out to determine what aspects of gliosis are regulated by Hippo/YAP signaling and the specific interactions between the Hippo components and gliosis triggers in the retina.

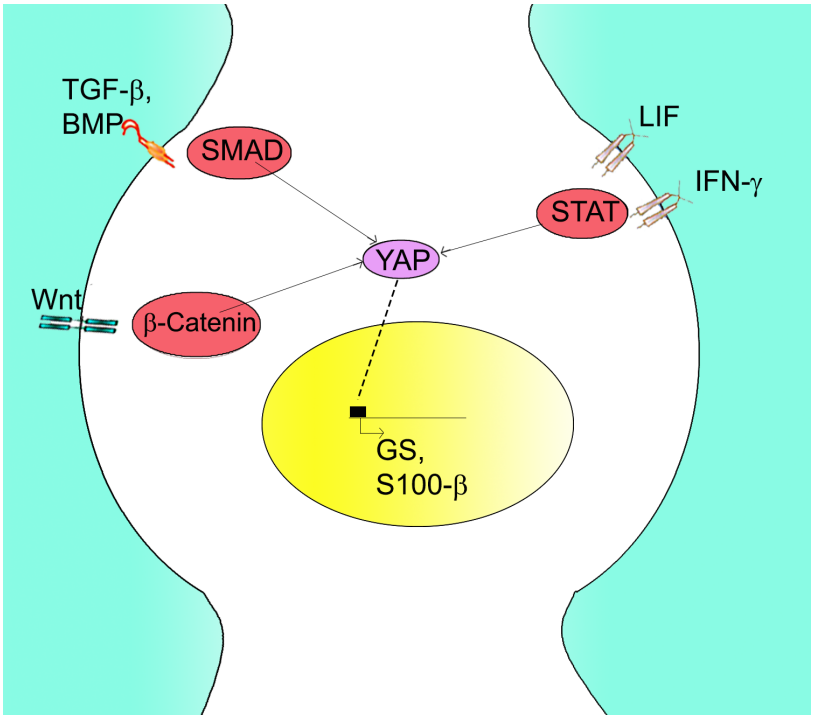

Fig. 5.2. Potential role of YAP as the common factor in regulating gliosis. YAP potentially regulates some of the responses associated with gliosis in retina. Furthermore, evidence of YAP interaction with transcription factors such as STAT and SMAD could suggest a potential role for YAP playing a central role in regulating certain common glial changes in response to different factors.

5.1 Future directions

The aim of this thesis is to characterize the gliosis response in the retina and the role of BMP7 in regulating this response. Using *in vitro* and *in vivo* approaches, we were able to show the mechanism for regulation of gliosis in the retina, which can be used for future research to help in manipulating gliosis to aid in functional recovery.

Throughout the studies we have primarily looked at RNA levels of gliosis markers representing various physiological changes in the glia. A subset of these markers were analyzed at the protein level. While this data does provide sufficient insight into the regulation of glial characteristics, future studies describing protein levels of the mark-

ers would be essential to elucidate the response in the glial cells. In chapter 2 and 3 of the studies, we observed differences in the levels of protein and RNA in the retinas induced treated with exogenic factors. This could be indicative of deregulation of the translation machinery, RNA stabilization or post translation modifications. Thus, it would be imperative to look into the regulation of proteins to provide a complete picture of regulation of gliosis in the retina.

In chapter 2, we showed that BMP7 triggers gliosis in the retina via activation of the canonical SMAD and non-canonical TAK pathway. This conclusion was based on the observation of the phosphorylated forms of these downstream signaling molecules. Thus, determining if gliosis is triggered preferentially by one pathway or the other, as well as identifying the downstream targets of these pathways in the retinal glia would be beneficial in developing treatments/inhibitory cues to prevent a prolonged gliosis response. While we observed an increase in phospho SMAD and phospho TAK levels in the retina, the source for BMP is still unclear. Identifying the source of BMP could be essential in developing treatment to aid in functional recovery in the retina by inhibiting long term changes of gliosis by blocking BMP signaling.

In chapter 3, we defined a model for reactive gliosis in the retina requiring activation of microglia. In our study we ablated retinal microglia for a maximum of 21 days and observed a decrease in BMP7 induced gliosis following microglial ablation. Further, we observed an increase in RNA levels of IL6 and RNA and protein levels of IFN-γ in the microglia following BMP7 treatment. Further work needs to be done 1) to determine if IL6 protein levels also increase corresponding to the RNA levels and 2) to determine if treatments with IFN-γ, IL6 and other growth factors (such as BMP) is sufficient to trigger gliosis in the absence of microglia. It would also be important to identify long term effects of microglia ablation on retinal function.

A more detailed study of the Hippo pathway in retinal gliosis will be essential in 1) determining if this pathway could be central to regulation of gliosis in different diseases and 2) if deregulation of the Hippo/YAP pathway can induce glial cells in to de-differentiation to generate retinal neurons lost due to injury or disease. In chapter 4, we described the expression of AMOT and YAP in the retina under normal conditions and in IFN-γ induced gliosis. The inhibitor used in the study, which blocks the interaction of YAP with TEADs to prevent activation of YAP/TEAD targets, lead to a decrease in the RNA levels of extracellular markers. Thus, it would be important to determine if this change is translated to the protein level. Future studies should also be aimed at determining if inhibition of YAP in disease models can aid in functional recovery or if YAP overexpression can induce proliferation and de-differentiation of Müller glia to aid with regeneration. Furthermore, overexpression or loss of expression of AMOT in the retinal glia should also be performed in disease models or gliosis induced retinas to determine the mechanism of regulation of Hippo/YAP pathway during gliosis.

Overall, these studies outlined above will provide more insight into the mechanism regulating retinal gliosis. This will help in studies which can lay the foundation to identify appropriate timepoint in the gliosis response which mediates the switch from beneficial to detrimental effects. The topics explored in this thesis have provide a basis for understanding gliosis regulation which can ultimately lead to development therapeutic approaches which can aid in the functional recovery as well regeneration in the retina.

REFERENCES

REFERENCES

[1] L. Lamport, *LaTeX: A Document Preparation System*. Reading Massachusetts: Addison-Wesley, 1994.

[2] B. E. Reese, "Development of the retina and optic pathway," *Vision Res*, vol. 51, no. 7, pp. 613–32, 2011. [Online]. Available: http://www.ncbi.nlm.nih.gov/pubmed/20647017

[3] T. L. Belecky-Adams, E. C. Chernoff, J. M. Wilson, and S. Dharmarajan, *Reactive Muller Glia as Potential Retinal Progenitors*, ser. Neural Stem Cells - New Perspectives, 2013. [Online]. Available: http://www.intechopen.com/books/export/citation/EndNote/neural-stem-cells-new-perspectives/reactive-muller-glia-as-potential-retinal-progenitors

[4] V. J. Kefalov, "Rod and cone visual pigments and phototransduction through pharmacological, genetic, and physiological approaches," *Journal of Biological Chemistry*, vol. 287, no. 3, pp. 1635–1641, 2012. [Online]. Available: ¡Go to ISI¿://WOS:000299321000005

[5] Y. B. Fu and K. W. Yau, "Phototransduction in mouse rods and cones," *Pflugers Archiv-European Journal of Physiology*, vol. 454, no. 5, pp. 805–819, 2007. [Online]. Available: ¡Go to ISI¿://WOS:000247465100010

[6] B. Roska and M. Meister, "The retina dissects the visual scene into distinct features," *New Visual Neurosciences*, pp. 163–182, 2014. [Online]. Available: ¡Go to ISI¿://WOS:000330033700014

[7] *Central Projections of Retinal Ganglion Cells*, ser. Neuroscience. Sunderland (MA): Sinauer Associates, 2001, vol. 2nd edition. [Online]. Available: https://www.ncbi.nlm.nih.gov/books/NBK10799/

[8] W. Heavner and L. Pevny, "Eye development and retinogenesis," *Cold Spring Harbor Perspectives in Biology*, vol. 4, no. 12, 2012. [Online]. Available: ¡Go to ISI¿://WOS:000312363400005

[9] S. Fuhrmann, "Eye morphogenesis and patterning of the optic vesicle," *Curr Top Dev Biol*, vol. 93, pp. 61–84, 2010. [Online]. Available: http://www.ncbi.nlm.nih.gov/pubmed/20959163

[10] T. D. Lamb, S. P. Collin, and J. Pugh, E. N., "Evolution of the vertebrate eye: opsins, photoreceptors, retina and eye cup," *Nat Rev Neurosci*, vol. 8, no. 12, pp. 960–76, 2007. [Online]. Available: http://www.ncbi.nlm.nih.gov/pubmed/18026166

[11] A. P. Jadhav, K. Roesch, and C. L. Cepko, "Development and neurogenic potential of muller glial cells in the vertebrate retina," *Prog Retin Eye Res*, vol. 28, no. 4, pp. 249–62, 2009. [Online]. Available: http://www.ncbi.nlm.nih.gov/pubmed/19465144

[12] G. D. Dakubo, S. T. Beug, C. J. Mazerolle, S. Thurig, Y. P. Wang, and V. A. Wallace, "Control of glial precursor cell development in the mouse optic nerve by sonic hedgehog from retinal ganglion cells," *Brain Research*, vol. 1228, pp. 27–42, 2008. [Online]. Available: ¡Go to ISI¿://WOS:000259512000005

[13] K. R. Huxlin, A. J. Sefton, and J. H. Furby, "The origin and development of retinal astrocytes in the mouse," *J Neurocytol*, vol. 21, no. 7, pp. 530–44, 1992. [Online]. Available: http://www.ncbi.nlm.nih.gov/pubmed/1500949

[14] F. Ginhoux, S. Lim, G. Hoeffel, D. Low, and T. Huber, "Origin and differentiation of microglia," *Frontiers in Cellular Neuroscience*, vol. 7, 2013. [Online]. Available: ¡Go to ISI¿://WOS:000317593700001

[15] K. Ono, T. Tsumori, T. Kishi, S. Yokota, and Y. Yasui, "Developmental appearance of oligodendrocytes in the embryonic chick retina," *J Comp Neurol*, vol. 398, no. 3, pp. 309–22, 1998. [Online]. Available: http://www.ncbi.nlm.nih.gov/pubmed/9714145

[16] C. P. Zelinka, M. A. Scott, L. Volkov, and A. J. Fischer, "The reactivity, distribution and abundance of non-astrocytic inner retinal glial (nirg) cells are regulated by microglia, acute damage, and igf1," *Plos One*, vol. 7, no. 9, 2012. [Online]. Available: ¡Go to ISI¿://WOS:000308577600060

[17] E. A. Newman, "Acid efflux from retinal glial cells generated by sodium bicarbonate cotransport," *Journal of Neuroscience*, vol. 16, no. 1, pp. 159–168, 1996. [Online]. Available: ¡Go to ISI¿://WOS:A1996TL99000018

[18] P. Mergenthaler, U. Lindauer, G. A. Dienel, and A. Meisel, "Sugar for the brain: the role of glucose in physiological and pathological brain function," *Trends Neurosci*, vol. 36, no. 10, pp. 587–97, 2013. [Online]. Available: http://www.ncbi.nlm.nih.gov/pubmed/23968694

[19] J. B. Hurley, K. J. Lindsay, and J. H. Du, "Glucose, lactate, and shuttling of metabolites in vertebrate retinas," *Journal of Neuroscience Research*, vol. 93, no. 7, pp. 1079–1092, 2015. [Online]. Available: ¡Go to ISI¿://WOS:000354822900010

[20] J. A. PerezLeon, I. Osorio-Paz, L. Francois, and R. Salceda, "Immunohistochemical localization of glycogen synthase and gsk3 beta: Control of glycogen content in retina," *Neurochemical Research*, vol. 38, no. 5, pp. 1063–1069, 2013. [Online]. Available: ¡Go to ISI¿://WOS:000316903200018

[21] A. Bringmann, T. Pannicke, B. Biedermann, M. Francke, I. Iandiev, J. Grosche, P. Wiedemann, J. Albrecht, and A. Reichenbach, "Role of retinal glial cells in neurotransmitter uptake and metabolism," *Neurochemistry International*, vol. 54, no. 3-4, pp. 143–160, 2009. [Online]. Available: ¡Go to ISI¿://WOS:000264697100001

[22] D. V. Pow and S. R. Robinson, "Glutamate in some retinal neurons is derived solely from glia," *Neuroscience*, vol. 60, no. 2, pp. 355–366, 1994. [Online]. Available: ¡Go to ISI¿://WOS:A1994NK70800008

[23] W. S. Chung, N. J. Allen, and C. Eroglu, "Astrocytes control synapse formation, function, and elimination," *Cold Spring Harb Perspect Biol*, vol. 7, no. 9, p. a020370, 2015. [Online]. Available: http://www.ncbi.nlm.nih.gov/pubmed/25663667

[24] M. T. Heneka, J. J. Rodriguez, and A. Verkhratsky, "Neuroglia in neurodegeneration," *Brain Research Reviews*, vol. 63, no. 1-2, pp. 189–211, 2010. [Online]. Available: ¡Go to ISI¿://WOS:000278034500018

[25] S. Tout, T. Chanling, H. Hollander, and J. Stone, "The role of muller cells in the formation of the blood-retinal barrier," *Neuroscience*, vol. 55, no. 1, pp. 291–301, 1993. [Online]. Available: ¡Go to ISI¿://WOS:A1993LL16300024

[26] J. Cunha-Vaz, "The blood-retinal barrier in the management of retinal disease: Euretina award lecture," *Ophthalmologica*, vol. 237, no. 1, pp. 1–10, 2017. [Online]. Available: ¡Go to ISI¿://WOS:000395356700001

[27] P. Kofuji, B. Biedermann, V. Siddharthan, M. Raap, I. Iandiev, I. Milenkovic, A. Thomzig, R. W. Veh, A. Bringmann, and A. Reichenbach, "Kir potassium channel subunit expression in retinal glial cells: Implications for spatial potassium buffering," *Glia*, vol. 39, no. 3, pp. 292–303, 2002. [Online]. Available: ¡Go to ISI¿://WOS:000177802100011

[28] A. Reichenbach, A. Wurm, T. Pannicke, I. Iandiev, P. Wiedemann, and A. Bringmann, "Muller cells as players in retinal degeneration and edema," *Graefes Archive for Clinical and Experimental Ophthalmology*, vol. 245, no. 5, pp. 627–636, 2007. [Online]. Available: ¡Go to ISI¿://WOS:000246183300002

[29] E. A. Nagelhus, Y. Horio, A. Inanobe, A. Fujita, F. M. Haug, S. Nielsen, Y. Kurachi, and O. P. Ottersen, "Immunogold evidence suggests that coupling of k+ siphoning and water transport in rat retinal muller cells is mediated by a coenrichment of kir4.1 and aqp4 in specific membrane domains," *Glia*, vol. 26, no. 1, pp. 47–54, 1999. [Online]. Available: ¡Go to ISI¿://WOS:000078911800005

[30] J. W. Deitmer, "A role for co2 and bicarbonate transporters in metabolic exchanges in the brain," *Journal of Neurochemistry*, vol. 80, no. 5, pp. 721–726, 2002. [Online]. Available: ¡Go to ISI¿://WOS:000174169500001

[31] T. Langmann, "Microglia activation in retinal degeneration," *Journal of Leukocyte Biology*, vol. 81, no. 6, pp. 1345–1351, 2007. [Online]. Available: ¡Go to ISI¿://WOS:000246988600002

[32] M. E. Tremblay, R. L. Lowery, and A. K. Majewska, "Microglial interactions with synapses are modulated by visual experience," *Plos Biology*, vol. 8, no. 11, 2010. [Online]. Available: ¡Go to ISI¿://WOS:000284762300004

[33] L. Li, N. Eter, and P. Heiduschka, "The microglia in healthy and diseased retina," *Experimental Eye Research*, vol. 136, pp. 116–130, 2015. [Online]. Available: ¡Go to ISI¿://WOS:000356562100015

[34] M. Ueno, Y. Fujita, T. Tanaka, Y. Nakamura, J. Kikuta, M. Ishii, and T. Yamashita, "Layer v cortical neurons require microglial support for survival during postnatal development," *Nature Neuroscience*, vol. 16, no. 5, pp. 543–+, 2013. [Online]. Available: ¡Go to ISI¿://WOS:000318029300010

[35] M. Noda, Y. Doi, J. F. Liang, J. Kawanokuchi, Y. Sonobe, H. Takeuchi, T. Mizuno, and A. Suzumura, "Fractalkine attenuates excito-neurotoxicity via microglial clearance of damaged neurons and antioxidant enzyme heme oxygenase-1 expression," *Journal of Biological Chemistry*, vol. 286, no. 3, pp. 2308–2319, 2011. [Online]. Available: ¡Go to ISI¿://WOS:000286191500070

[36] K. Takahashi, C. D. P. Rochford, and H. Neumann, "Clearance of apoptotic neurons without inflammation by microglial triggering receptor expressed on myeloid cells-2," *Journal of Experimental Medicine*, vol. 201, no. 4, pp. 647–657, 2005. [Online]. Available: ¡Go to ISI¿://WOS:000227306900019

[37] H. Wake, A. J. Moorhouse, S. Jinno, S. Kohsaka, and J. Nabekura, "Resting microglia directly monitor the functional state of synapses in vivo and determine the fate of ischemic terminals," *Journal of Neuroscience*, vol. 29, no. 13, pp. 3974–3980, 2009. [Online]. Available: ¡Go to ISI¿://WOS:000264767500002

[38] T. Arnold and C. Betsholtz, "The importance of microglia in the development of the vasculature in the central nervous system," *Vasc Cell*, vol. 5, no. 1, p. 4, 2013. [Online]. Available: http://www.ncbi.nlm.nih.gov/pubmed/23422217

[39] M. R. Ritter, E. Banin, S. K. Moreno, E. Aguilar, M. I. Dorrell, and M. Friedlander, "Myeloid progenitors differentiate into microglia and promote vascular repair in a model of ischemic retinopathy," *Journal of Clinical Investigation*, vol. 116, no. 12, pp. 3266–3276, 2006. [Online]. Available: ¡Go to ISI¿://WOS:000242606900026

[40] J. E. Lee, K. J. Liang, R. N. Fariss, and W. T. Wong, "Ex vivo dynamic imaging of retinal microglia using time-lapse confocal microscopy," *Investigative Ophthalmology and Visual Science*, vol. 49, no. 9, pp. 4169–4176, 2008. [Online]. Available: ¡Go to ISI¿://WOS:000258896500057

[41] M. Pekny, U. Wilhelmsson, and M. Pekna, "The dual role of astrocyte activation and reactive gliosis," *Neuroscience Letters*, vol. 565, pp. 30–38, 2014. [Online]. Available: ¡Go to ISI¿://WOS:000335114400006

[42] A. Reichenbach and A. Bringmann, "Muller cells in the healthy and diseased retina," *Muller Cells in the Healthy and Diseased Retina*, pp. 1–417, 2010. [Online]. Available: ¡Go to ISI¿://WOS:000276927400006

[43] M. V. Sofroniew, "Molecular dissection of reactive astrogliosis and glial scar formation," *Trends in Neurosciences*, vol. 32, no. 12, pp. 638–647, 2009. [Online]. Available: ¡Go to ISI¿://WOS:000272643900005

[44] J. L. Ridet, S. K. Malhotra, A. Privat, and F. H. Gage, "Reactive astrocytes: cellular and molecular cues to biological function," *Trends in Neurosciences*, vol. 20, no. 12, pp. 570–577, 1997. [Online]. Available: ¡Go to ISI¿://WOS:A1997YJ58000010

[45] R. de Hoz, B. Rojas, A. I. Ramirez, J. J. Salazar, B. I. Gallego, A. Trivino, and J. M. Ramirez, "Retinal macroglial responses in health and disease," *Biomed Research International*, 2016. [Online]. Available: ¡Go to ISI¿://WOS:000376915000001

[46] A. Bringmann, I. Iandiev, T. Pannicke, A. Wurm, M. Hollborn, P. Wiedemann, N. N. Osborne, and A. Reichenbach, "Cellular signaling and factors involved in muller cell gliosis: neuroprotective and detrimental effects," *Prog Retin Eye Res*, vol. 28, no. 6, pp. 423–51, 2009. [Online]. Available: http://www.ncbi.nlm.nih.gov/pubmed/19660572

[47] K. M. Drescher and J. A. WhittumHudson, "Modulation of immune-associated surface markers and cytokine production by murine retinal glial cells," *Journal of Neuroimmunology*, vol. 64, no. 1, pp. 71–81, 1996. [Online]. Available: ¡Go to ISI¿://WOS:A1996TW36800009

[48] I. Iandiev, A. Wurm, M. Hollborn, P. Wiedemann, C. Grimm, C. E. Reme, A. Reichenbach, T. Pannicke, and A. Bringmann, "Muller cell response to blue light injury of the rat retina," *Invest Ophthalmol Vis Sci*, vol. 49, no. 8, pp. 3559–67, 2008. [Online]. Available: http://www.ncbi.nlm.nih.gov/pubmed/18450590

[49] S. Ooto, T. Akagi, R. Kageyama, J. Akita, M. Mandai, Y. Honda, and M. Takahashi, "Potential for neural regeneration after neurotoxic injury in the adult mammalian retina," *Proc Natl Acad Sci U S A*, vol. 101, no. 37, pp. 13 654–9, 2004. [Online]. Available: http://www.ncbi.nlm.nih.gov/pubmed/15353594

[50] A. Bringmann, T. Pannicke, J. Grosche, M. Francke, P. Wiedemann, S. N. Skatchkov, N. N. Osborne, and A. Reichenbach, "Muller cells in the healthy and diseased retina," *Progress in Retinal and Eye Research*, vol. 25, no. 4, pp. 397–424, 2006. [Online]. Available: ¡Go to ISI¿://WOS:000239884500003

[51] E. Vecino, F. D. Rodriguez, N. Ruzafa, X. Pereiro, and S. C. Sharma, "Glia-neuron interactions in the mammalian retina," *Prog Retin Eye Res*, vol. 51, pp. 1–40, 2016. [Online]. Available: http://www.ncbi.nlm.nih.gov/pubmed/26113209

[52] E. Garcia, J. Aguilar-Cevallos, R. Silva-Garcia, and A. Ibarra, "Cytokine and growth factor activation in vivo and in vitro after spinal cord injury," *Mediators of Inflammation*, 2016. [Online]. Available: ¡Go to ISI¿://WOS:000379054700001

[53] A. M. Smith, H. M. Gibbons, R. L. Oldfield, P. M. Bergin, E. W. Mee, M. A. Curtis, R. L. M. Faull, and M. Dragunow, "M-csf increases proliferation and phagocytosis while modulating receptor and transcription factor expression in adult human microglia," *Journal of Neuroinflammation*, vol. 10, 2013. [Online]. Available: ¡Go to ISI¿://WOS:000322536500001

[54] M. Karlstetter, R. Scholz, M. Rutar, W. T. Wong, J. M. Provis, and T. Langmann, "Retinal microglia: Just bystander or target for therapy?" *Progress in Retinal and Eye Research*, vol. 45, pp. 30–57, 2015. [Online]. Available: ¡Go to ISI¿://WOS:000350836300002

[55] D. Boche, V. H. Perry, and J. A. R. Nicoll, "Review: Activation patterns of microglia and their identification in the human brain," *Neuropathology and Applied Neurobiology*, vol. 39, no. 1, pp. 3–18, 2013. [Online]. Available: ¡Go to ISI¿://WOS:000313909200002

[56] J. D. Cherry, J. A. Olschowka, and M. K. O'Banion, "Neuroinflammation and m2 microglia: the good, the bad, and the inflamed," *Journal of Neuroinflammation*, vol. 11, 2014. [Online]. Available: ¡Go to ISI¿://WOS:000338140600001

[57] Y. Li, X. F. Du, C. S. Liu, Z. L. Wen, and J. L. Du, "Reciprocal regulation between resting microglial dynamics and neuronal activity in vivo," *Developmental Cell*, vol. 23, no. 6, pp. 1189–1202, 2012. [Online]. Available: ¡Go to ISI¿://WOS:000312429200015

[58] O. Uckermann, A. Wolf, F. Kutzera, F. Kalisch, A. G. Beck-Sickinger, P. Wiedemann, A. Reichenbach, and A. Bringmann, "Glutamate release by neurons evokes a purinergic inhibitory mechanism of osmotic glial cell swelling in the rat retina: Activation by neuropeptide y," *Journal of Neuroscience Research*, vol. 83, no. 4, pp. 538–550, 2006. [Online]. Available: ¡Go to ISI¿://WOS:000236263400003

[59] W. Q. Wang, J. Huang, and J. J. Chen, "Angiomotin-like proteins associate with and negatively regulate yap1," *Journal of Biological Chemistry*, vol. 286, no. 6, pp. 4364–4370, 2011. [Online]. Available: ¡Go to ISI¿://WOS:000286975700036

[60] C. Rohl and J. Sievers, "Microglia is activated by astrocytes in trimethyltin intoxication," *Toxicology and Applied Pharmacology*, vol. 204, no. 1, pp. 36–45, 2005. [Online]. Available: ¡Go to ISI¿://WOS:000228253300005

[61] Z. W. Gao, Q. S. Zhu, Y. P. Zhang, Y. Z. Zhao, L. Cai, C. Shields, and J. Cai, "Reciprocal modulation between microglia and astrocyte in reactive gliosis following the cns injury," *Molecular Neurobiology*, vol. 48, no. 3, pp. 690–701, 2013. [Online]. Available: ¡Go to ISI¿://WOS:000326714700024

[62] T. Schilling, R. Nitsch, U. Heinemann, D. Haas, and C. Eder, "Astrocyte-released cytokines induce ramification and outward k+ channel expression in microglia via distinct signalling pathways," *European Journal of Neuroscience*, vol. 14, no. 3, pp. 463–473, 2001. [Online]. Available: ¡Go to ISI¿://WOS:000171184400006

[63] A. Rolls, R. Shechter, A. London, Y. Segev, J. Jacob-Hirsch, N. Amariglio, G. Rechavi, and M. Schwartz, "Two faces of chondroitin sulfate proteoglycan in spinal cord repair: A role in microglia/macrophage activation," *Plos Medicine*, vol. 5, no. 8, pp. 1262–1277, 2008. [Online]. Available: ¡Go to ISI¿://WOS:000258739200016

[64] R. Herrera-Molina and R. von Bernhardi, "Transforming growth factor-beta 1 produced by hippocampal cells modulates microglial reactivity in culture," *Neurobiology of Disease*, vol. 19, no. 1-2, pp. 229–236, 2005. [Online]. Available: ¡Go to ISI¿://WOS:000228672900024

[65] D. Goldman, "Muller glial cell reprogramming and retina regeneration," *Nat Rev Neurosci*, vol. 15, no. 7, pp. 431–42, 2014. [Online]. Available: http://www.ncbi.nlm.nih.gov/pubmed/24894585

[66] L. Zhang, W. Q. Zhao, B. S. Li, D. L. Alkon, J. L. Barker, Y. H. Chang, M. Wu, and D. R. Rubinow, "Tnf-alpha induced over-expression of gfap is associated with mapks," *Neuroreport*, vol. 11, no. 2, pp. 409–412, 2000. [Online]. Available: ¡Go to ISI¿://WOS:000084992200038

[67] A. Cotinet, O. Goureau, D. Hicks, B. Thillaye-Goldenberg, and Y. de Kozak, "Tumor necrosis factor and nitric oxide production by retinal muller glial cells from rats exhibiting inherited retinal dystrophy," *Glia*, vol. 20, no. 1, pp. 59–69, 1997. [Online]. Available: http://www.ncbi.nlm.nih.gov/pubmed/9145305

[68] W. Xue, R. I. Cojocaru, V. J. Dudley, M. Brooks, A. Swaroop, and V. P. Sarthy, "Ciliary neurotrophic factor induces genes associated with inflammation and gliosis in the retina: a gene profiling study of flow-sorted, muller cells," *PLoS One*, vol. 6, no. 5, p. e20326, 2011. [Online]. Available: http://www.ncbi.nlm.nih.gov/pubmed/21637858

[69] A. J. Fischer, G. Omar, J. Eubanks, C. R. McGuire, B. D. Dierks, and T. A. Reh, "Different aspects of gliosis in retinal muller glia can be induced by cntf, insulin, and fgf2 in the absence of damage," *Molecular Vision*, vol. 10, no. 115-16, pp. 973–986, 2004. [Online]. Available: ¡Go to ISI¿://WOS:000225975500002

[70] X. F. Zhao, J. Wan, C. Powell, R. Ramachandran, J. Myers, M. G., and D. Goldman, "Leptin and il-6 family cytokines synergize to stimulate muller glia reprogramming and retina regeneration," *Cell Rep*, vol. 9, no. 1, pp. 272–84, 2014. [Online]. Available: http://www.ncbi.nlm.nih.gov/pubmed/25263554

[71] H. Yamada, E. Yamada, A. Ando, M. S. Seo, N. Esumi, N. Okamoto, M. Vinores, W. LaRochelle, D. J. Zack, and P. A. Campochiaro, "Platelet-derived growth factor-a-induced retinal gliosis protects against ischemic retinopathy," *Am J Pathol*, vol. 156, no. 2, pp. 477–87, 2000. [Online]. Available: http://www.ncbi.nlm.nih.gov/pubmed/10666377

[72] N. Jahan and S. S. Hannila, "Transforming growth factor beta-induced expression of chondroitin sulfate proteoglycans is mediated through non-smad signaling pathways," *Experimental Neurology*, vol. 263, pp. 372–384, 2015. [Online]. Available: ¡Go to ISI¿://WOS:000346626100039

[73] K. Miyazono, Y. Kamiya, and M. Morikawa, "Bone morphogenetic protein receptors and signal transduction," *Journal of Biochemistry*, vol. 147, no. 1, pp. 35–51, 2010. [Online]. Available: ¡Go to ISI¿://WOS:000273501300005

[74] P. Rajan, D. M. Panchision, L. E. Newell, and R. D. G. McKay, "Bmps signal alternately through a smad or frap-stat pathway to regulate fate choice in cns stem cells," *Journal of Cell Biology*, vol. 161, no. 5, pp. 911–921, 2003. [Online]. Available: ¡Go to ISI¿://WOS:000183504700008

[75] B. Bragdon, O. Moseychuk, S. Saldanha, D. King, J. Julian, and A. Nohe, "Bone morphogenetic proteins: A critical review," *Cellular Signalling*, vol. 23, no. 4, pp. 609–620, 2011. [Online]. Available: ¡Go to ISI¿://WOS:000287565400002

[76] C. Liu, Y. Li, P. J. Lein, and B. D. Ford, "Spatiotemporal patterns of gfap upregulation in rat brain following acute intoxication with diisopropylfluorophosphate (dfp)," *Curr Neurobiol*, vol. 3, no. 2, pp. 90–97, 2012. [Online]. Available: http://www.ncbi.nlm.nih.gov/pubmed/24039349

[77] M. L. Fuller, A. K. DeChant, B. Rothstein, A. Caprariello, R. Wang, A. K. Hall, and R. H. Miller, "Bone morphogenetic proteins promote gliosis in demyelinating spinal cord lesions," *Annals of Neurology*, vol. 62, no. 3, pp. 288–300, 2007. [Online]. Available: ¡Go to ISI¿://WOS:000249937000015

[78] Y. Ueki and T. A. Reh, "Activation of bmp-smad1/5/8 signaling promotes survival of retinal ganglion cells after damage in vivo," *Plos One*, vol. 7, no. 6, 2012. [Online]. Available: ¡Go to ISI¿://WOS:000305348400086

[79] A. J. Fischer, M. A. Scott, C. Zelinka, and P. Sherwood, "A novel type of glial cell in the retina is stimulated by insulin-like growth factor 1 and may exacerbate damage to neurons and muller glia," *Glia*, vol. 58, no. 6, pp. 633–649, 2010. [Online]. Available: ¡Go to ISI¿://000275939500001

[80] J. P. D. Vaccari, A. Marcillo, D. Nonner, W. D. Dietrich, and R. W. Keane, "Neuroprotective effects of bone morphogenetic protein 7 (bmp7) treatment after spinal cord injury," *Neuroscience Letters*, vol. 465, no. 3, pp. 226–229, 2009. [Online]. Available: ¡Go to ISI¿://WOS:000271066800006

[81] V. Sahni, A. Mukhopadhyay, V. Tysseling, A. Hebert, D. Birch, T. L. Mcguire, S. I. Stupp, and J. A. Kessler, "Bmpr1a and bmpr1b signaling exert opposing effects on gliosis after spinal cord injury," *Journal of Neuroscience*, vol. 30, no. 5, pp. 1839–1855, 2010. [Online]. Available: ¡Go to ISI¿://WOS:000274246700027

[82] S. Piccolo, S. Dupont, and M. Cordenonsi, "The biology of yap/taz: Hippo signaling and beyond," *Physiological Reviews*, vol. 94, no. 4, pp. 1287–1312, 2014. [Online]. Available: ¡Go to ISI¿://WOS:000343216300008

[83] J. S. Bae, S. M. Kim, and H. Lee, "The hippo signaling pathway provides novel anti-cancer drug targets," *Oncotarget*, vol. 8, no. 9, pp. 16 084–16 098, 2017. [Online]. Available: ¡Go to ISI¿://WOS:000396013700150

[84] F. X. Yu and K. L. Guan, "The hippo pathway: regulators and regulations," *Genes and Development*, vol. 27, no. 4, pp. 355–371, 2013. [Online]. Available: ¡Go to ISI¿://WOS:000315286300002

[85] F. Zanconato, M. Forcato, G. Battilana, L. Azzolin, E. Quaranta, B. Bodega, A. Rosato, S. Bicciato, M. Cordenonsi, and S. Piccolo, "Genome-wide association between yap/taz/tead and ap-1 at enhancers drives oncogenic growth," *Nature Cell Biology*, vol. 17, no. 9, pp. 1218–+, 2015. [Online]. Available: ¡Go to ISI¿://WOS:000361113700017

[86] B. Zhao, L. Li, L. Wang, C. Y. Wang, J. Yu, and K. L. Guan, "Cell detachment activates the hippo pathway via cytoskeleton reorganization to induce anoikis," *Genes Dev*, vol. 26, no. 1, pp. 54–68, 2012. [Online]. Available: http://www.ncbi.nlm.nih.gov/pubmed/22215811

[87] Y. J. Zheng, Y. Y. Zhang, G. Barutello, K. C. Chiu, M. Arigoni, C. Giampietro, F. Cavallo, and L. Holmgren, "Angiomotin like-1 is a novel component of the n-cadherin complex affecting endothelial/pericyte interaction in normal and tumor angiogenesis," *Scientific Reports*, vol. 6, 2016. [Online]. Available: ¡Go to ISI¿://WOS:000380978200001

[88] C. Yi, S. Troutman, D. Fera, A. Stemmer-Rachamimov, J. L. Avila, N. Christian, N. L. Persson, A. Shimono, D. W. Speicher, R. Marmorstein, L. Holmgren, and J. L. Kissil, "A tight junction-associated merlin-angiomotin complex mediates merlin's regulation of mitogenic signaling and tumor suppressive functions," *Cancer Cell*, vol. 19, no. 4, pp. 527–40, 2011. [Online]. Available: http://www.ncbi.nlm.nih.gov/pubmed/21481793

[89] W. Kim, S. K. Khan, J. Gvozdenovic-Jeremic, Y. Kim, J. Dahlman, H. Kim, O. Park, T. Ishitani, E. H. Jho, B. Gao, and Y. Yang, "Hippo signaling interactions with wnt/beta-catenin and notch signaling repress liver tumorigenesis," *Journal of Clinical Investigation*, vol. 127, no. 1, pp. 137–152, 2017. [Online]. Available: ¡Go to ISI¿://WOS:000392271300018

[90] R. Tsutsumi, M. Masoudi, A. Takahashi, Y. Fujii, T. Hayashi, I. Kikuchi, Y. Satou, M. Taira, and M. Hatakeyama, "Yap and taz, hippo signaling targets, act as a rheostat for nuclear shp2 function," *Developmental Cell*, vol. 26, no. 6, pp. 658–665, 2013. [Online]. Available: ¡Go to ISI¿://WOS:000326305100014

[91] M. Imajo, K. Miyatake, A. Iimura, A. Miyamoto, and E. Nishida, "A molecular mechanism that links hippo signalling to the inhibition of wnt/beta-catenin signalling," *Embo Journal*, vol. 31, no. 5, pp. 1109–1122, 2012. [Online]. Available: ¡Go to ISI¿://WOS:000301342500007

[92] M. Xin, Y. Kim, L. B. Sutherland, X. X. Qi, J. McAnally, R. J. Schwartz, J. A. Richardson, R. Bassel-Duby, and E. N. Olson, "Regulation of insulin-like growth factor signaling by yap governs cardiomyocyte proliferation and embryonic heart size," *Science Signaling*, vol. 4, no. 196, 2011. [Online]. Available: ¡Go to ISI¿://WOS:000296560500002

[93] C. Alarcn, A.-I. Zaromytidou, Q. Xi, S. Gao, J. Yu, S. Fujisawa, A. Barlas, A. N. Miller, K. Manova-Todorova, M. J. Macias, G. Sapkota, D. Pan, and J. Massagu, "Cdk8/9 drive smad transcriptional action, turnover and yap interactions in bmp and tgf pathways," *Cell*, vol. 139, no. 4, pp. 757–769, 2009. [Online]. Available: http://www.ncbi.nlm.nih.gov/pmc/articles/PMC2818353/

[94] D. Yimlamai, C. Christodoulou, G. G. Galli, K. Yanger, B. Pepe-Mooney, B. Gurung, K. Shrestha, P. Cahan, B. Z. Stanger, and F. D. Camargo, "Hippo pathway activity influences liver cell fate," *Cell*, vol. 157, no. 6, pp. 1324–1338, 2014. [Online]. Available: ¡Go to ISI¿://WOS:000340881400010

[95] C. Ffrenchconstant, R. H. Miller, J. F. Burne, and M. C. Raff, "Evidence that migratory oligodendrocyte-type-2 astrocyte (o-2a) progenitor cells are kept out of the rat retina by a barrier at the eye-end of the optic-nerve," *Journal of Neurocytology*, vol. 17, no. 1, pp. 13–25, 1988. [Online]. Available: ¡Go to ISI¿://A1988N197400002

[96] A. J. Fischer, C. Zelinka, and M. A. Scott, "Heterogeneity of glia in the retina and optic nerve of birds and mammals," *PLoS One*, vol. 5, no. 6, p. e10774, 2010. [Online]. Available: http://www.ncbi.nlm.nih.gov/pubmed/20567503

[97] V. H. Perry and R. D. Lund, "Evidence that the lamina-cribrosa prevents intraretinal myelination of retinal ganglion-cell axons," *Journal of Neurocytology*, vol. 19, no. 2, pp. 265–272, 1990. [Online]. Available: ¡Go to ISI¿://A1990DC51100011

[98] M. Dubois-Dauphin, C. Poitry-Yamate, F. De Bilbao, A. K. Julliard, F. Jourdan, and G. Donati, "Early postnatal muller cell death leads to retinal but not optic nerve degeneration in nse-hu-bcl-2 transgenic mice," *Neuroscience*, vol. 95, no. 1, pp. 9–21, 2000. [Online]. Available: ¡Go to ISI¿://000084071000003

[99] S. Kuchler-Bopp, J. P. Delaunoy, J. C. Artault, M. Zaepfel, and J. B. Dietrich, "Astrocytes induce several blood-brain barrier properties in non-neural endothelial cells," *Neuroreport*, vol. 10, no. 6, pp. 1347–1353, 1999. [Online]. Available: ¡Go to ISI¿://000080488200036

[100] S. B. Rompani and C. L. Cepko, "A common progenitor for retinal astrocytes and oligodendrocytes," *The Journal of Neuroscience*, vol. 30, no. 14, pp. 4970–4980, 2010. [Online]. Available: https://www.ncbi.nlm.nih.gov/pmc/articles/PMC3536471/

[101] M. R. Hernandez, H. Miao, and T. Lukas, "Astrocytes in glaucomatous optic neuropathy," *Prog Brain Res*, vol. 173, pp. 353–73, 2008. [Online]. Available: http://www.ncbi.nlm.nih.gov/pubmed/18929121

[102] A. Bringmann and P. Wiedemann, "Muller glial cells in retinal disease," *Ophthalmologica*, vol. 227, no. 1, pp. 1–19, 2012. [Online]. Available: http://www.ncbi.nlm.nih.gov/pubmed/21921569

[103] R. A. Asher, D. A. Morgenstern, P. S. Fidler, K. H. Adcock, A. Oohira, J. E. Braistead, J. M. Levine, R. U. Margolis, J. H. Rogers, and J. W. Fawcett, "Neurocan is upregulated in injured brain and in cytokine-treated astrocytes," *Journal of Neuroscience*, vol. 20, no. 7, pp. 2427–2438, 2000. [Online]. Available: ¡Go to ISI¿://000086136600004

[104] P. E. Nickerson, M. C. McLeod, T. Myers, and D. B. Clarke, "Effects of epidermal growth factor and erythropoietin on muller glial activation and phenotypic plasticity in the adult mammalian retina," *J Neurosci Res*, vol. 89, no. 7, pp. 1018–30, 2011. [Online]. Available: http://www.ncbi.nlm.nih.gov/pubmed/21484851

[105] S. Ekmark-Lewen, A. Lewen, C. Israelsson, G. L. Li, M. Farooque, Y. Olsson, T. Ebendal, and L. Hillered, "Vimentin and gfap responses in astrocytes after contusion trauma to the murine brain," *Restor Neurol Neurosci*, vol. 28, no. 3, pp. 311–21, 2010. [Online]. Available: http://www.ncbi.nlm.nih.gov/pubmed/20479526

[106] W. T. Norton, D. A. Aquino, I. Hozumi, F. C. Chiu, and C. F. Brosnan, "Quantitative aspects of reactive gliosis: a review," *Neurochem Res*, vol. 17, no. 9, pp. 877–85, 1992. [Online]. Available: http://www.ncbi.nlm.nih.gov/pubmed/1407275

[107] M. V. Sofroniew and H. V. Vinters, "Astrocytes: biology and pathology," *Acta Neuropathol*, vol. 119, no. 1, pp. 7–35, 2010. [Online]. Available: http://www.ncbi.nlm.nih.gov/pubmed/20012068

[108] M. J. Lee, C. J. Chen, W. C. Huang, M. C. Huang, W. C. Chang, H. S. Kuo, M. J. Tsai, Y. L. Lin, and H. Cheng, "Regulation of chondroitin sulphate proteoglycan and reactive gliosis after spinal cord transection: effects of peripheral nerve graft and fibroblast growth factor 1," *Neuropathol Appl Neurobiol*, vol. 37, no. 6, pp. 585–99, 2011. [Online]. Available: http://www.ncbi.nlm.nih.gov/pubmed/21486314

[109] T. Nakazawa, A. Matsubara, K. Noda, T. Hisatomi, H. She, D. Skondra, S. Miyahara, L. Sobrin, K. L. Thomas, D. F. Chen, C. L. Grosskreutz, A. Hafezi-Moghadam, and J. W. Miller, "Characterization of cytokine responses to retinal detachment in rats," *Mol Vis*, vol. 12, pp. 867–78, 2006. [Online]. Available: http://www.ncbi.nlm.nih.gov/pubmed/16917487

[110] J. Silver and J. H. Miller, "Regeneration beyond the glial scar," *Nat Rev Neurosci*, vol. 5, no. 2, pp. 146–56, 2004. [Online]. Available: http://www.ncbi.nlm.nih.gov/pubmed/14735117

[111] T. Setoguchi, K. Yone, E. Matsuoka, H. Takenouchi, K. Nakashima, T. Sakou, S. Komiya, and S. Izumo, "Traumatic injury-induced bmp7 expression in the adult rat spinal cord," *Brain Research*, vol. 921, no. 1-2, pp. 219–25, 2001. [Online]. Available: http://www.ncbi.nlm.nih.gov/pubmed/11720729

[112] D. W. Hampton, R. A. Asher, T. Kondo, J. D. Steeves, M. S. Ramer, and J. W. Fawcett, "A potential role for bone morphogenetic protein signalling in glial cell fate determination following adult central nervous system injury in vivo," *European Journal of Neuroscience*, vol. 26, no. 11, pp. 3024–35, 2007. [Online]. Available: http://www.ncbi.nlm.nih.gov/pubmed/18028109

[113] L. Dai, C. A. Thu, X. Y. Liu, J. J. Xi, and P. C. F. Cheung, "Tak1, more than just innate immunity," *Iubmb Life*, vol. 64, no. 10, pp. 825–834, 2012. [Online]. Available: ¡Go to ISI¿://000309188500005

[114] I. Iandiev, A. Wurm, T. Pannicke, P. Wiedemann, A. Reichenbach, S. C. Robson, H. Zimmermann, and A. Bringmann, "Ectonucleotidases in muller glial cells of the rodent retina: Involvement in inhibition of osmotic cell swelling," *Purinergic Signal*, vol. 3, no. 4, pp. 423–33, 2007. [Online]. Available: http://www.ncbi.nlm.nih.gov/pubmed/18404455

[115] R. Sehgal, N. Sheibani, S. J. Rhodes, and T. L. Belecky Adams, "Bmp7 and shh regulate pax2 in mouse retinal astrocytes by relieving tlx repression," *Dev Biol*, vol. 332, no. 2, pp. 429–43, 2009. [Online]. Available: http://www.ncbi.nlm.nih.gov/pubmed/19505455

[116] E. Scheef, S. Wang, C. M. Sorenson, and N. Sheibani, "Isolation and characterization of murine retinal astrocytes," *Mol Vis*, vol. 11, pp. 613–24, 2005.

[117] P. Cassina, H. Peluffo, M. Pehar, L. Martinez-Palma, A. Ressia, J. S. Beckman, A. G. Estevez, and L. Barbeito, "Peroxynitrite triggers a phenotypic transformation in spinal cord astrocytes that induces motor neuron apoptosis," *J Neurosci Res*, vol. 67, no. 1, pp. 21–9, 2002. [Online]. Available: http://www.ncbi.nlm.nih.gov/pubmed/11754077

[118] G. A. Limb, T. E. Salt, P. M. Munro, S. E. Moss, and P. T. Khaw, "In vitro characterization of a spontaneously immortalized human muller cell line (mio-m1)," *Invest Ophthalmol Vis Sci*, vol. 43, no. 3, pp. 864–9, 2002. [Online]. Available: http://www.ncbi.nlm.nih.gov/pubmed/11867609

[119] M. T. Fitch and J. Silver, "Cns injury, glial scars, and inflammation: Inhibitory extracellular matrices and regeneration failure," *Exp Neurol*, vol. 209, no. 2, pp. 294–301, 2008. [Online]. Available: http://www.ncbi.nlm.nih.gov/pubmed/17617407

[120] A. Derouiche and T. Rauen, "Coincidence of l-glutamate/l-aspartate transporter (glast) and glutamine synthetase (gs) immunoreactions in retinal glia: evidence for coupling of glast and gs in transmitter clearance," *J Neurosci Res*, vol. 42, no. 1, pp. 131–43, 1995. [Online]. Available: http://www.ncbi.nlm.nih.gov/pubmed/8531222

[121] J. Grosche, W. Hartig, and A. Reichenbach, "Expression of glial fibrillary acidic protein (gfap), glutamine synthetase (gs), and bcl-2 protooncogene protein by muller (glial) cells in retinal light damage of rats," *Neuroscience Letters*, vol. 185, no. 2, pp. 119–22, 1995. [Online]. Available: http://www.ncbi.nlm.nih.gov/pubmed/7746501

[122] G. P. Lewis, P. A. Erickson, C. J. Guerin, D. H. Anderson, and S. K. Fisher, "Changes in the expression of specific muller cell proteins during long-term retinal detachment," *Exp Eye Res*, vol. 49, no. 1, pp. 93–111, 1989. [Online]. Available: http://www.ncbi.nlm.nih.gov/pubmed/2503391

[123] A. Reichenbach, J. U. Stolzenburg, H. Wolburg, W. Hartig, E. el Hifnawi, and H. Martin, "Effects of enhanced extracellular ammonia concentration on cultured mammalian retinal glial (muller) cells," *Glia*, vol. 13, no. 3, pp. 195–208, 1995. [Online]. Available: http://www.ncbi.nlm.nih.gov/pubmed/7782105

[124] M. L. Chang, C. H. Wu, Y. F. Jiang-Shieh, J. Y. Shieh, and C. Y. Wen, "Reactive changes of retinal astrocytes and muller glial cells in kainate-induced neuroexcitotoxicity," *J Anat*, vol. 210, no. 1, pp. 54–65, 2007. [Online]. Available: http://www.ncbi.nlm.nih.gov/pubmed/17229283

[125] M. Mizutani, C. Gerhardinger, and M. Lorenzi, "Muller cell changes in human diabetic retinopathy," *Diabetes*, vol. 47, no. 3, pp. 445–9, 1998. [Online]. Available: http://www.ncbi.nlm.nih.gov/pubmed/9519752

[126] H. Chen and A. J. Weber, "Expression of glial fibrillary acidic protein and glutamine synthetase by muller cells after optic nerve damage and intravitreal application of brain-derived neurotrophic factor," *Glia*, vol. 38, no. 2, pp. 115–25, 2002. [Online]. Available: http://www.ncbi.nlm.nih.gov/pubmed/11948805

[127] M. Cui, Y. Huang, C. Tian, Y. Zhao, and J. Zheng, "Foxo3a inhibits tnf-alpha- and il-1beta-induced astrocyte proliferation:implication for reactive astrogliosis," *Glia*, vol. 59, no. 4, pp. 641–54, 2011. [Online]. Available: http://www.ncbi.nlm.nih.gov/pubmed/21294163

[128] V. Fontaine, S. Mohand-Said, N. Hanoteau, C. Fuchs, K. Pfizenmaier, and U. Eisel, "Neurodegenerative and neuroprotective effects of tumor necrosis factor (tnf) in retinal ischemia: opposite roles of tnf receptor 1 and tnf receptor 2," *J Neurosci*, vol. 22, no. 7, p. RC216, 2002. [Online]. Available: http://www.ncbi.nlm.nih.gov/pubmed/11917000

[129] I. Matsuura, J. Taniguchi, K. Hata, N. Saeki, and T. Yamashita, "Bmp inhibition enhances axonal growth and functional recovery after spinal cord injury," *J Neurochem*, vol. 105, no. 4, pp. 1471–9, 2008. [Online]. Available: http://www.ncbi.nlm.nih.gov/pubmed/18221366

[130] A. Masumoto, Y. Hirooka, K. Hironaga, K. Eshima, S. Setoguchi, K. Egashira, and A. Takeshita, "Effect of pravastatin on endothelial function in patients with coronary artery disease (cholesterol-independent effect of pravastatin)," *Am J Cardiol*, vol. 88, no. 11, pp. 1291–4, 2001. [Online]. Available: http://www.ncbi.nlm.nih.gov/pubmed/11728357

[131] A. Masumoto, Y. Hirooka, H. Shimokawa, K. Hironaga, S. Setoguchi, and A. Takeshita, "Possible involvement of rho-kinase in the pathogenesis of hypertension in humans," *Hypertension*, vol. 38, no. 6, pp. 1307–10, 2001. [Online]. Available: http://www.ncbi.nlm.nih.gov/pubmed/11751708

[132] R. Fuchshofer, A. H. Yu, U. Welge-Lussen, and E. R. Tamm, "Bone morphogenetic protein-7 is an antagonist of transforming growth factor-beta2 in human trabecular meshwork cells," *Invest Ophthalmol Vis Sci*, vol. 48, no. 2, pp. 715–26, 2007. [Online]. Available: http://www.ncbi.nlm.nih.gov/pubmed/17251470

[133] R. J. Wordinger, D. L. Fleenor, P. E. Hellberg, I. H. Pang, T. O. Tovar, G. S. Zode, J. A. Fuller, and A. F. Clark, "Effects of tgf-beta2, bmp-4, and gremlin in the trabecular meshwork: implications for glaucoma," *Invest Ophthalmol Vis Sci*, vol. 48, no. 3, pp. 1191–200, 2007. [Online]. Available: http://www.ncbi.nlm.nih.gov/pubmed/17325163

[134] G. S. Zode, A. F. Clark, and R. J. Wordinger, "Activation of the bmp canonical signaling pathway in human optic nerve head tissue and isolated optic nerve head astrocytes and lamina cribrosa cells," *Invest Ophthalmol Vis Sci*, vol. 48, no. 11, pp. 5058–67, 2007. [Online]. Available: http://www.ncbi.nlm.nih.gov/pubmed/17962458

[135] Y. Ueki and T. A. Reh, "Egf stimulates muller glial proliferation via a bmp-dependent mechanism," *Glia*, vol. 61, no. 5, pp. 778–89, 2013. [Online]. Available: http://www.ncbi.nlm.nih.gov/pubmed/23362023

[136] A. J. Fischer, M. Schmidt, G. Omar, and T. A. Reh, "Bmp4 and cntf are neuroprotective and suppress damage-induced proliferation of muller glia in the retina," *Molecular and Cellular Neuroscience*, vol. 27, no. 4, pp. 531–542, 2004. [Online]. Available: ¡Go to ISI¿://WOS:000225448600016

[137] B. Tucker, H. Klassen, L. Yang, D. F. Chen, and M. J. Young, "Elevated mmp expression in the mrl mouse retina creates a permissive environment for retinal regeneration," *Invest Ophthalmol Vis Sci*, vol. 49, no. 4, pp. 1686–95, 2008. [Online]. Available: http://www.ncbi.nlm.nih.gov/pubmed/18385092

[138] B. S. Ganesh and S. K. Chintala, "Inhibition of reactive gliosis attenuates excitotoxicity-mediated death of retinal ganglion cells," *PLoS One*, vol. 6, no. 3, p. e18305, 2011. [Online]. Available: http://www.ncbi.nlm.nih.gov/pubmed/21483783

[139] O. Steward, M. S. Kelley, and E. R. Torre, "The process of reinnervation in the dentate gyrus of adult rats: temporal relationship between changes in the levels of glial fibrillary acidic protein (gfap) and gfap mrna in reactive astrocytes," *Experimental Neurology*, vol. 124, no. 2, pp. 167–83, 1993. [Online]. Available: http://www.ncbi.nlm.nih.gov/pubmed/8287920

[140] D. M. Inman and P. J. Horner, "Reactive nonproliferative gliosis predominates in a chronic mouse model of glaucoma," *Glia*, vol. 55, no. 9, pp. 942–53, 2007. [Online]. Available: http://www.ncbi.nlm.nih.gov/pubmed/17457855

[141] X. Wu, H. Hsuchou, A. J. Kastin, P. K. Mishra, and W. Pan, "Upregulation of astrocytic leptin receptor in mice with experimental autoimmune encephalomyelitis," *J Mol Neurosci*, vol. 49, no. 3, pp. 446–56, 2013. [Online]. Available: http://www.ncbi.nlm.nih.gov/pubmed/22684620

[142] R. W. Wong and T. Hagen, "Mechanistic target of rapamycin (mtor) dependent regulation of thioredoxin interacting protein (txnip) transcription in hypoxia," *Biochem Biophys Res Commun*, vol. 433, no. 1, pp. 40–6, 2013. [Online]. Available: http://www.ncbi.nlm.nih.gov/pubmed/23454121

[143] D. Baek, J. Villen, C. Shin, F. D. Camargo, S. P. Gygi, and D. P. Bartel, "The impact of micrornas on protein output," *Nature*, vol. 455, no. 7209, pp. 64–U38, 2008. [Online]. Available: ¡Go to ISI¿://000258890200037

[144] C. M. Di Liegro, G. Schiera, and I. Di Liegro, "Regulation of mrna transport, localization and translation in the nervous system of mammals (review)," *Int J Mol Med*, vol. 33, no. 4, pp. 747–62, 2014. [Online]. Available: http://www.ncbi.nlm.nih.gov/pubmed/24452120

[145] K. C. Kim, S. Hyun Joo, and C. Y. Shin, "Cpeb1 modulates lipopolysaccharide-mediated inos induction in rat primary astrocytes," *Biochem Biophys Res Commun*, vol. 409, no. 4, pp. 687–92, 2011. [Online]. Available: http://www.ncbi.nlm.nih.gov/pubmed/21620800

[146] M. Cargnello and P. P. Roux, "Activation and function of the mapks and their substrates, the mapk-activated protein kinases (vol 75, pg 50, 2011)," *Microbiology and Molecular Biology Reviews*, vol. 76, no. 2, pp. 496–496, 2012. [Online]. Available: ¡Go to ISI¿://000305508000011

[147] L. Hackler, J. Wan, A. Swaroop, J. Qian, and D. J. Zack, "Microrna profile of the developing mouse retina," *Investigative Ophthalmology and Visual Science*, vol. 51, no. 4, pp. 1823–1831, 2010. [Online]. Available: ¡Go to ISI¿://000275995800005

[148] E. de Sousa, L. T. Walter, G. S. V. Higa, O. Augusto, N. Casado, and A. H. Kihara, "Developmental and functional expression of mirna-stability related genes in the nervous system," *Plos One*, vol. 8, no. 6, 2013. [Online]. Available: ¡Go to ISI¿://000319966400001

[149] B. N. Davis, A. C. Hilyard, G. Lagna, and A. Hata, "Smad proteins control drosha-mediated microrna maturation," *Nature*, vol. 454, no. 7200, pp. 56–61, 2008. [Online]. Available: http://www.ncbi.nlm.nih.gov/pubmed/18548003

[150] G. Ning, X. Liu, M. Dai, A. Meng, and Q. Wang, "Microrna-92a upholds bmp signaling by targeting noggin3 during pharyngeal cartilage formation," *Dev Cell*, vol. 24, no. 3, pp. 283–95, 2013. [Online]. Available: http://www.ncbi.nlm.nih.gov/pubmed/23410941

[151] O. G. Bhalala, M. Srikanth, and J. A. Kessler, "The emerging roles of micrornas in cns injuries," *Nature Reviews Neurology*, vol. 9, no. 6, pp. 328–339, 2013. [Online]. Available: ¡Go to ISI¿://000320678400007

[152] S. K. Ling, Y. Birnbaum, M. K. Nanhwan, B. Thomas, M. Bajaj, and Y. M. Ye, "Microrna-dependent cross-talk between vegf and hif1 alpha in the diabetic retina," *Cell Signal*, vol. 25, no. 12, pp. 2840–2847, 2013. [Online]. Available: ¡Go to ISI¿://000328179800053

[153] M. A. Pizzi and M. J. Crowe, "Matrix metalloproteinases and proteoglycans in axonal regeneration," *Exp Neurol*, vol. 204, no. 2, pp. 496–511, 2007. [Online]. Available: http://www.ncbi.nlm.nih.gov/pubmed/17254568

[154] T. Watanabe and M. C. Raff, "Retinal astrocytes are immigrants from the optic nerve," *Nature*, vol. 332, no. 6167, pp. 834–7, 1988. [Online]. Available: http://www.ncbi.nlm.nih.gov/pubmed/3282180

[155] J. H. Seo, Y. G. Haam, S. W. Park, D. W. Kim, G. S. Jeon, C. Lee, D. H. Hwang, Y. S. Kim, and S. S. Cho, "Oligodendroglia in the avian retina: immunocytochemical demonstration in the adult bird," *J Neurosci Res*, vol. 65, no. 2, pp. 173–83, 2001. [Online]. Available: http://www.ncbi.nlm.nih.gov/pubmed/11438986

[156] G. A. Lutty, "Effects of diabetes on the eye," *Investigative Ophthalmology and Visual Science*, vol. 54, no. 14, 2013. [Online]. Available: ¡Go to ISI¿://000328884600014

[157] S. Dharmarajan, Z. Gurel, S. Wang, C. M. Sorenson, N. Sheibani, and T. L. Belecky-Adams, "Bone morphogenetic protein 7 regulates reactive gliosis in retinal astrocytes and muller glia," *Mol Vis*, vol. 20, pp. 1085–108, 2014. [Online]. Available: http://www.ncbi.nlm.nih.gov/pubmed/25253985

[158] G. Martinez, M. L. Carnazza, C. Di Giacomo, V. Sorrenti, and A. Vanella, "Expression of bone morphogenetic protein-6 and transforming growth factor-beta1 in the rat brain after a mild and reversible ischemic damage," *Brain Res*, vol. 894, no. 1, pp. 1–11, 2001. [Online]. Available: http://www.ncbi.nlm.nih.gov/pubmed/11245809

[159] L. J. Luan, X. M. Yang, C. M. Zhou, K. Wang, and L. H. Qin, "Post-hypoxic and ischemic neuroprotection of bmp-7 in the cerebral cortex and caudate-putamen tissue of rat," *Acta Histochemica*, vol. 117, no. 2, pp. 148–154, 2015. [Online]. Available: ¡Go to ISI¿://000355232600002

[160] C. Woiciechowsky, B. Schoning, G. Stoltenburg-Didinger, F. Stockhammer, and H. D. Volk, "Brain-il-1 beta triggers astrogliosis through induction of il-6: Inhibition by propranolol and il-10," *Medical Science Monitor*, vol. 10, no. 9, pp. Br325–Br330, 2004. [Online]. Available: ¡Go to ISI¿://000224833800003

[161] K. A. Hussein, K. Choksi, S. Akeel, S. Ahmad, S. Megyerdi, M. El-Sherbiny, M. Nawaz, A. Abu El-Asrar, and M. Al-Shabrawey, "Bone morphogenetic protein 2: a potential new player in the pathogenesis of diabetic retinopathy," *Exp Eye Res*, vol. 125, pp. 79–88, 2014. [Online]. Available: http://www.ncbi.nlm.nih.gov/pubmed/24910902

[162] A. M. Santos, R. Calvente, M. Tassi, M. C. Carrasco, D. Martin-Oliva, J. L. Marin-Teva, J. Navascues, and M. A. Cuadros, "Embryonic and postnatal development of microglial cells in the mouse retina," *J Comp Neurol*, vol. 506, no. 2, pp. 224–39, 2008. [Online]. Available: http://www.ncbi.nlm.nih.gov/pubmed/18022954

[163] L. Chen, P. Yang, and A. Kijlstra, "Distribution, markers, and functions of retinal microglia," *Ocul Immunol Inflamm*, vol. 10, no. 1, pp. 27–39, 2002. [Online]. Available: http://www.ncbi.nlm.nih.gov/pubmed/12461701

[164] A. Bosco, M. R. Steele, and M. L. Vetter, "Early microglia activation in a mouse model of chronic glaucoma," *J Comp Neurol*, vol. 519, no. 4, pp. 599–620, 2011. [Online]. Available: http://www.ncbi.nlm.nih.gov/pubmed/21246546

[165] M. Wang and W. T. Wong, "Microglia-muller cell interactions in the retina," *Adv Exp Med Biol*, vol. 801, pp. 333–8, 2014. [Online]. Available: http://www.ncbi.nlm.nih.gov/pubmed/24664715

[166] J. M. Crain, M. Nikodemova, and J. J. Watters, "Microglia express distinct m1 and m2 phenotypic markers in the postnatal and adult central nervous system in male and female mice," *J Neurosci Res*, vol. 91, no. 9, pp. 1143–51, 2013. [Online]. Available: http://www.ncbi.nlm.nih.gov/pubmed/23686747

[167] V. Chhor, T. Le Charpentier, S. Lebon, M. V. Ore, I. L. Celador, J. Josserand, V. Degos, E. Jacotot, H. Hagberg, K. Savman, C. Mallard, P. Gressens, and B. Fleiss, "Characterization of phenotype markers and neuronotoxic potential of polarised primary microglia in vitro," *Brain Behav Immun*, vol. 32, pp. 70–85, 2013. [Online]. Available: http://www.ncbi.nlm.nih.gov/pubmed/23454862

[168] M. Jaguin, N. Houlbert, O. Fardel, and V. Lecureur, "Polarization profiles of human m-csf-generated macrophages and comparison of m1-markers in classically activated macrophages from gm-csf and m-csf origin," *Cell Immunol*, vol. 281, no. 1, pp. 51–61, 2013. [Online]. Available: http://www.ncbi.nlm.nih.gov/pubmed/23454681

[169] M. J. Crane, J. M. Daley, O. van Houtte, S. K. Brancato, J. Henry, W. L., and J. E. Albina, "The monocyte to macrophage transition in the murine sterile wound," *PLoS One*, vol. 9, no. 1, p. e86660, 2014. [Online]. Available: http://www.ncbi.nlm.nih.gov/pubmed/24466192

[170] G. J. Harry, "Microglia during development and aging," *Pharmacology and Therapeutics*, vol. 139, no. 3, pp. 313–326, 2013. [Online]. Available: ¡Go to ISI¿://WOS:000323398900002

[171] H. Y. Zeng, X. A. Zhu, C. Zhang, L. P. Yang, L. M. Wu, and M. O. Tso, "Identification of sequential events and factors associated with microglial activation, migration, and cytotoxicity in retinal degeneration in rd mice," *Invest Ophthalmol Vis Sci*, vol. 46, no. 8, pp. 2992–9, 2005. [Online]. Available: http://www.ncbi.nlm.nih.gov/pubmed/16043876

[172] A. Kumar and N. Shamsuddin, "Retinal muller glia initiate innate response to infectious stimuli via toll-like receptor signaling," *Plos One*, vol. 7, no. 1, 2012. [Online]. Available: ¡Go to ISI¿://000315865800016

[173] V. Balasingam and V. W. Yong, "Attenuation of astroglial reactivity by interleukin-10," *Journal of Neuroscience*, vol. 16, no. 9, pp. 2945–2955, 1996. [Online]. Available: ¡Go to ISI¿://A1996UF71100009

[174] A. J. Fischer, C. Zelinka, D. Gallina, M. A. Scott, and L. Todd, "Reactive microglia and macrophage facilitate the formation of muller glia-derived retinal progenitors," *Glia*, vol. 62, no. 10, pp. 1608–28, 2014. [Online]. Available: http://www.ncbi.nlm.nih.gov/pubmed/24916856

[175] R. S. Roque and R. B. Caldwell, "Isolation and culture of retinal microglia," *Curr Eye Res*, vol. 12, no. 3, pp. 285–90, 1993. [Online]. Available: http://www.ncbi.nlm.nih.gov/pubmed/7683260

[176] S. Srinivas, T. Watanabe, C.-S. Lin, C. M. William, Y. Tanabe, T. M. Jessell, and F. Costantini, "Cre reporter strains produced by targeted insertion of eyfp and ecfp into the rosa26 locus," *BMC Developmental Biology*, vol. 1, pp. 4–4, 2001. [Online]. Available: http://www.ncbi.nlm.nih.gov/pmc/articles/PMC31338/

[177] S. Tual-Chalot, K. R. Allinson, M. Fruttiger, and H. M. Arthur, "Whole mount immunofluorescent staining of the neonatal mouse retina to investigate angiogenesis in vivo," *J Vis Exp*, no. 77, p. e50546, 2013. [Online]. Available: http://www.ncbi.nlm.nih.gov/pubmed/23892721

[178] M. Hollborn, S. Tenckhoff, K. Jahn, I. Iandiev, B. Biedermann, U. E. Schnurrbusch, G. A. Limb, A. Reichenbach, S. Wolf, P. Wiedemann, L. Kohen, and A. Bringmann, "Changes in retinal gene expression in proliferative vitreoretinopathy: glial cell expression of hb-egf," *Mol Vis*, vol. 11, pp. 397–413, 2005. [Online]. Available: http://www.ncbi.nlm.nih.gov/pubmed/15988409

[179] B. N. Lilley, Y. A. Pan, and J. R. Sanes, "Sad kinases sculpt axonal arbors of sensory neurons through long- and short-term responses to neurotrophin signals," *Neuron*, vol. 79, no. 1, pp. 39–53, 2013. [Online]. Available: ¡Go to ISI¿://WOS:000321802000008

[180] M. Neubert, D. A. Ridder, P. Bargiotas, S. Akira, and M. Schwaninger, "Acute inhibition of tak1 protects against neuronal death in cerebral ischemia," *Cell Death and Differentiation*, vol. 18, no. 9, pp. 1521–1530, 2011. [Online]. Available: ¡Go to ISI¿://WOS:000293998100015

[181] T. Haynes, C. Gutierrez, J. C. Aycinena, P. A. Tsonis, and K. Del Rio-Tsonis, "Bmp signaling mediates stem/progenitor cell-induced retina regeneration," *Proc Natl Acad Sci U S A*, vol. 104, no. 51, pp. 20 380–5, 2007. [Online]. Available: http://www.ncbi.nlm.nih.gov/pubmed/18093961

[182] N. Yoshida, Y. Ikeda, S. Notomi, K. Ishikawa, Y. Murakami, T. Hisatomi, H. Enaida, and T. Ishibashi, "Laboratory evidence of sustained chronic inflammatory reaction in retinitis pigmentosa," *Ophthalmology*, vol. 120, no. 1, pp. E5–E12, 2013. [Online]. Available: ¡Go to ISI¿://WOS:000313011700001

[183] J. G. Grigsby, S. M. Cardona, C. E. Pouw, A. Muniz, A. S. Mendiola, A. T. C. Tsin, D. M. Allen, and A. E. Cardona, "The role of microglia in diabetic retinopathy," *Journal of Ophthalmology*, 2014. [Online]. Available: ¡Go to ISI¿://WOS:000344253400001

[184] J. W. Wang, S. D. Chen, X. L. Zhang, and J. B. Jonas, "Retinal microglia in glaucoma," *Journal of Glaucoma*, vol. 25, no. 5, pp. 459–465, 2016. [Online]. Available: ¡Go to ISI¿://WOS:000375150000014

[185] A. J. Fischer, C. Zelinka, and N. Milani-Nejad, "Reactive retinal microglia, neuronal survival, and the formation of retinal folds and detachments," *Glia*, vol. 63, no. 2, pp. 313–327, 2015. [Online]. Available: ¡Go to ISI¿://WOS:000346250400010

[186] M. Karlstetter, S. Ebert, and T. Langmann, "Microglia in the healthy and degenerating retina: Insights from novel mouse models," *Immunobiology*, vol. 215, no. 9-10, pp. 685–691, 2010. [Online]. Available: ¡Go to ISI¿://WOS:000281536800003

[187] X. G. Luo and S. D. Chen, "The changing phenotype of microglia from homeostasis to disease," *Transl Neurodegener*, vol. 1, no. 1, p. 9, 2012. [Online]. Available: http://www.ncbi.nlm.nih.gov/pubmed/23210447

[188] G. Luna, G. P. Lewis, C. D. Banna, O. Skalli, and S. K. Fisher, "Expression profiles of nestin and synemin in reactive astrocytes and muller cells following retinal injury: a comparison with glial fibrillar acidic protein and vimentin," *Mol Vis*, vol. 16, pp. 2511–23, 2010. [Online]. Available: http://www.ncbi.nlm.nih.gov/pubmed/21139996

[189] L. Fernandez-Sanchez, P. Lax, L. Campello, I. Pinilla, and N. Cuenca, "Astrocytes and muller cell alterations during retinal degeneration in a transgenic rat model of retinitis pigmentosa," *Front Cell Neurosci*, vol. 9, p. 484, 2015. [Online]. Available: http://www.ncbi.nlm.nih.gov/pubmed/26733810

[190] A. Kanamori, M. Nakamura, Y. Nakanishi, Y. Yamada, and A. Negi, "Long-term glial reactivity in rat retinas ipsilateral and contralateral to experimental glaucoma," *Exp Eye Res*, vol. 81, no. 1, pp. 48–56, 2005. [Online]. Available: http://www.ncbi.nlm.nih.gov/pubmed/15978254

[191] A. I. Ramirez, J. J. Salazar, R. de Hoz, B. Rojas, B. I. Gallego, M. Salinas-Navarro, L. Alarcon-Martinez, A. Ortin-Martinez, M. Aviles-Trigueros, M. Vidal-Sanz, A. Trivino, and J. M. Ramirez, "Quantification of the effect of different levels of iop in the astroglia of the rat retina ipsilateral and contralateral to experimental glaucoma," *Invest Ophthalmol Vis Sci*, vol. 51, no. 11, pp. 5690–6, 2010. [Online]. Available: http://www.ncbi.nlm.nih.gov/pubmed/20538983

[192] B. I. Gallego, J. J. Salazar, R. de Hoz, B. Rojas, A. I. Ramirez, M. Salinas-Navarro, A. Ortin-Martinez, F. J. Valiente-Soriano, M. Aviles-Trigueros, M. P. Villegas-Perez, M. Vidal-Sanz, A. Trivino, and J. M. Ramirez, "Iop induces upregulation of gfap and mhc-ii and microglia reactivity in mice retina contralateral to experimental glaucoma," *J Neuroinflammation*, vol. 9, p. 92, 2012. [Online]. Available: http://www.ncbi.nlm.nih.gov/pubmed/22583833

[193] N. Jin, L. Gao, X. Fan, and H. Xu, "Friend or foe? resident microglia vs bone marrow-derived microglia and their roles in the retinal degeneration," *Molecular Neurobiology*, pp. 1–19, 2016. [Online]. Available: http://dx.doi.org/10.1007/s12035-016-9960-9

[194] T. Harada, C. Harada, S. Kohsaka, E. Wada, K. Yoshida, S. Ohno, H. Mamada, K. Tanaka, L. F. Parada, and K. Wada, "Microglia-muller glia cell interactions control neurotrophic factor production during light-induced retinal degeneration," *Journal of Neuroscience*, vol. 22, no. 21, pp. 9228–36, 2002. [Online]. Available: http://www.ncbi.nlm.nih.gov/pubmed/12417648

[195] G. T. Lee, S. J. Kwon, J. H. Lee, S. S. Jeon, K. T. Jang, H. Y. Choi, H. M. Lee, W. J. Kim, S. J. Kim, and I. Y. Kim, "Induction of interleukin-6 expression by bone morphogenetic protein-6 in macrophages requires both smad and p38 signaling pathways," *Journal of Biological Chemistry*, vol. 285, no. 50, pp. 39 401–39 408, 2010. [Online]. Available: ¡Go to ISI¿://000284941300067

[196] J. H. Hong, G. T. Lee, J. H. Lee, S. J. Kwon, S. H. Park, S. J. Kim, and I. Y. Kim, "Effect of bone morphogenetic protein-6 on macrophages," *Immunology*, vol. 128, no. 1, pp. e442–e450, 2009. [Online]. Available: ¡Go to ISI¿://000268703800028

[197] S. J. Kwon, G. T. Lee, J. H. Lee, W. J. Kim, and I. Y. Kim, "Bone morphogenetic protein-6 induces the expression of inducible nitric oxide synthase in macrophages," *Immunology*, vol. 128, no. 1, pp. e758–e765, 2009. [Online]. Available: ¡Go to ISI¿://000268703800061

[198] D. K. Singla, R. Singla, and J. Wang, "Bmp-7 treatment increases m2 macrophage differentiation and reduces inflammation and plaque formation in apo e-/- mice," *Plos One*, vol. 11, no. 1, 2016. [Online]. Available: ¡Go to ISI¿://000369528600068

[199] C. Rocher and D. K. Singla, "Smad-pi3k-akt-mtor pathway mediates bmp-7 polarization of monocytes into m2 macrophages," *Plos One*, vol. 8, no. 12, 2013. [Online]. Available: ¡Go to ISI¿://000328745100152

[200] P. Urbina and D. K. Singla, "Bmp-7 attenuates adverse cardiac remodeling mediated through m2 macrophages in prediabetic cardiomyopathy," *American Journal of Physiology-Heart and Circulatory Physiology*, vol. 307, no. 5, pp. H762–H772, 2014. [Online]. Available: ¡Go to ISI¿://000341081200014

[201] C. Rocher, R. Singla, P. K. Singal, S. Parthasarathy, and D. K. Singla, "Bone morphogenetic protein 7 polarizes thp-1 cells into m2 macrophages," *Canadian Journal of Physiology and Pharmacology*, vol. 90, no. 7, pp. 947–951, 2012. [Online]. Available: ¡Go to ISI¿://000306110100014

[202] H. Wake, A. J. Moorhouse, and J. Nabekura, "Functions of microglia in the central nervous system–beyond the immune response," *Neuron Glia Biol*, vol. 7, no. 1, pp. 47–53, 2011. [Online]. Available: http://www.ncbi.nlm.nih.gov/pubmed/22613055

[203] R. K. Nuttall, C. Silva, W. Hader, A. Bar-Or, K. D. Patel, D. R. Edwards, and V. W. Yong, "Metalloproteinases are enriched in microglia compared with leukocytes and they regulate cytokine levels in activated microglia," *Glia*, vol. 55, no. 5, pp. 516–26, 2007. [Online]. Available: http://www.ncbi.nlm.nih.gov/pubmed/17216595

[204] G. J. del Zoppo, R. Milner, T. Mabuchi, S. Hung, X. Wang, G. I. Berg, and J. A. Koziol, "Microglial activation and matrix protease generation during focal cerebral ischemia," *Stroke*, vol. 38, no. 2 Suppl, pp. 646–51, 2007. [Online]. Available: http://www.ncbi.nlm.nih.gov/pubmed/17261708

[205] G. A. Limb, J. T. Daniels, R. Pleass, D. G. Charteris, P. J. Luthert, and P. T. Khaw, "Differential expression of matrix metalloproteinases 2 and 9 by glial muller cells: response to soluble and extracellular matrix-bound tumor necrosis factor-alpha," *Am J Pathol*, vol. 160, no. 5, pp. 1847–55, 2002. [Online]. Available: http://www.ncbi.nlm.nih.gov/pubmed/12000736

[206] A. Koussounadis, S. P. Langdon, I. H. Um, D. J. Harrison, and V. A. Smith, "Relationship between differentially expressed mrna and mrna-protein correlations in a xenograft model system," *Scientific Reports*, vol. 5, p. 10775, 2015. [Online]. Available: http://www.ncbi.nlm.nih.gov/pmc/articles/PMC4459080/

[207] T. Maier, M. Guell, and L. Serrano, "Correlation of mrna and protein in complex biological samples," *FEBS Lett*, vol. 583, no. 24, pp. 3966–73, 2009. [Online]. Available: http://www.ncbi.nlm.nih.gov/pubmed/19850042

[208] L. Liu, T. Sun, Z. Liu, X. Chen, L. Zhao, G. Qu, and Q. Li, "Traumatic brain injury dysregulates micrornas to modulate cell signaling in rat hippocampus," *PLoS One*, vol. 9, no. 8, p. e103948, 2014. [Online]. Available: http://www.ncbi.nlm.nih.gov/pubmed/25089700

[209] K. Rajaram, R. L. Harding, T. Bailey, J. G. Patton, and D. R. Hyde, "Dynamic mirna expression patterns during retinal regeneration in zebrafish: reduced dicer or mirna expression suppresses proliferation of muller glia-derived neuronal progenitor cells," *Dev Dyn*, vol. 243, no. 12, pp. 1591–605, 2014. [Online]. Available: http://www.ncbi.nlm.nih.gov/pubmed/25220904

[210] M. Cargnello and P. P. Roux, "Activation and function of the mapks and their substrates, the mapk-activated protein kinases," *Microbiology and Molecular Biology Reviews : MMBR*, vol. 75, no. 1, pp. 50–83, 2011. [Online]. Available: http://www.ncbi.nlm.nih.gov/pmc/articles/PMC3063353/

[211] Y. Ouchi, E. Yoshikawa, Y. Sekine, M. Futatsubashi, T. Kanno, T. Ogusu, and T. Torizuka, "Microglial activation and dopamine terminal loss in early parkinson's disease," *Ann Neurol*, vol. 57, no. 2, pp. 168–75, 2005. [Online]. Available: http://www.ncbi.nlm.nih.gov/pubmed/15668962

[212] K. Miyoshi, K. Obata, T. Kondo, H. Okamura, and K. Noguchi, "Interleukin-18-mediated microglia/astrocyte interaction in the spinal cord enhances neuropathic pain processing after nerve injury," *Journal of Neuroscience*, vol. 28, no. 48, pp. 12 775–12 787, 2008. [Online]. Available: ¡Go to ISI¿://000261191700018

[213] O. Goureau, D. Hicks, Y. Courtois, and Y. De Kozak, "Induction and regulation of nitric oxide synthase in retinal muller glial cells," *Journal of Neurochemistry*, vol. 63, no. 1, pp. 310–7, 1994. [Online]. Available: http://www.ncbi.nlm.nih.gov/pubmed/7515948

[214] A. Matteucci, L. Gaddini, M. Villa, M. Varano, M. Parravano, V. Monteleone, F. Cavallo, L. Leo, C. Mallozzi, F. Malchiodi-Albedi, and F. Pricci, "Neuroprotection by rat mller glia against high glucose-induced neurodegeneration through a mechanism involving erk1/2 activation," *Experimental Eye Research*, vol. 125, pp. 20–29, 2014. [Online]. Available: http://www.sciencedirect.com/science/article/pii/S0014483514001328

[215] X. F. Ye, G. Z. Xu, Q. Chang, J. W. Fan, Z. C. Sun, Y. W. Qin, and A. C. Jiang, "Erk1/2 signaling pathways involved in vegf release in diabetic rat retina," *Investigative Ophthalmology and Visual Science*, vol. 51, no. 10, pp. 5226–5233, 2010. [Online]. Available: ¡Go to ISI¿://WOS:000282275500048

[216] W. Eichler, Y. Yafai, P. Wiedemann, and A. Reichenbach, "Angiogenesis-related factors derived from retinal glial (muller) cells in hypoxia," *Neuroreport*, vol. 15, no. 10, pp. 1633–1637, 2004. [Online]. Available: ¡Go to ISI¿://WOS:000225140700020

[217] G. P. Lewis, P. A. Erickson, C. J. Guerin, D. H. Anderson, and S. K. Fisher, "Basic fibroblast growth-factor - a potential regulator of proliferation and intermediate filament expression in the retina," *Journal of Neuroscience*, vol. 12, no. 10, pp. 3968–3978, 1992. [Online]. Available: ¡Go to ISI¿://WOS:A1992JT19700023

[218] A. Rattner and J. Nathans, "The genomic response to retinal disease and injury: Evidence for endothelin signaling from photoreceptors to glia," *Journal of Neuroscience*, vol. 25, no. 18, pp. 4540–4549, 2005. [Online]. Available: ¡Go to ISI¿://WOS:000228895200012

[219] T. Hisatomi, T. Sakamoto, I. Yamanaka, Y. Sassa, T. Kubota, H. Ueno, Y. Ohnishi, and T. Ishibashi, "Photocoagulation-induced retinal gliosis is inhibited by systemically expressed soluble tgf-beta receptor type ii via adenovirus mediated gene transfer," *Laboratory Investigation*, vol. 82, no. 7, pp. 863–870, 2002. [Online]. Available: ¡Go to ISI¿://WOS:000176831200006

[220] W. Cao, F. Li, R. H. Steinberg, and M. M. Lavail, "Development of normal and injury-induced gene expression of afgf, bfgf, cntf, bdnf, gfap and igf-i in the rat retina," *Experimental Eye Research*, vol. 72, no. 5, pp. 591–604, 2014. [Online]. Available: ¡Go to ISI¿://WOS:000168509500011

[221] K. Valter, S. Bisti, C. Gargini, S. Di Loreto, R. Maccarone, L. Cervetto, and J. Stone, "Time course of neurotrophic factor upregulation and retinal protection against light-induced damage after optic nerve section," *Investigative Ophthalmology and Visual Science*, vol. 46, no. 5, pp. 1748–1754, 2005. [Online]. Available: ¡Go to ISI¿://WOS:000228708000032

[222] S. F. Geller, G. P. Lewis, and S. K. Fisher, "Fgfr1, signaling, and ap-1 expression after retinal detachment: reactive muller and rpe cells," *Invest Ophthalmol Vis Sci*, vol. 42, no. 6, pp. 1363–9, 2001. [Online]. Available: http://www.ncbi.nlm.nih.gov/pubmed/11328752

[223] H. Q. Zhang, M. Deo, R. C. Thompson, M. D. Uhler, and D. L. Turner, "Negative regulation of yap during neuronal differentiation," *Developmental Biology*, vol. 361, no. 1, pp. 103–115, 2012. [Online]. Available: ¡Go to ISI¿://WOS:000297898700009

[224] T. P. Driscoll, B. D. Cosgrove, S. J. Heo, Z. E. Shurden, and R. L. Mauck, "Cytoskeletal to nuclear strain transfer regulates yap signaling in mesenchymal stem cells," *Biophys J*, vol. 108, no. 12, pp. 2783–93, 2015. [Online]. Available: http://www.ncbi.nlm.nih.gov/pubmed/26083918

[225] B. Zhao, X. Wei, W. Li, R. S. Udan, Q. Yang, J. Kim, J. Xie, T. Ikenoue, J. Yu, L. Li, P. Zheng, K. Ye, A. Chinnaiyan, G. Halder, Z. C. Lai, and K. L. Guan, "Inactivation of yap oncoprotein by the hippo pathway is involved in cell contact inhibition and tissue growth control," *Genes and Development*, vol. 21, no. 21, pp. 2747–2761, 2007. [Online]. Available: ¡Go to ISI¿://WOS:000250618100007

[226] M. R. Silvis, B. T. Kreger, W. H. Lien, O. Klezovitch, G. M. Rudakova, F. D. Camargo, D. M. Lantz, J. T. Seykora, and V. Vasioukhin, "alpha-catenin is a tumor suppressor that controls cell accumulation by regulating the localization and activity of the transcriptional coactivator yap1," *Science Signaling*, vol. 4, no. 174, 2011. [Online]. Available: ¡Go to ISI¿://WOS:000290908900001

[227] H. W. Park, Y. C. Kim, B. Yu, T. Moroishi, J. S. Mo, S. W. Plouffe, Z. P. Meng, K. C. Lin, F. X. Yu, C. M. Alexander, C. Y. Wang, and K. L. Guan, "Alternative wnt signaling activates yap/taz," *Cell*, vol. 162, no. 4, pp. 780–794, 2015. [Online]. Available: ¡Go to ISI¿://WOS:000359741400012

[228] R. Fan, N. G. Kim, and B. M. Gumbiner, "Regulation of hippo pathway by mitogenic growth factors via phosphoinositide 3-kinase and phosphoinositide-dependent kinase-1," *Proceedings of the National Academy of Sciences of the United States of America*, vol. 110, no. 7, pp. 2569–2574, 2013. [Online]. Available: ¡Go to ISI¿://WOS:000315812800043

[229] K. Schlegelmilch, M. Mohseni, O. Kirak, J. Pruszak, J. R. Rodriguez, D. Zhou, B. T. Kreger, V. Vasioukhin, J. Avruch, T. R. Brummelkamp, and F. D. Camargo, "Yap1 acts downstream of alpha-catenin to control epidermal proliferation," *Cell*, vol. 144, no. 5, pp. 782–95, 2011. [Online]. Available: http://www.ncbi.nlm.nih.gov/pubmed/21376238

[230] W. Q. Wang, J. Huang, X. Wang, J. S. Yuan, X. Li, L. Feng, J. I. Park, and J. J. Chen, "Ptpn14 is required for the density-dependent control of yap1," *Genes and Development*, vol. 26, no. 17, pp. 1959–1971, 2012. [Online]. Available: ¡Go to ISI¿://WOS:000308391800007

[231] B. Zhao, L. Li, Q. Lu, L. H. Wang, C. Y. Liu, Q. Y. Lei, and K. L. Guan, "Angiomotin is a novel hippo pathway component that inhibits yap oncoprotein," *Genes and Development*, vol. 25, no. 1, pp. 51–63, 2011. [Online]. Available: ¡Go to ISI¿://WOS:000285870300006

[232] M. Ernkvist, O. Birot, I. Sinha, N. Veitonmaki, S. Nystrom, K. Aase, and L. Holmgren, "Differential roles of p80-and p130-angiomotin in the switch between migration and stabilization of endothelial cells," *Biochimica Et Biophysica Acta-Molecular Cell Research*, vol. 1783, no. 3, pp. 429–437, 2008. [Online]. Available: ¡Go to ISI¿://WOS:000254185100008

[233] S. Moleirinho, W. Guerrant, and J. L. Kissil, "The angiomotins - from discovery to function," *Febs Letters*, vol. 588, no. 16, pp. 2693–2703, 2014. [Online]. Available: ¡Go to ISI¿://WOS:000340317800016

[234] S. Dharmarajan, D. L. Fisk, C. M. Sorenson, N. Sheibani, and T. L. Belecky-Adams, "Microglia activation is essential for bmp7-mediated retinal reactive gliosis," *Journal of Neuroinflammation*, vol. 14, 2017. [Online]. Available: ¡Go to ISI¿://WOS:000399758500002

[235] H. W. Peng, M. Slattery, and R. S. Mann, "Transcription factor choice in the hippo signaling pathway: homothorax and yorkie regulation of the microrna bantam in the progenitor domain of the drosophila eye imaginal disc," *Genes and Development*, vol. 23, no. 19, pp. 2307–2319, 2009. [Online]. Available: ¡Go to ISI¿://WOS:000270389600008

[236] Q. Jiang, D. Liu, Y. B. Gong, Y. X. Wang, S. N. Sun, Y. H. Gui, and H. Y. Song, "yap is required for the development of brain, eyes, and neural crest in zebrafish," *Biochemical and Biophysical Research Communications*, vol. 384, no. 1, pp. 114–119, 2009. [Online]. Available: ¡Go to ISI¿://WOS:000266462400022

[237] Y. Asaoka, S. Hata, M. Namae, M. Furutani-Seiki, and H. Nishina, "The hippo pathway controls a switch between retinal progenitor cell proliferation and photoreceptor cell differentiation in zebrafish," *Plos One*, vol. 9, no. 5, 2014. [Online]. Available: ¡Go to ISI¿://WOS:000336857400085

[238] E. Wittkorn, A. Sarkar, K. Garcia, M. Kango-Singh, and A. Singh, "The hippo pathway effector yki downregulates wg signaling to promote retinal differentiation in the drosophila eye," *Development*, vol. 142, no. 11, pp. 2002–2013, 2015. [Online]. Available: ¡Go to ISI¿://WOS:000355209700011

[239] Z. H. Huang, D. Sun, J. X. Hu, F. L. Tang, D. H. Lee, Y. Wang, G. Q. Hu, X. J. Zhu, J. L. Zhou, L. Mei, and W. C. Xiong, "Neogenin promotes bmp2 activation of yap and smad1 and enhances astrocytic differentiation in developing mouse neocortex," *Journal of Neuroscience*, vol. 36, no. 21, pp. 5833–5849, 2016. [Online]. Available: ¡Go to ISI¿://WOS:000378345000016

[240] C. Powell, E. Cornblath, F. Elsaeidi, J. Wan, and D. Goldman, "Zebrafish muller glia-derived progenitors are multipotent, exhibit proliferative biases and regenerate excess neurons," *Sci Rep*, vol. 6, p. 24851, 2016. [Online]. Available: http://www.ncbi.nlm.nih.gov/pubmed/27094545

[241] M. Nagashima, L. K. Barthel, and P. A. Raymond, "A self-renewing division of zebrafish mller glial cells generates neuronal progenitors that require n-cadherin to regenerate retinal neurons," *Development (Cambridge, England)*, vol. 140, no. 22, pp. 4510–4521, 2013. [Online]. Available: http://www.ncbi.nlm.nih.gov/pmc/articles/PMC3817940/

[242] M. J. Lee, M. R. Byun, M. Furutani-Seiki, J. H. Hong, and H. S. Jung, "Yap and taz regulate skin wound healing," *Journal of Investigative Dermatology*, vol. 134, no. 2, pp. 518–525, 2014. [Online]. Available: ¡Go to ISI¿://WOS:000329896000031

[243] E. R. Barry, T. Morikawa, B. L. Butler, K. Shrestha, R. de la Rosa, K. S. Yan, C. S. Fuchs, S. T. Magness, R. Smits, S. Ogino, C. J. Kuo, and F. D. Camargo, "Restriction of intestinal stem cell expansion and the regenerative response by yap," *Nature*, vol. 493, no. 7430, pp. 106–+, 2013. [Online]. Available: ¡Go to ISI¿://WOS:000312933800040

[244] A. Hamon, C. Masson, J. Bitard, L. Gieser, J. E. Roger, and M. Perron, "Retinal degeneration triggers the activation of yap/tead in reactive muller cells," *Invest Ophthalmol Vis Sci*, vol. 58, no. 4, pp. 1941–1953, 2017. [Online]. Available: http://www.ncbi.nlm.nih.gov/pubmed/28384715

[245] B. Troyanovsky, T. Levchenko, G. Mansson, O. Matvijenko, and L. Holmgren, "Angiomotin: An angiostatin binding protein that regulates endothelial cell migration and tube formation," *Journal of Cell Biology*, vol. 152, no. 6, pp. 1247–1254, 2001. [Online]. Available: ¡Go to ISI¿://WOS:000167715600012

[246] M. Ernkvist, K. Aase, C. Ukomadu, J. Wohlschlegel, R. Blackman, N. Veitonmaki, A. Bratt, A. Dutta, and L. Holmgren, "p130-angiomotin associates to actin and controls endothelial cell shape," *Febs Journal*, vol. 273, no. 9, pp. 2000–2011, 2006. [Online]. Available: ¡Go to ISI¿://WOS:000237357500012

[247] B. T. Susarla, E. D. Laing, P. Yu, Y. Katagiri, H. M. Geller, and A. J. Symes, "Smad proteins differentially regulate transforming growth factor-beta-mediated induction of chondroitin sulfate proteoglycans," *J Neurochem*, vol. 119, no. 4, pp. 868–78, 2011. [Online]. Available: http://www.ncbi.nlm.nih.gov/pubmed/21895657

[248] M. Fanjul-Fernandez, A. R. Folgueras, S. Cabrera, and C. Lopez-Otin, "Matrix metalloproteinases: Evolution, gene regulation and functional analysis in mouse models," *Biochimica Et Biophysica Acta-Molecular Cell Research*, vol. 1803, no. 1, pp. 3–19, 2010. [Online]. Available: ¡Go to ISI¿://WOS:000275508500002

[249] M. DeRan, J. Yang, C. H. Shen, E. C. Peters, J. Fitamant, P. Chan, M. Hsieh, S. Zhu, J. M. Asara, B. Zheng, N. Bardeesy, J. Liu, and X. Wu, "Energy stress regulates hippo-yap signaling involving ampk-mediated regulation of angiomotin-like 1 protein," *Cell Rep*, vol. 9, no. 2, pp. 495–503, 2014. [Online]. Available: http://www.ncbi.nlm.nih.gov/pubmed/25373897

[250] Z. H. Huang, Y. Wang, G. Q. Hu, J. L. Zhou, L. Mei, and W. C. Xiong, "Yap is a critical inducer of socs3, preventing reactive astrogliosis," *Cerebral Cortex*, vol. 26, no. 5, pp. 2299–2310, 2016. [Online]. Available: ¡Go to ISI¿://WOS:000377469500037

VITA

VITA

Personal Details

Name: Subramanian Dharmarajan

Email : sdharmar@iupui.edu

Education

- Bachelors of Biotechnology, Dr. D.Y. Patil University, Navi Mumbai, 2009
- Masters in Biology, Indiana University-Purdue University Indianapolis, 2012
- PhD in Biology, Indiana University-Purdue University Indianapolis, 2017

Research Presentations

- Association for Research in Vision and Ophthalmology Annual Meeting (Posters, 2012, 2013, 2016)
- Society For Neuroscience Annual Meeting (Poster, 2015)
- Indianapolis Chapter for Society For Neuroscience (Poster, 2017)
- Midwest Eye Research Symposium (Poster, 2016)
- Glick Eye Research Symposium (Talk, 2012)

Teaching and Mentoring Experience

- Taught and trained six undergraduate students and helped manage their experiments
- Assisted undergraduates in securing 5 UROP grants for research.
- Led two laboratory sessions of 30 students for six semesters.
- Conducted experiments on topics of cell biology, anatomy, physiology, principles of diversity, plant biology and molecular biology.

Publications

- Dharmarajan S, Fisk DL, Sorenson CM, Sheibani N, Belecky-Adams TL, Microglia activation is essential for BMP7-mediated retinal reactive gliosis, J Neuro. 2017 Apr 5 2017, DOI: 10.1186/s12974-017-0855-0.
- Dharmarajan S, Gurel Z, Wang S, Sorenson CM, Sheibani N, Belecky-Adams TL, Bone morphogenetic protein 7 regulates reactive gliosis in retinal astrocytes and Mller glia, Mol Vis. 2014 Jul 31;20:1085-108.
- Tiwari S, Dharmarajan S, Shivanna M, Otteson DC, Belecky-Adams TL, Histone deacetylase expression patterns in developing murine optic nerve, BMC Dev Biol. 2014 Jul 9;14:30. doi: 10.1186/1471-213X-14-30.
- Teri L. Belecky-Adams, Ellen C. Chernoff, Jonathan M. Wilson and Subramanian Dharmarajan, Reactive Muller Glia as Potential Retinal Progenitors, Neural Stem Cells - New Perspectives, Dr. Luca Bonfanti (Ed.), ISBN: 978-953-51-1069-9, InTech, DOI: 10.5772/55150 (2013).

Professional Organizations and Societies

- Member of the Society for Neuroscience (2015-2016)
- Member of the Association for Research in Vision and Ophthalmology (2010-2016)
- Student representative to the graduate and professional student government (2015-2016)
- Student representative to the school of science graduate student council (2011-2012)